# Towards non-invasive monitoring of mitochondrial function

Floor Harms

# Towards non-invasive monitoring of mitochondrial function

Floor Harms

ISBN: 978-90-5335-934-1

Druk: Ridderprint BV, Ridderkerk

Cover: Bart Lukkes and Ridderprint B.V. Layout and printing.

# Towards non-invasive monitoring of mitochondrial function

## Op weg naar niet-invasieve monitoring van mitochondriale functie

**PROEFSCHRIFT**

ter verkrijging van de graad van doctor aan de
Erasmus Universiteit Rotterdam
op gezag van de
rector magnificus

Prof.dr. H.A.P. Pols

en volgens besluit van het College voor Promoties.
De openbare verdediging zal plaatsvinden op
woensdag 26 november 2014 om 11.30 uur

door

**Floortje Anneleen Harms**
geboren te 's-Gravenhage

**PROMOTIECOMMISSIE**

| | |
|---|---|
| **Promotor:** | Prof.dr. R.J. Stolker |
| **Overige leden:** | Dr. D.A.M.P.J. Gommers |
| | Prof.dr. C. Ince |
| | Prof.dr. C.D. Spies |
| **Copromotor:** | Dr. E.G. Mik |

Financial support for the studies published in this thesis was obtained from ZonMW (the Netherlands Organisation for Health Research Development).

Further financial support for this thesis was generously provided by: Erasmus MC and Photonic Health Care B.V.

**CONTENTS**


PREFACE
AND
OUTLINE

**PREFACE**

Maintaining optimal tissue oxygenation to safeguard oxygen supply and aerobic metabolism plays an important role in the daily clinical practice of anesthesiologists and intensivists. The mitochondria are the ultimate destination of oxygen in the body. The mitochondria produce energy-rich phosphates by the process of oxidative phosphorylation. Sustained mitochondrial energy production is essential for survival of tissue cells and the organism. Several pathophysiological circumstances are known to lead to mitochondrial dysfunction and, eventually, cell death. For example, lack of oxygen (anoxia) and prolonged reduced oxygen availability (hypoxia) are detrimental for mitochondrial function. Therefore, the amount of effort put into restoring and maintaining adequate tissue oxygenation in the critically ill patient seems justifiable. However, the question remains whether such clinical focus on optimizing oxygen supply is adequate under all circumstances.

An increasing number of studies have described the impact of mitochondrial dysfunction in a variety of human disorders. Examples include the process of cellular aging and cancer [1] and cardiovascular diseases [2-6]. Interestingly, mitochondrial dysfunction is also suggested to play a key role in the pathophysiology of and recovery from sepsis and septic shock [3-7]. The latter are both life-threatening disorders with a high mortality rate of 30-60% [8]. Besides actual treatment of the cause, the main cornerstones in the treatment of sepsis are mainly supportive. Such supportive measures are aimed at restoring the hemodynamic state, ventilation, and the 'milieu interieur'. However, even after achievement of these goals, some patients do not recover from sepsis. Part of the failure to recover can be attributed to mitochondrial dysfunction. This may explain why the mortality and morbidity of sepsis has not been substantially reduced in the last years, despite progression in terms of monitoring techniques and medical treatment options.

Notwithstanding the role of mitochondrial dysfunction in the pathophysiology of sepsis, no current treatment is specifically directed to protect or improve mitochondrial function. One reason for this might be the lack of availability of a non-invasive monitor for mitochondrial function [9]. Current techniques to assess mitochondrial function are limited in several ways, i.e. they are either invasive, locally destructive, semi-quantitative, indirect, measure in the wrong compartment, have low temporal resolution, or are not feasible for clinical use because of toxicity. The protoporphyrin IX-triplet state lifetime technique (PpIX-TSLT) for measurement of mitochondrial oxygen tension *in vivo* can potentially overcome such constraints [10].

Therefore, the work in this thesis is aimed at further developing PpIX-TSLT into a clinical monitoring tool that enables early assessment of mitochondrial function in critically ill patients.

PpIX-TSLT in itself allows us to measure mitochondrial oxygen tension (mitoPO$_2$) in an optical manner. It is the first technique that enables measurement of mitoPO$_2$ in living cells and tissues, and can be applied *in vivo* [11, 12]. The principles of the measurement are shown in Figure 1.

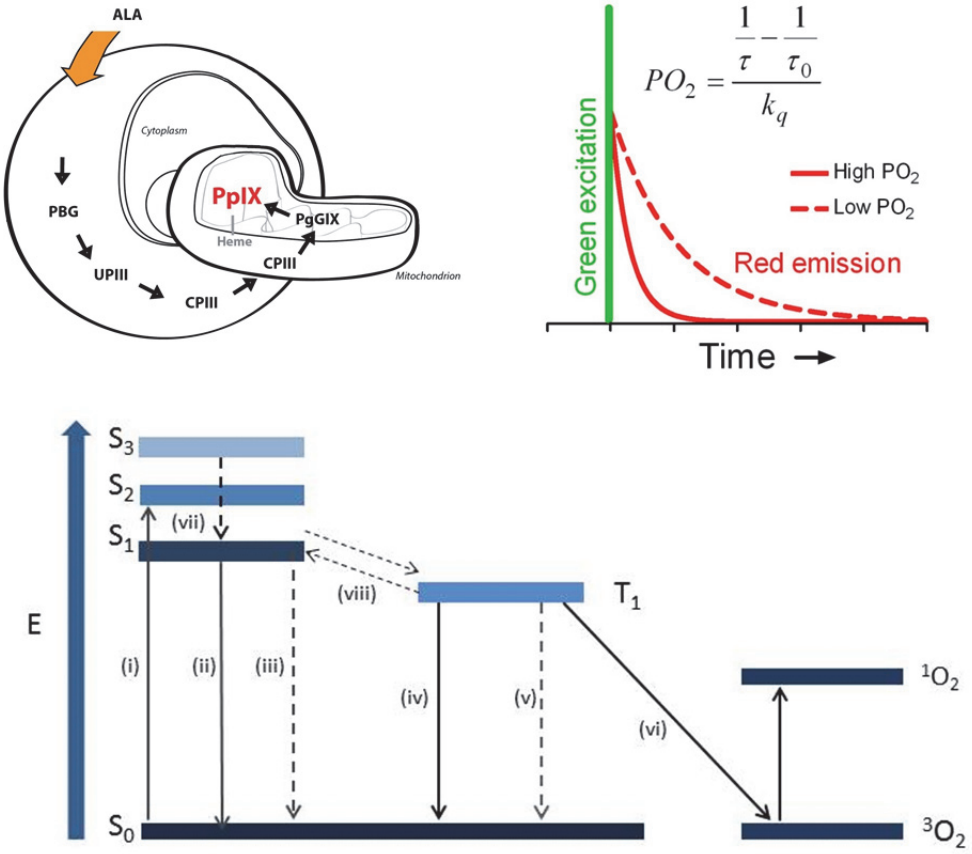


**FIGURE 1.** Principle of mitoPO$_2$ measurement by oxygen-dependent quenching of ALA enhanced PpIX. Principle by which ALA administration enhances mitochondrial PpIX levels. ALA, 5-aminolevulinic acid; PBG, porphobilinogen; UPIII, uroporphyrinogen III; CPIII, coporporphyrinogen III; and PpIX, protoporphyrin IX. PpIX emits delayed fluorescence after excitation by a pulse of green (510 nm) light. The delayed fluorescence lifetime is oxygen-dependent according to the Stern-Volmer equation (inset), in which $k_q$ is the quenching constant and $\tau_0$ is the lifetime at zero oxygen. Jablonski diagram of states and state transitions of PpIX and its interaction with oxygen. $S_0$, $S_1$, and $S_2$ represent the ground state and first and second excited singlet states, respectively. $T_0$, $T_1$, and $T_2$ represent the ground (triplet) state and first and second excited triplet states, respectively. $k_q$ is the rate constant of $T_1$ quenching by oxygen.

The technique was developed and calibrated on cell cultures, isolated organs (heart and liver), and for *in vivo* use [10-12]. A notable finding of the first *in vivo* measurements was that the level of mitoPO$_2$ appeared to be much higher than classically anticipated. This finding was recently discussed in our review on the delayed fluorescence of protoporphyrin IX (PpIX) technique [13] as follows: *"Most studies report rather low PO$_2$ values ranging from 10-17 mmHg for vascular and interstitial compartments [14, 15]. As a consequence, mitoPO$_2$ has been derived and estimated to be in the order of several mmHg [16, 17]. However, with the advent of new techniques with less invasiveness and increased accuracy it appears that the levels of oxygen in tissue are much higher than originally thought [18-20]. These more recent findings suggest that the classical estimations of mitoPO$_2$ in vivo might be too low. Indeed, our first direct measurements of mitoPO$_2$ in vivo also indicated that mitochondrial oxygen levels might well exceed a few mmHg. While mitoPO$_2$ appeared to be highly heterogeneous, average mitoPO$_2$ in rat liver was around 45 mmHg [12], in rat heart around 35 mmHg [11]."*

The possibility to measure mitoPO$_2$ *in vivo* is only a first step towards clinical measurement of mitochondrial function at the bedside.
In this thesis we describe further developments of the PpIX-TSLM technique, for example, for use in humans. Furthermore, we have initiated the first measurements of additional mitochondrial parameters, i.e. mitochondrial oxygen consumption (mitoVO$_2$) and oxygen affinity of the respiratory chain. These developments are important steps towards the clinical use of PpIX-TSLM. The ultimate goal is to enable bedside monitoring of oxygen tension and oxygen consumption at the subcellular level. This will allow physicians to study oxygen supply and demand at the place where it matters most, the mitochondria.

**REFERENCES**


1. Navarro, A. and A. Boveris, *The mitochondrial energy transduction system and the aging process.* Am J Physiol Cell Physiol, 2007. **292**(2): p. C670-86.
2. Ballinger, S.W., *Mitochondrial dysfunction in cardiovascular disease.* Free Radic Biol Med, 2005. **38**(10): p. 1278-95.
3. Brealey, D., et al., *Mitochondrial dysfunction in a long-term rodent model of sepsis and organ failure.* American Journal of Physiology - Regulatory Integrative and Comparative Physiology, 2004. **286**(3 55-3): p. R491-R497.
4. Fink, M.P., *Bench-to-bedside review: Cytopathic hypoxia.* Crit Care, 2002. **6**(6): p. 491-9.

5. Galley, H.F., *Oxidative stress and mitochondrial dysfunction in sepsis.* Br J Anaesth, 2011. **107**(1): p. 57-64.
6. Gellerich, F.N., et al., *Impaired energy metabolism in hearts of septic baboons: Diminished activities of complex I and complex II of the mitochondrial respiratory chain.* Shock, 1999. **11**(5): p. 336-341.
7. Garrabou, G., et al., *The effects of sepsis on mitochondria.* J Infect Dis, 2012. **205**(3): p. 392-400.
8. Bakker, J., et al., *[Sepsis, a complicated syndrome with major medical and social consequences] Sepsis, een gecompliceerd syndroom met belangrijke medische en maatschappelijke consequenties.* Ned Tijdschr Geneeskd, 2004. **148**(20): p. 975-8.
9. Jeger, V., et al., *Mitochondrial function in sepsis.* Eur J Clin Invest, 2013. **43**(5): p. 532-42.
10. Mik, E.G., et al., *Mitochondrial PO2 measured by delayed fluorescence of endogenous protoporphyrin IX.* Nat Methods, 2006. **3**(11): p. 939-45.
11. Mik, E.G., et al., *Mitochondrial oxygen tension within the heart.* J Mol Cell Cardiol, 2009. **46**(6): p. 943-51.
12. Mik, E.G., et al., *In vivo mitochondrial oxygen tension measured by a delayed fluorescence lifetime technique.* Biophys J, 2008. **95**(8): p. 3977-90.
13. Mik, E.G., *Measuring Mitochondrial Oxygen Tension: From Basic Principles to Application in Humans.* Anesth Analg, Anesth Analg, 2013. **117**(4): p. 834-46.
14. Rumsey, W.L., et al., *Oxygen pressure distribution in the heart in vivo and evaluation of the ischemic "border zone".* Am J Physiol, 1994. **266**(4 Pt 2): p. H1676-80.
15. Trochu, J.N., et al., *Role of endothelium-derived nitric oxide in the regulation of cardiac oxygen metabolism: implications in health and disease.* Circ Res, 2000. **87**(12): p. 1108-17.
16. Wittenberg, B.A. and J.B. Wittenberg, *Transport of oxygen in muscle.* Annu Rev Physiol, 1989. **51**: p. 857-78.
17. Gnaiger, E., et al., *Mitochondrial oxygen affinity, respiratory flux control and excess capacity of cytochrome c oxidase.* J Exp Biol, 1998. **201**(Pt 8): p. 1129-39.
18. Wilson, D.F., *Quantifying the role of oxygen pressure in tissue function.* Am J Physiol Heart Circ Physiol, 2008. **294**(1): p. H11-3.
19. Bodmer, S.I., et al., *Microvascular and mitochondrial PO(2) simultaneously measured by oxygen-dependent delayed luminescence.* J Biophotonics, 2012. **5**(2): p. 140-51.

20. Giraudeau, C., et al., *High sensitivity 19F MRI of a perfluorooctyl bromide emulsion: application to a dynamic biodistribution study and oxygen tension mapping in the mouse liver and spleen.* NMR Biomed, 2012. **25**(4): p. 654-60.
21. Silva, A.M. and P.J. Oliveira, *Evaluation of respiration with clark type electrode in isolated mitochondria and permeabilized animal cells.* Methods Mol Biol, 2012. **810**: p. 7-24.

**OUTLINE OF THE THESIS**

The work presented in this thesis describes the development of a non-invasive and clinically usable system to monitor important aspects of mitochondrial function. This translational research project started with the validation of PpIX-TSLT for cutaneous use in an animal model and finished with the first study performed in healthy human volunteers.

**Chapter 1** explores the possibility of using PpIX-TSLT to measure oxygen-dependent delayed fluorescence in skin after topical application of the PpIX precursor 5-aminolevulinic acid. To enable reliable cutaneous mito$PO_2$ measurements on the skin, calibration of the signals was necessary. Previous calibrations of PpIX-TSLT were performed in cultured cells [10], heart and liver [11, 12]. However, the calibration procedures used for cultured cells and isolated organs were not applicable in skin tissue. Therefore, we developed a novel approach that enables simultaneous measurements of cutaneous mito$PO_2$ and microvascular oxygen tension in rats (**Chapter 2)**. Subsequently, in **Chapter 3**, we validated the previously found calibration constants for application on skin by means of these simultaneous measurements.

The absolute value of mito$PO_2$ is an important physiological parameter indicating mitochondrial oxygen availability. However, as investigated in **Chapter 4**, measurement of the kinetics of delayed fluorescence lifetime (indicative of changes in mito$PO_2$) after artificially blocking local oxygen supply, provides additional information on mitochondrial oxygen consumption (mito$VO_2$) and oxygen affinity of the respiratory chain.

Having established the feasibility of measuring cutaneous mito$PO_2$ and mito$VO_2$ we then examined the changes in mitochondrial oxygenation and oxygen consumption in an endotoxin-induced septic animal model with and without fluid resuscitation **(Chapter 5)**.

The substrate succinate improves mitochondrial complex II activity in sepsis-induced mitochondrial dysfunction, as previously shown by classical respirometry in isolated mitochondria from muscle biopsies [21]. If we are capable of *in vivo* monitoring of alterations in mitochondrial function, the administration of succinate in an endotoxin-induced sepsis model should provide results similar to those observed in isolated mitochondria. Therefore, in **Chapter 6,** we performed validation of the mito$VO_2$ measurements by means of infusing succinate under endotoxin-induced septic conditions in rats.

Other important steps essential for the clinical applicability of PpIX-TSLT are described in **Chapter 7**. Here we investigated whether alterations in mitochondrial parameters in skin reflect similar alterations in other organs and tissues. Furthermore, in this chapter we describe a clinical prototype of the PpIX-TSLT device ready for human use. Finally, after extensive testing in animal studies, we describe the first results of measurements with our new clinical prototype in healthy volunteers **(Chapter 8)**.

**Chapter 9** provides a detailed description of the PpIX–TSLT. This user-friendly manual enables researchers to measure mito$PO_2$ and mito$VO_2$ in small animal models.


CHAPTER
1

# *Oxygen-dependent delayed fluorescence measured in skin after topical application of 5-aminolevulinic acid*

Floor A. Harms[1], Wadim M. I. de Boon[1], Gianmarco M. Balestra[1,2], Sander I.A. Bodmer[1], Tanja Johannes[1], Robert J. Stolker[1], and Egbert G. Mik[1,3]

1 Department of Anesthesiology, Laboratory of Experimental Anesthesiology, ErasmusMC, University Medical Center Rotterdam, Rotterdam, The Netherlands

2 Department of Intensive Care, University Hospital Basel, Basel, Switzerland

3 Department of Intensive Care, Erasmus University Medical Center Rotterdam, 's-Gravendijkwal 230, 3015 CE Rotterdam, The Netherlands

**Short title:** Oxygen-dependent delayed fluorescence measured in skin

Published in: J. Biophotonics, 2011. 4(10): p. 731-9

**ABSTRACT**

Mitochondrial oxygen tension can be measured *in vivo* by means of oxygen-dependent quenching of delayed fluorescence of protoporphyrin IX (PpIX). Here we demonstrate that delayed fluorescence is readily observed from skin in rat and man after topical application of the PpIX precursor 5-aminolevulinic acid (ALA). Delayed fluorescence lifetimes respond to changes in inspired oxygen fraction and blood supply. The signals contain lifetime distributions and the fitting of rectangular distributions to the data appears more adequate than mono-exponential fitting. The use of topically applied ALA for delayed fluorescence lifetime measurements might pave the way for clinical use of this technique.

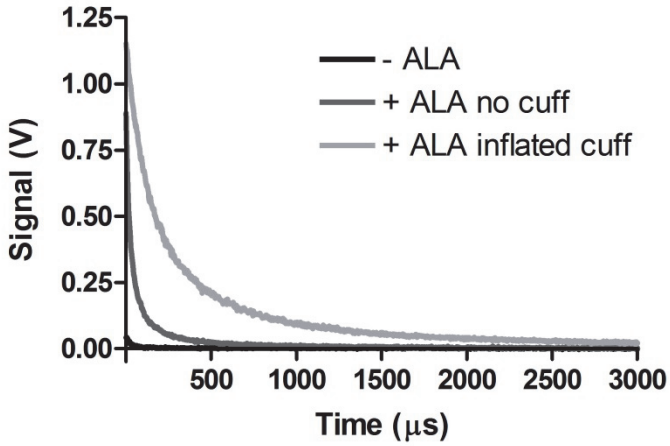


**Abstract figure.** Oxygen-dependent delayed fluorescence measured on the forearm of a volunteer before and after inflation of a blood pressure cuff.

## INTRODUCTION

The adequate supply of oxygen by inhalation and subsequent transport to tissues via the circulating blood is a conditio sine qua non for mammalian cells to sustain life. Molecular oxygen is the primary oxidant in biological systems and its ultimate destination *in vivo* is the mitochondria where it is used in oxidative phosphorylation [2]. Besides being indispensible for the energy production of our cells, oxygen is known to play a role in many other biochemical processes and mammalian tissue contains a large number of oxygen consuming enzymes [3].

Many techniques have been developed for measuring oxygen *in vivo* [4], because of the importance of adequate oxygen supply. However, due to invasiveness or the need of injection of foreign compounds into the circulation, most techniques have been restricted to preclinical use in laboratory animals. An excellent example of this is the phosphorescence quenching technique, originally developed by Vanderkooi and Wilson in the late 1980s [5].

Oxygen-dependent quenching of phosphorescence of metallo-porphyrin–based dyes relies on the injection of the dye in experimental animals. This allows for the measurement of oxygen tension ($PO_2$) in the microcirculation [6, 7] or interstitium [8, 9], depending on the site of injection. The oxygen tension ($PO_2$) can be calculated from the phosphorescence decay kinetics. Once calibrated, phosphorescence lifetime measurements do not require recalibration [10]. Furthermore, because the technique measures lifetimes, and not intensities, it is insensitive to changes in tissue optical properties. Despite these favorable properties, the need for injection of potentially toxic oxygen-sensitive dyes has prevented its clinical use till today.

In order to circumvent this drawback we researched the possibilities to use endogenous porphyrin for measuring oxygen. Recently we demonstrated that the optical properties of endogenous protoporphyrin IX (PpIX) enables quantitative oxygen measurements by means of oxygen-dependent quenching of delayed fluorescence [11]. 5-Aminolevulinic acid (ALA) enhanced PpIX is synthesized inside the mitochondria [12] and can act as mitochondrially located oxygen-sensitive dye. We successfully measured mitochondrial $PO_2$ (mito$PO_2$) in cultured cells [11], rat liver [13] and rat heart [14].

ALA is a precursor in porphyrin synthesis and its application induces the accumulation of PpIX inside mitochondria [15]. ALA is clinically used in photodynamic diagnosis and

therapy of cancer [16-18]. Besides systemic application by oral intake or intravenous injection, ALA can be topically applied to tissue in order to enhance PpIX levels locally [19, 20]. If the latter approach would prove to be feasible for delayed fluorescence measurements this could pave the way for exploring its clinical applications.

In this study we tested the feasibility of measuring oxygen-dependent delayed fluorescence in skin after topical application of ALA. To this end, 2.5% ALA cream was topically applied for 3 hours on the skin of anesthetized and mechanically ventilated rats. Delayed fluorescence was detected from the side of application and the oxygen-dependency of the lifetime was tested by various measures. Three different methods to analyze the delayed fluorescence signals were compared. We also performed a pilot experiment on the forearm of a healthy volunteer.

## MATERIALS AND METHODS

### PRINCIPLE OF MEASUREMENT

The background of the PpIX delayed fluorescence technology is described in detail elsewhere [11, 13]. In short, PpIX is the final precursor of heme in the heme biosynthetic pathway (figure 1a). PpIX is synthesized in the mitochondria, and administration of ALA substantially enhances the PpIX concentration. Since the conversion of PpIX to heme is a rate-limiting step, administration of ALA causes accumulation of PpIX inside the mitochondria. PpIX possesses a triplet state ($T_1$) that reacts strongly with oxygen, making the $T_1$ lifetime oxygen-dependent (Figure 1b). Population of $T_1$ occurs upon photo-excitation with a pulse of light, and bidirectional intersystem crossing causes the emission of red delayed fluorescence. The lifetime of the delayed fluorescence reflects the $T_1$ lifetime and is therefore also oxygen-dependent.

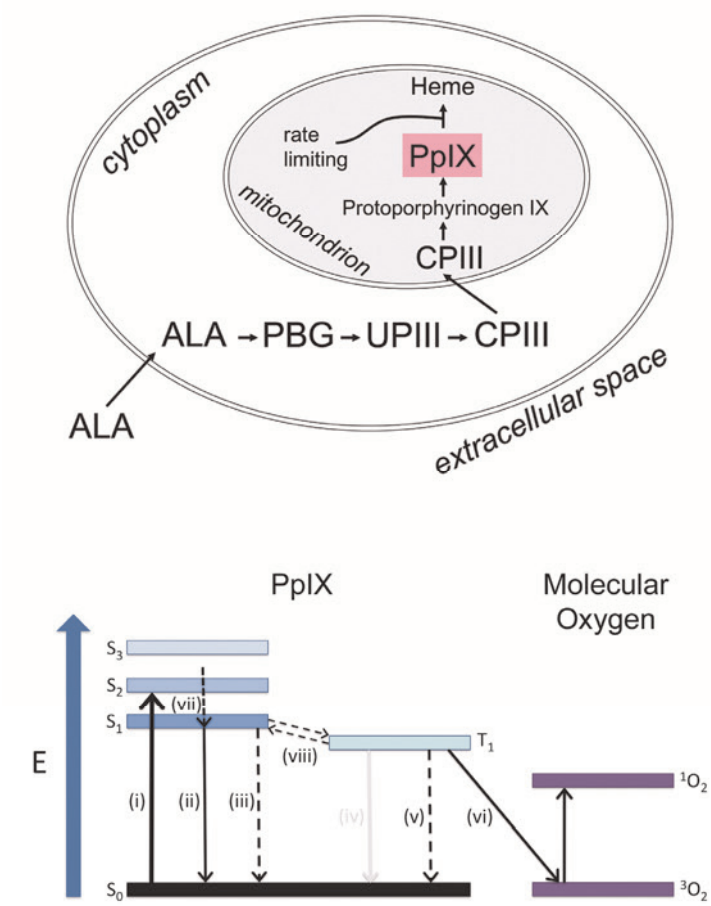


**Figure 1.** Principle by which ALA administration enhances mitochondrial PpIX levels (upper panel) and the Jablonski diagram of states and state transitions of PpIX and its interaction with oxygen (lower panel). ALA, 5-aminolevulinic acid; PBG, porphobilinogen; UPIII, uroporphyrinogen III; CPIII, coporporphyrinogen III; and PpIX, protoporphyrin IX. $S_0$, $S_1$, $S_2$ and $S_3$ represent the ground state and first, second and third excited singlet states, respectively. $T_1$ represent the first excited triplet states of PpIX and $^3O_2$ and $^1O_2$ are the triplet ground state and excited singlet state of oxygen. Absorption (i), fluorescence and delayed fluorescence (ii), radiationless transitions (iii and v), phosphorescence (iv), energy transfer (vi), internal conversion (vii) and bi-directional intersystemcrossing (viii).

## LIFETIME ANALYSIS

When excited by a light pulse, the delayed fluorescence (~610-740 nm) intensity decreases at a rate dependent on the surrounding oxygen pressure. The relationship between the measured decay time and the $PO_2$ is given by the Stern-Volmer equation:

$$PO_2 = \frac{\frac{1}{\tau} - \frac{1}{\tau_0}}{k_q} \quad (1)$$

where $\tau$ is the measured decay time, $\tau_0$ is the decay time at an oxygen pressure of zero and $k_q$ is the quenching constant. Although the calibration constants have been determined in rat liver [13] and rat heart [14], $\tau_0$ and $k_q$ are not validated for our current application in skin. Especially the temperature dependency of $\tau_0$ and $k_q$ remain to be determined. Therefore, instead of providing quantitative $PO_2$ values we restrict ourselves to reporting our data in terms of reciprocal lifetimes ($R_\tau$):

$$R_\tau = \frac{1}{\tau} = k_q PO_2 + \frac{1}{\tau_0} \quad (2)$$

Equations 1 and 2 describe the relationship between the $PO_2$ and the phosphorescence lifetime in case of a homogeneous oxygen distribution. However, large nonuniformities in oxygen pressure exist *in vivo*, resulting in a phosphorescence signal that in general can be described by an integral over an exponential kernel:

$$y(t) = \int_0^t \exp(-\lambda t) f(\lambda) d\lambda \quad (3)$$

where $f(\lambda)$ denotes the spectrum of reciprocal lifetimes that should be determined from the finite data set $y(t)$. The Exponential Series Method (ESM) has been proven reliable and robust [13, 21] for retrieving information about the spectrum $f(\lambda)$ in the case of delayed luminescence lifetime measurements. According to ESM the reciprocal lifetime distribution can be retrieved from the data by finding the weight factors of a finite set of discrete reciprocal lifetimes:

$$Y^*(t) = \sum w_i \exp\left(-R_{\tau_i} t\right) \quad (4)$$

where $Y^*(t)$ are the normalized phosphorescence data and $w_i$ is the weight factor for the according reciprocal lifetime $R_{\tau i}$ ($w_i \geq 0$ and $\sum w_i = 1$). For analysis of our data we used a set

of 15 equally distributed $R_\tau$'s in the range 0.005 to 0.122 $\mu s^{-1}$, corresponding to a broad lifetime range from 8 till 200 µs. The average value of $R_\tau$, denoted by $< R_\tau >$, can be retrieved from the distribution by:

$$\langle R_\tau \rangle = \sum w_i R_{\tau_i} \tag{5}$$

Besides the ESM method, we used Mono-Exponential Analysis (MEA) and the approach published by Golub et al. [22] in which the heterogeneity in oxygen pressure is analyzed by fitting distributions of quencher concentration to the delayed luminescence data. Corresponding to their work, the fitting function for a simple rectangular distribution with a mean $PO_2$ $Q_m$ and a $PO_2$ range from $Q_m - \delta$ till $Q_m + \delta$ is:

$$Y_R(t) = \exp[-(k_0 + k_q Q_m)t] \cdot \sinh(k_q \delta t) / k_q \delta t \tag{6}$$

where $Y_R(t)$ is the normalized phosphorescence data, $k_0$ is the first-order rate constant for phosphorescent decay in the absence of quencher, and $\delta$ is half the width of the rectangular distribution. For the case of unknown calibration constants equation 5 can be rewritten as:

$$Y_R(t) = \exp[-R_\tau t] \cdot \sinh(\Delta t) / \Delta t \tag{7}$$

where $\Delta$ is a measure of the heterogeneity in reciprocal lifetime $R_\tau$. We refer to this approach as the Rectangular Distribution Method (RDM).

EXPERIMENTAL SETUP

The excitation source was an Opolette 355-I (Opotek, Carlsbad, CA, USA), a compact computer-controlled tunable laser providing pulses with a specified duration of 4-10 ns and typically 2-4 mJ/pulse over the tunable range of 410 to 670 nm. The laser was coupled into a Fiber Delivery System (Opotek, Carlsbad, CA, USA) consisting of 50 mm planoconvex lens, X-Y fibermount and a 2 meter fiber with a core diameter of 1000 µm. This fiber was coupled to a custom made reflection probe by an In-Line Fiber Optic Attenuator (FOA-Inline, Avantes b.v., Eerbeek, The Netherlands). The reflection probe consisted of two 1000 µm fibers with a length of 2 meters (P1000-2-VIS-NIR, Ocean Optics, Dunedin, FL, USA) mounted at the common end into a stainless steel holder with a

separation of 1 mm between the fibers. The light output of the excitation branch was set at 200 µJ/pulse as measured by a FieldMate laser power meter with PowerMax PS19 measuring head (Coherent Inc., Santa Clara, CA, USA). Measurements were performed with the reflection probe at 5 mm from the skin. Due to an output angle of 25.4° this resulted in an illuminated spot with a diameter of approximately 3.3 mm. Corresponding fluencies were 2.4 mJ/cm$^2$ per pulse and 0.15 J/cm$^2$ per measurement.

The PpIX signal was detected by a gated microchannel plate photomultiplier tube (MCP-PMT R5916U series, Hamamatsu Photonics, Hamamatsu, Japan). The MCP-PMT was custom adapted with an enhanced red-sensitive photocathode having a quantum efficiency of 24% at 650 nm. The MCP-PMT was mounted on a gated socket assembly (E3059-501, Hamamatsu Photonics, Hamamatsu, Japan) and cooled to –30 °C by a thermoelectric cooler (C10373, Hamamatsu Photonics, Hamamatsu, Japan). The MCP-PMT was operated at a voltage in the range of 2300V-3000V by a regulated high-voltage DC power supply (C4848-02, Hamamatsu Photonics, Hamamatsu, Japan). The detection fiber was fit into an Oriel Fiber Bundle Focusing Assembly (Model 77799, Newport, Irvine, CA, USA) which was coupled to the MCP-PMT by an in-house built optics consisting of a filter-holder, a plano convex lens (BK7, OptoSigma, Santa Ana, CA, USA) with focal length of 90 mm and an electronic shutter (04 UTS 203, Melles Griot, Albuquerque, NM, USA). The shutter was controlled by an OEM Shutter Controller Board (59 OSC 205, Melles Griot, Albuquerque, NM, USA) and served as protection for the PMT, which was configured for the “normally on” mode. The PpIX emission light was filtered by a combination of a 590 nm longpass filter (OG590, Newport, Irvine, CA, USA) and a broadband (600-750 nm) bandpassfilter (Omega Optical, Brattleboro, VT, USA).

The output current of the photomultiplier was voltage-converted by an in-house built amplifier with an input impedance of 440 ohm, 400 times voltage amplification and a bandwidth around 20 Mhz. Data-acquisition was performed by a PC-based data-acquisition system containing a 10 MS/s simultaneous sampling data-acquisition board (NI-PCI-6115, National Instruments, Austin, TX). The amplifiers were coupled to the DAQ-board by a BNC interface (BNC-2090A, National Instruments, Austin, TX). The data-acquisition ran at a rate of 10 mega samples per second and 64 laser pulses (repetition rate 20 Hz) were averaged prior to analysis. Control of the setup and analysis of the data was performed with software written in LabView (Version 8.6, National Instruments, Austin, TX, USA).

EXPERIMENTAL PROCEDURES

The protocol was approved by the Animal Research Committee of the ErasmusMC University Medical Center Rotterdam. Animal care and handling were performed in accordance with the guidelines for Institutional and Animal Care and Use Committees.

A total of 6 male Wistar rats (Charles River, Wilmington, MA, USA, body weight 292 ± 25,5 g) were used in this study. The animals were anesthetized by an intraperitoneal injection of a mixture of ketamine 90 mg $kg^{-1}$ (Alfasan, Woerden, The Netherlands), medetomidine 0.5 mg $kg^{-1}$ (Sedator Eurovet Animal Health BV, Bladel, The Netherlands), and atropine 0.05 mg $kg^{-1}$ (Centrofarm Services BV, Etten-Leur, The Netherlands). Mechanical ventilation was performed via tracheotomy. Ventilation was adjusted on end-tidal $PCO_2$, keeping the arterial $PCO_2$ between 35 and 40 mmHg. Variations in $FiO_2$, the fraction of inspired oxygen, were made by mixtures of oxygen and nitrogen.

A polyethylene catheter (outer diameter 0.9 mm) was inserted into the right jugular vein for the intravenous administration of fluids. Arterial blood pressure and heart rate were monitored with a similar catheter in the right carotid artery. Ketamine (50 mg $kg^{-1}$ $h^{-1}$) and crystalloid solution (Ringer lactate, 5 mL $kg^{-1}$ $h^{-1}$) were infused intravenously for maintaining anaesthesia and fluid balance. Body temperature was rectally measured and kept at 38°C ± 0.5°C by means of a heating pad.

PpIX was induced by topical application of 2.5% ALA cream. A mixture of hydrophilic cremor lanette (Lanettecrème I FNA, Bipharma, Weesp, The Netherlands) and 2.5% 5-aminolevulinic acid (Sigma-Aldrich, St. Louis, MO, USA) was made just before use and administered topically on the abdominal skin after hair removal. The latter was accomplished by shaving and hair removal cream (Veet, Reckitt Benckiser Co., Slough, UK). The exposed skin was covered with an adhesive film and, to prevent premature exposure of PpIX to light, the area was covered with aluminium foil. The delayed fluorescence lifetime measurements were started three hours after the application of ALA cream. First the baseline delayed fluorescence was measured at an $FiO_2$ of 0.4 and subsequently, after a stabilisation period of 5 minutes, measurements were performed during 1.0 $FiO_2$ ventilation. The experiment was terminated by euthanasia of the animal using an overdose of Euthasol (ST Farma, Raamsdonksveer, The Netherlands).

The experiment in human skin was voluntarily performed on the forearm of the principal investigator (E.G.M.). A small aliquot of 2.5% ALA-cream was topically applied under adhesive foil and protection from light for 3 hours. Delayed fluorescence was measured

under normal conditions and 2 minutes after cessation of blood flow by inflation of a blood-pressure cuff around the arm.

**RESULTS**

Topical application of ALA to the abdominal skin of rats induced detectable delayed fluorescence signal. Figure 2 shows the signals observed in a rat from areas of the skin with and without direct ALA exposure. The area on which ALA was topically applied shows a clear signal. This is in contrast to the area without ALA in which the signal is very faint. The latter was most probably due to some systemic ALA uptake and distribution. No signal was detectable in skin from rats not exposed to ALA.

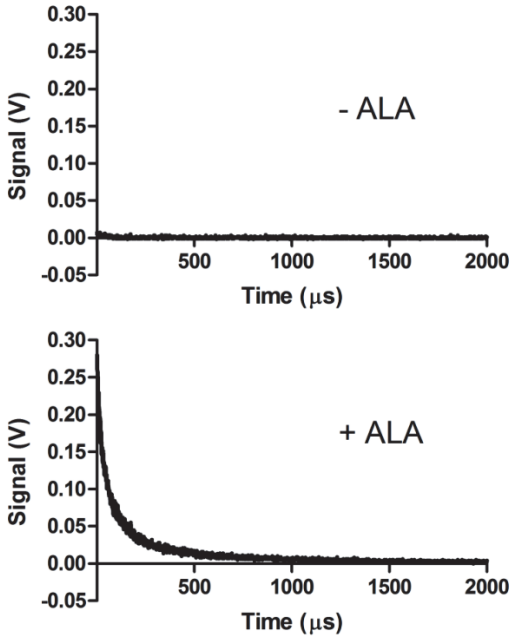


**Figure 2.** Examples of signals obtained from areas of skin on the abdomen of a rat not exposed (upper panel) and exposed to topically administered ALA for 3 hours.

The oxygen-dependency of the delayed fluorescence is demonstrated in figure 3. A change in inspired oxygen fraction from 0.4 (40% oxygen in the ventilation gas) to 1.0 (breathing with 100% oxygen) resulted in a faster decay of the delayed fluorescence signal, corresponding to higher oxygen levels in the skin tissue. Conversely, cessation of

microvascular blood flow by applying pressure to the skin with the detection probe resulted in a slower decay. This is in accordance with decreased oxygen levels in the skin tissue due to oxygen consumption under blocked oxygen supply.

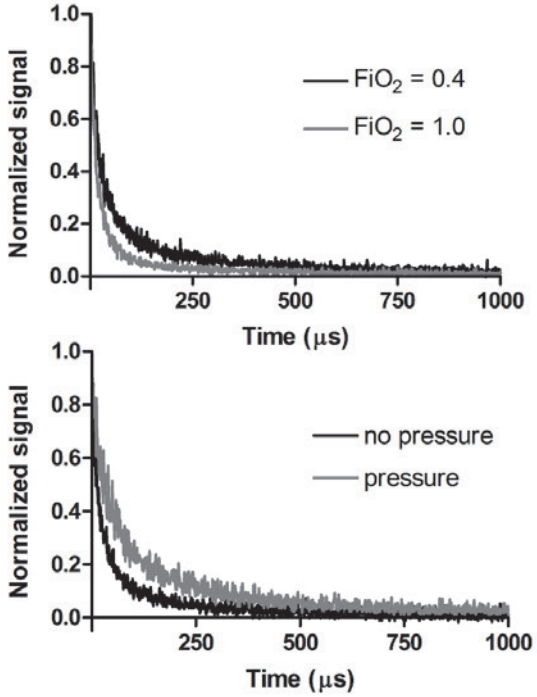


**Figure 3.** Normalized delayed fluorescence traces measured in abdominal skin of rats after 3 hours exposure to topically administered ALA. Increasing $FiO_2$ from 0.4 to 1.0 results in faster decay of delayed fluorescence (upper panel). Application of pressure on the skin by the measurement probe results in a slower decay of delayed fluorescence (lower panel).

Analysis of the delayed fluorescence by means of the ESM method reveals that the delayed fluorescence signal is not simply mono-exponential, as would be the case if oxygen would be homogeneously distributed in the skin. The distribution of reciprocal lifetimes shows a much more complex pattern of which examples are shown in figure 4. The ESM analysis generally shows a left-skewed distribution (i.e. towards short reciprocal lifetimes corresponding to low oxygen levels) with a considerable part of the signal arising from areas emitting long lived delayed fluorescence. Upon increasing the $FiO_2$ from 0.4 to 1.0 the distribution moves towards the right and the fraction of the shortest reciprocal lifetime decreases. Both phenomena correspond to an increase in oxygen levels in the skin.

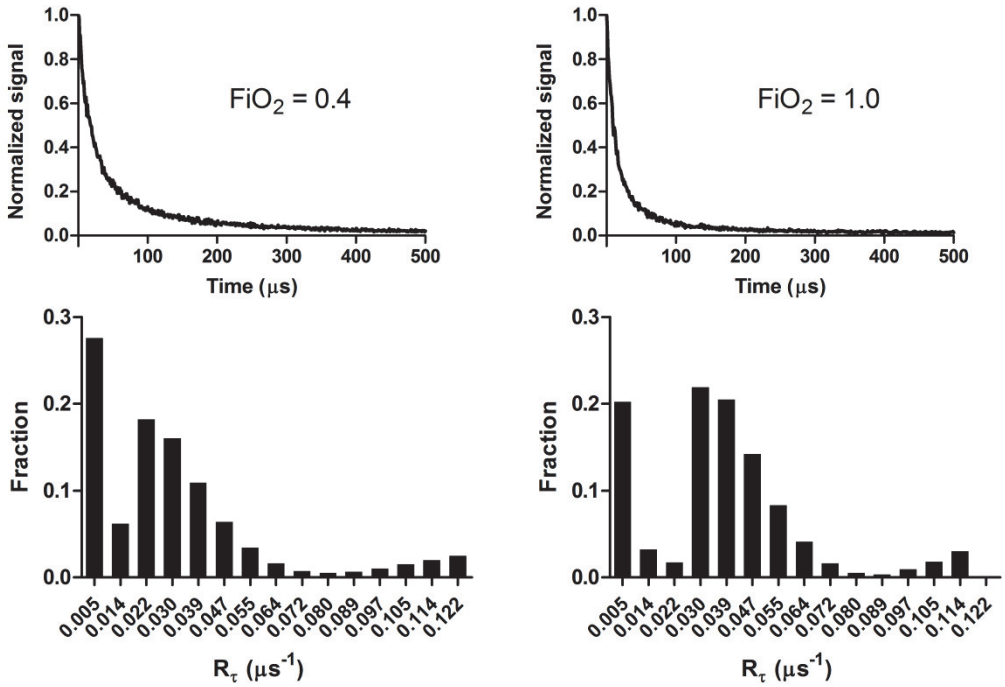


**Figure 4.** Examples of delayed fluorescence signals at different $FiO_2$ (upper panel) and the corresponding distributions of reciprocal lifetimes as obtained by ESM (lower panel).

Although the exponential series method (ESM) has been proven to be reliable and robust for delayed fluorescence measurements, the calculations are relatively time consuming (seconds to tens of seconds) and in its current form too slow for real-time implementation under non-steady state circumstances. Therefore we compared the average lifetimes retrieved by both mono-exponential analysis (MEA) and the rectangular distribution method (RDM) to the ESM. Figure 5 shows the effects of increasing $FiO_2$ in 6 rats on the average reciprocal lifetime $\langle R_\tau \rangle$ as found with the ESM. 5 out of 6 rats respond to an increase in $FiO_2$ with the expected increase in $\langle R_\tau \rangle$. The lower two panels show that in general MEA has the tendency to overestimate the average delayed fluorescence lifetime. The average lifetimes obtained by RDM are in good agreement with the ESM.

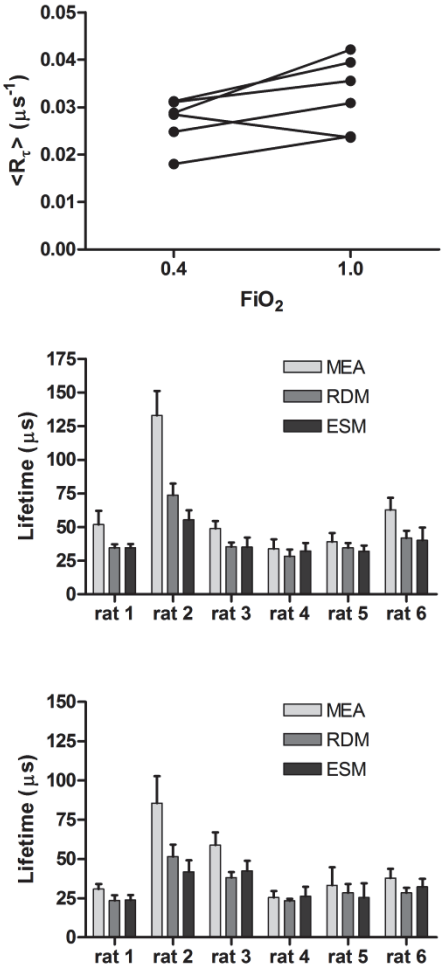


**Figure 5.** Effect of the increase in $FiO_2$ from 0.4 to 1.0 on the average reciprocal lifetime $<R_\tau>$ as obtained with ESM (upper panel). Average lifetime obtained by mono-exponential analysis (MEA), rectangular distribution method (RDM) and exponential series method (ESM) at $FiO_2$ = 0.4 (middle panel) and at $FiO_2$ = 1.0 (lower panel).

To test whether topical application of ALA also induces measurable oxygen-dependent delayed fluorescence in hairless human skin we conducted a pilot experiment on inside of the forearm of the principal investigator. Figure 6 shows that delayed fluorescence is readily measured after 3 hours of topical application of ALA. Also, cessation of blood flow to the limb by inflating a cuff around the arm leads to slower decay kinetics of the delayed fluorescence signal.

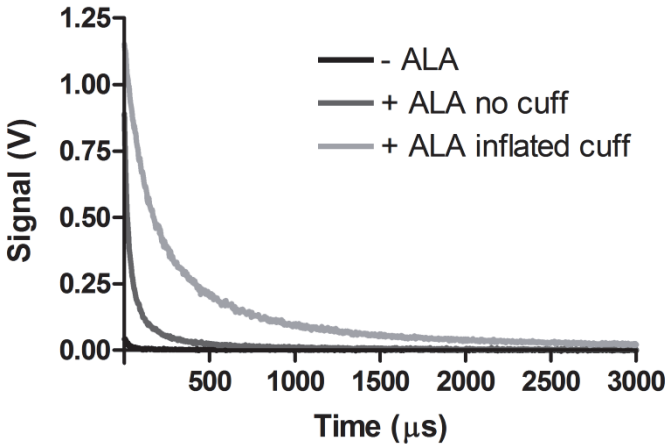


**Figure 6.** Measurement of delayed fluorescence on the forearm of a volunteer. Topical ALA administration induced a delayed fluorescence signal of which the lifetime increased upon inflation of a blood pressure cuff around the arm.

## DISCUSION AND CONCLUSION

In this work, we present a method to induce and measure oxygen-dependent delayed fluorescence in skin. The clear advantage of topical application of ALA over systemic administration is the reduction of potential side effects. The measurement equipment is fiber-based and robust and can be adapted for clinical use. We demonstrate that 3 hours after topical application of a low-dose ALA crème (2.5%), oxygen-dependent delayed fluorescence is easily observed from abdominal skin in rats and also human skin on the forearm. The delayed fluorescence signal contained a complex (reciprocal) lifetime distribution as determined with ESM. While MEA had the tendency to overestimate the average lifetime, RDM provided results that were comparable to ESM analysis.

Although ALA is systemically administered to patients in the setting of photodynamic therapy and diagnosis [15-17] without significant side effects, the photosensitization of the entire skin and retina asks for special precautions. The topical application of ALA derivatives has become a widely used method in photodynamic therapy of non-melanoma skin cancers [23]. Since concerns about photosensitization are limited to the exposed skin area, which can easily be protected from light, patients remain ambulant and are often treated in an out-of-hospital setting. Furthermore, the safety of this approach has led to the use of photodynamic therapy on benign skin lesions, like acne [24] and hidradenitis

[25]. Therefore, our finding that topical application of a relatively low dose of ALA crème induces measurable levels of oxygen-dependent delayed fluorescence might prove an important step in bringing this technique to applications in human beings. However, repeated delayed fluorescence measurements could exceed the light doses used for photodynamic therapy. Therefore, for clinical use one should strive to minimize excitation light levels.

In its calibrated form, the technique of oxygen-dependent quenching of delayed fluorescence of PpIX allows for the measurement of mitochondrial oxygen tension in living cells [11] and ex vivo and *in vivo* tissues [13, 14]. For its application in skin, the calibration constants remain to be determined, but the oxygen-dependence of the signal was evident in the present study from analysis of the reciprocal lifetime distributions. The reciprocal lifetimes are linearly dependent on the oxygen levels and this makes the technique useful even in the absence of true calibration. For example, dynamic measurement of the reciprocal lifetimes during photodynamic therapy can give insight in the rate of oxygen disappearance due to oxygen-radical formation. This could be helpful for optimizing the effect of treatment [26, 27].

The ESM in its current form is too slow for real-time analysis of delayed fluorescence signals and therefore we applied two other methods for lifetime analysis, mono-exponential analysis (MEA) and the rectangular distribution method (RDM). As in the case of phosphorescence lifetime measurements, the MEA overestimates the average lifetime [28]. Although the underlying distributions are more complex than a simple rectangular distribution, the RDM provided average lifetimes comparable to those obtained by ESM.

Overall, our study shows that implementation of the technique of oxygen-dependent quenching of delayed fluorescence is feasible in skin using topical application of ALA crème. The delayed fluorescence signals contain complex lifetime distributions and the lifetime analysis has to be adapted accordingly. The RDM is a fast and easy to implement alternative to the ESM if one needs real-time analysis in non-steady state situations. Clinical applications of the technique might range from measuring oxygen during photodynamic therapy to monitoring cellular oxygen availability in the skin of critically ill patients.

**ACKNOWLEDGEMENTS**

This work is financially supported by a Life Sciences Pre-Seed Grant (grant no 40-41300-98-9037) from the Netherlands Organization for Health Research and Development (ZonMW) and, in part, by the Young Investigator Grant 2009 (awarded to E.G.M.) from the Dutch Society of Anesthesiology.

**CONFLICT OF INTEREST STATEMENT**

E.G.M is founder and shareholder of Photonics Healthcare B.V., a company aimed at making the delayed fluorescence lifetime technology available to a broad public. Photonics Healthcare B.V. holds the exclusive licenses to several patents regarding this technology, filed and owned by the Academic Medical Center in Amsterdam and the Erasmus Medical Center in Rotterdam, The Netherlands.

**REFERENCES**

1. Golub, A.S., et al., *Analysis of phosphorescence in heterogeneous systems using distributions of quencher concentration.* Biophys J, 1997. **73**(1): p. 452-65.
2. Mitchell, P. and J. Moyle, *Chemiosmotic hypothesis of oxidative phosphorylation.* Nature, 1967. **213**(5072): p. 137-9.
3. Vanderkooi, J.M., M. Erecinska, and I.A. Silver, *Oxygen in mammalian tissue: methods of measurement and affinities of various reactions.* The American journal of physiology, 1991. **260**(6 Pt 1): p. C1131-50.
4. Springett, R. and H.M. Swartz, *Measurements of oxygen in vivo: overview and perspectives on methods to measure oxygen within cells and tissues.* Antioxidants & redox signaling, 2007. **9**(8): p. 1295-301.
5. Vanderkooi, J.M., et al., *An optical method for measurement of dioxygen concentration based upon quenching of phosphorescence.* The Journal of biological chemistry, 1987. **262**(12): p. 5476-82.
6. Johannes, T., et al., *Iloprost preserves renal oxygenation and restores kidney function in endotoxemia-related acute renal failure in the rat.* Critical care medicine, 2009. **37**(4): p. 1423-32.

7. Johannes, T., et al., *Influence of fluid resuscitation on renal microvascular PO2 in a normotensive rat model of endotoxemia.* Critical care, 2006. **10**(3): p. R88.
8. Golub, A.S., M.A. Tevald, and R.N. Pittman, *Phosphorescence quenching microrespirometry of skeletal muscle in situ.* American journal of physiology. Heart and circulatory physiology, 2011. **300**(1): p. H135-43.
9. Wilson, D.F., et al., *Oxygen pressures in the interstitial space and their relationship to those in the blood plasma in resting skeletal muscle.* Journal of applied physiology, 2006. **101**(6): p. 1648-56.
10. Mik, E.G., et al., *Excitation pulse deconvolution in luminescence lifetime analysis for oxygen measurements in vivo.* Photochemistry and photobiology, 2002. **76**(1): p. 12-21.
11. Mik, E.G., et al., *Mitochondrial PO2 measured by delayed fluorescence of endogenous protoporphyrin IX.* Nature methods, 2006. **3**(11): p. 939-45.
12. Gardner, L.C., S.J. Smith, and T.M. Cox, *Biosynthesis of delta-aminolevulinic acid and the regulation of heme formation by immature erythroid cells in man.* The Journal of biological chemistry, 1991. **266**(32): p. 22010-8.
13. Mik, E.G., et al., *In vivo mitochondrial oxygen tension measured by a delayed fluorescence lifetime technique.* Biophysical journal, 2008. **95**(8): p. 3977-90.
14. Mik, E.G., et al., *Mitochondrial oxygen tension within the heart.* Journal of molecular and cellular cardiology, 2009. **46**(6): p. 943-51.
15. Morgan, J. and A.R. Oseroff, *Mitochondria-based photodynamic anti-cancer therapy.* Advanced drug delivery reviews, 2001. **49**(1-2): p. 71-86.
16. Fukuda, H., A. Casas, and A. Batlle, *Aminolevulinic acid: from its unique biological function to its star role in photodynamic therapy.* The international journal of biochemistry & cell biology, 2005. **37**(2): p. 272-6.
17. Kelty, C.J., et al., *The use of 5-aminolaevulinic acid as a photosensitiser in photodynamic therapy and photodiagnosis.* Photochemical & photobiological sciences : Official journal of the European Photochemistry Association and the European Society for Photobiology, 2002. **1**(3): p. 158-68.
18. Peng, Q., et al., *5-Aminolevulinic acid-based photodynamic therapy. Clinical research and future challenges.* Cancer, 1997. **79**(12): p. 2282-308.
19. Becker, T.L., et al., *Monitoring blood flow responses during topical ALA-PDT.* Biomedical optics express, 2010. **2**(1): p. 123-30.
20. Juzeniene, A., P. Juzenas, and J. Moan, *Application of 5-aminolevulinic acid and its derivatives for photodynamic therapy in vitro and in vivo.* Methods in molecular biology, 2010. **635**: p. 97-106.

21. Bezemer, R., et al., *Evaluation of multi-exponential curve fitting analysis of oxygen-quenched phosphorescence decay traces for recovering microvascular oxygen tension histograms.* Medical & biological engineering & computing, 2010. **48**(12): p. 1233-42.
22. Golub, A.S., et al., *Analysis of phosphorescence in heterogeneous systems using distributions of quencher concentration.* Biophysical journal, 1997. **73**(1): p. 452-65.
23. De Vijlder, H.C., et al., *Optimizing ALA-PDT in the management of non-melanoma skin cancer by fractionated illumination.* Giornale italiano di dermatologia e venereologia : organo ufficiale, Societa italiana di dermatologia e sifilografia, 2009. **144**(4): p. 433-9.
24. Orringer, J.S., et al., *Photodynamic therapy for acne vulgaris: a randomized, controlled, split-face clinical trial of topical aminolevulinic acid and pulsed dye laser therapy.* Journal of cosmetic dermatology, 2010. **9**(1): p. 28-34.
25. Schweiger, E.S., C.C. Riddle, and D.J. Aires, *Treatment of hidradenitis suppurativa by photodynamic therapy with aminolevulinic acid: preliminary results.* Journal of drugs in dermatology : JDD, 2011. **10**(4): p. 381-6.
26. Manifold, R.N. and C.D. Anderson, *Increased cutaneous oxygen availability by topical application of hydrogen peroxide cream enhances the photodynamic reaction to topical 5-aminolevulinic acid-methyl ester.* Archives of dermatological research, 2011. **303**(4): p. 285-92.
27. Piffaretti, F.M., et al., *Optical fiber-based setup for in vivo measurement of the delayed fluorescence lifetime of oxygen sensors.* Journal of biomedical optics, 2011. **16**(3): p. 037005.
28. Johannes, T., E.G. Mik, and C. Ince, *Dual-wavelength phosphorimetry for determination of cortical and subcortical microvascular oxygenation in rat kidney.* Journal of applied physiology, 2006. **100**(4): p. 1301-10.

# CHAPTER 2

# *Microvascular and mitochondrial $PO_2$ simultaneously measured by oxygen-dependent delayed luminescence*

Sander I. A. Bodmer[1], Gianmarco M. Balestra[2], Floor A. Harms[1], Tanja Johannes[1], Nicolaas J. H. Raat[1], Robert J. Stolker[1] and Egbert G. Mik[1,3]

1 Department of Anesthesiology, Laboratory of Experimental Anesthesiology, ErasmusMC, University Medical Center Rotterdam, Rotterdam, The Netherlands

2 Department of Intensive Care, University Hospital Basel, Basel, Switzerland

3 Department of Intensive Care, Erasmus University Medical Center Rotterdam, 's-Gravendijkwal 230, 3015 CE Rotterdam, The Netherlands

**Short title:** Microvascular and mitochondrial $PO_2$

Published in: J. Biophotonics, 2012. **5**(2): p. 140-51

**ABSTRACT**

Measurement of tissue oxygenation is a complex task and various techniques have led to a wide range of tissue $PO_2$ values and contradictory results. Tissue is compartmentalized in microcirculation, interstitium and intracellular space and current techniques are biased towards a certain compartment. Simultaneous oxygen measurements in various compartments might be of great benefit for our understanding of determinants of tissue oxygenation. Here we report simultaneous measurement of microvascular $PO_2$ ($\mu PO_2$) and mitochondrial $PO_2$ ($mitoPO_2$) in rats. The $\mu PO_2$ measurements are based on oxygen-dependent quenching of phosphorescence of the near-infrared phosphor Oxyphor G2. The $mitoPO_2$ measurements are based on oxygen-dependent quenching of delayed fluorescence of protoporphyrin IX (PpIX). Favorable spectral properties of these porphyrins allow simultaneous measurement of the delayed luminescence lifetimes. A dedicated fiber-based time-domain setup consisting of a tunable pulsed laser, 2 red-sensitive gated photomultiplier tubes and a simultaneous sampling data-acquisition system is described in detail. The absence of cross talk between the channels is shown and the feasibility of simultaneous $\mu PO_2$ and $mitoPO_2$ measurements is demonstrated in rat liver *in vivo*. It is anticipated that this novel approach will greatly contribute to our understanding of tissue oxygenation in physiological and pathological circumstances.

**INTRODUCTION**

The study into the determinants of tissue oxygenation in physiological and pathological circumstances is a complex field of ongoing research. Tissue oxygen tension ($tPO_2$) is a key parameter for physiological function. Because of its importance many techniques have been developed to measure $tPO_2$ *in vivo* [1]. Concerning oxygenation, tissue can be regarded to consist of three main compartments, the microcirculation, the interstitial space and the intracellular space. Due to the technological and physical-chemical background of the available techniques to measure $tPO_2$, each is biased towards a certain compartment. Oxygen electrodes [2] tend to measure interstitial $PO_2$ while e.g. phosphorescence quenching [3] and electron paramagnetic resonance oximetry [4] are biased towards the microcirculation. Since oxygen gradients exist between the compartments this results in a bias towards a specific $PO_2$ range. This bias, together with technical differences like response time and sample volume, have made the interpretation and comparison of *in vivo* oxygen measurements difficult [5]. Therefore, the simultaneous

measurement of $PO_2$ in different tissue compartments is needed to further our understanding of oxygen delivery and utilization under various pathophysiological circumstances.

Oxygen-dependent quenching of phosphorescence is a powerful method for quantitative measurement of $PO_2$ in biological samples [6]. Pd-meso-tetra-(4-carboxyphenyl)-tetrabenzoporphyrin (Oxyphor G2) is a relatively new phosphor which is excellently suited for oxygen measurements *in vivo* [7-9]. It is highly soluble in blood plasma, where it binds to albumin and confines to the circulation [10]. Upon intravascular injection oxygen-dependent phosphorescence lifetimes can be measured at the surface of tissues and organs using e.g. fiber-based phosphorimeters [11, 12]. In this way, Oxyphor G2 has been successfully used for measurement of the distribution of microvascular oxygen pressure ($\mu PO_2$) in e.g. solid tumors [13] and kidney [14, 15]. Oxyphor G2 has its absorption maxima at 440 and 632 nm and its emission near 800 nm.

Recently we reported that the delayed fluorescence lifetime of endogenous PpIX can be used to measure mitochondrial $PO_2$ ($mitoPO_2$) in cultured cells [16] and *in vivo* [[17-19]. Administration of the precursor 5-aminolevulinic acid (ALA) increases the intramitochondrial levels of PpIX and $mitoPO_2$ can subsequently be measured by its oxygen-dependent delayed fluorescence lifetime. Delayed fluorescence has much in common with phosphorescence and it shares the useful possibility to determine heterogeneity in $PO_2$ within a volume of tissue with high temporal resolution [20, 21]. Moreover, the basic setup for delayed fluorescence lifetime measurements resembles the equipment for phosphorescence quenching experiments. Therefore, simultaneous measurement of phosphorescence and delayed fluorescence should be possible. The spectral properties of Oxyphor G2 and PpIX are very favorable in this respect with having a common excitation band (632 nm) and widely separated emission bands (~800 nm for Oxyphor G2 and ~690 nm for PpIX). The successful combination of the two techniques would provide a powerful means to measure simultaneously $\mu PO_2$ and $mitoPO_2$ *in vivo*.

Accordingly, we have developed a delayed luminescence lifetime technique that quantitatively and simultaneously measures $\mu PO_2$ using the oxygen-dependent optical properties of injectable Oxyphor G2 and $mitoPO_2$ using the oxygen-dependent optical properties of ALA-enhanced PpIX. In this paper we describe in detail the setup and the applicability of this technique for simultaneous measurements of $\mu PO_2$ and $mitoPO_2$ in intact tissue. The lack of crossover in the detection channels is demonstrated *in vivo* in the

rat. Ultimately we provide the first simultaneous measurements of $\mu PO_2$ and $mitoPO_2$ in the rat liver *in vivo*.

## MATERIALS AND METHODS

### MEASUREMENT CONCEPT

Both Oxyphor G2 and PpIX possess a first excited triplet state ($T_1$) that reacts strongly with oxygen. Population of $T_1$ occurs upon photo excitation with light at one of the porphyrin-specific absorption bands. Energy transfer between the excited porphyrin and oxygen results in an oxygen-dependent $T_1$ lifetime. Spontaneous relaxation of the $T_1$ state to the ground state ($S_1$) produces delayed luminescence (i.e. phosphorescence or delayed fluorescence) that can be used to measure the $T_1$ lifetime (figure 1). The lifetime of the delayed luminescence is quantitatively related to the oxygen tension by the Stern-Volmer relationship:

$$PO_2 = \frac{\frac{1}{\tau} - \frac{1}{\tau_0}}{k_q} \qquad (1)$$

where $PO_2$ is the oxygen tension (in mmHg), $\tau$ is the measured decay time, $k_q$ is the quenching constant (in $mmHg^{-1}s^{-1}$) and $\tau_0$ is the lifetime at an oxygen pressure of zero.

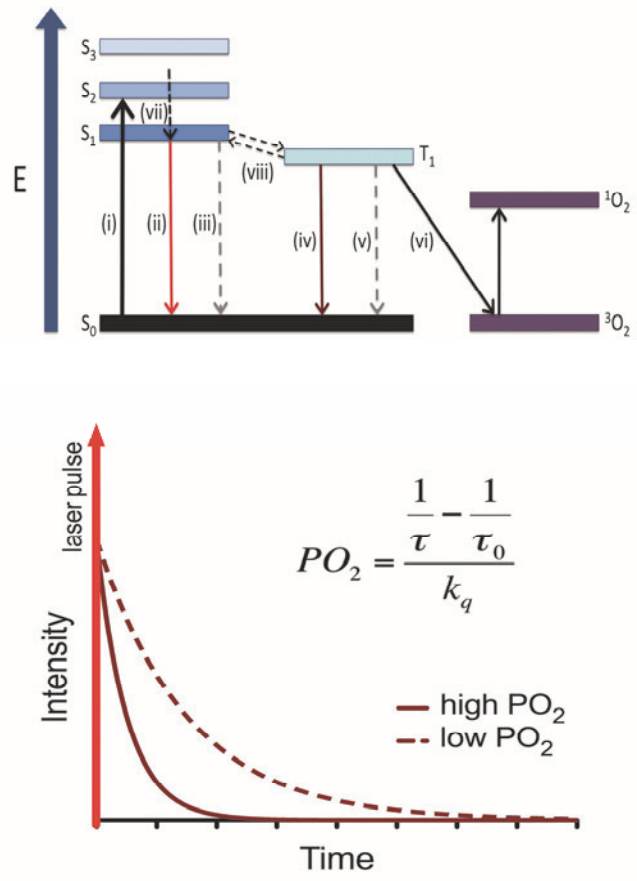


$$PO_2 = \frac{\frac{1}{\tau} - \frac{1}{\tau_0}}{k_q}$$

**Figure 1** Jablonski diagram of states and state transitions of PpIX and its interaction with oxygen (upper panel) and the principle of measuring oxygen tension ($PO_2$) by oxygen dependent quenching of delayed luminescence (lower panel). $S_0$, $S_1$, $S_2$ and $S_3$ represent the ground state and first, second and third excited singlet states, respectively. $T_1$ represent the first excited triplet states of PpIX and $^3O_2$ and $^1O_2$ are the triplet ground state and excited singlet state of oxygen. Absorption (i), fluorescence and delayed fluorescence (ii), radiationless transitions (iii and v), phosphorescence (iv), energy transfer (vi), internal conversion (vii) and bi-directional intersystem crossing (viii). The inserted equation in the lower panel is the Stern-Volmer relationship in which $PO_2$ is the oxygen tension, $\tau$ is the measured lifetime, $k_q$ is the quenching constant and $\tau_0$ is the lifetime in the absence of oxygen.

Oxyphor G2 is a water-soluble synthetic porphyrin especially developed as oxygen-sensitive phosphorescent dye. Absorption maxima of Oxyphor G2 are 440 and 632 nm and emission peaks around 800 nm. The calibration constants of Oxyphor G2 for *in vivo* conditions are $k_q$ = 270 $mmHg^{-1}s^{-1}$ and $\tau_0$ = 250 µs and the quantum efficiency of phosphorescence is approximately 12% [9]. The oxygen-dependent quenching of phosphorescence of Oxyphor G2 has been successfully used for microvascular ($\mu PO_2$) measurements [11, 13-15] and $PO_2$ measurements in macrovessels [22]. To this end, Oxyphor G2 is injected into the blood stream of experimental animals where the probe

binds to albumin and is confined to the circulation [10]. Typical *in vivo* concentrations of Oxyphor G2 for microvascular oxygen measurements are around 1 nmol/g (tissue wet weight).

Protoporphyrin IX (PpIX) is the final precursor of heme in the heme biosynthetic pathway. PpIX is synthesized in the mitochondria [23] and administration of its precursor 5-aminolevulinic acid (ALA) to cells and organisms substantially enhances PpIX concentration [24]. Since the conversion of PpIX to heme is a rate-limiting step, administration of ALA causes accumulation of PpIX in the mitochondria [19]. Besides the absorption maximum around 420 nm the absorption spectrum of PpIX contains several smaller peaks including one around 634 nm (figure 2). The fluorescence spectrum is typically two-peaked. Because of the spectral overlap with the excitation pulse only the peak around 690 nm is used for delayed fluorescence detection. The oxygen-dependent delayed fluorescence of PpIX has been successfully introduced as a technique for mitochondrial oxygen measurements [16, 18, 19]. The calibration constants of PpIX for *in vivo* conditions are $k_q$ = 830 $mmHg^{-1}s^{-1}$ and $\tau_0$ = 0.8 ms. ALA-induced PpIX levels have been reported to be in the order of 20 nmol/g (tissue wet weight) in liver [25]

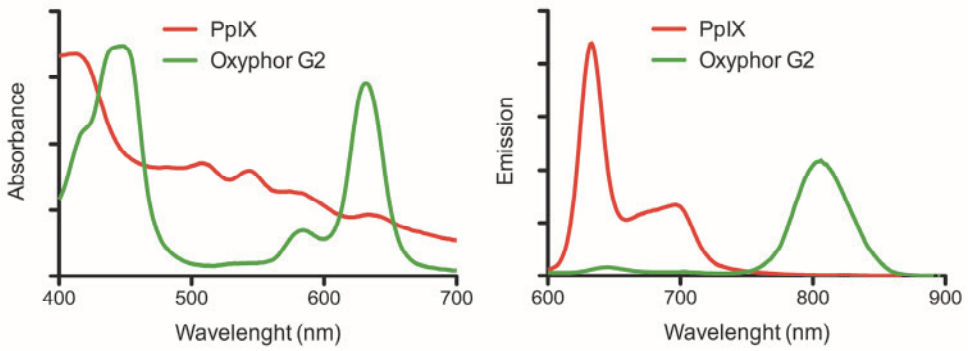


**Figure 2.** Absorption spectra (upper panel) and emission spectra (lower panel) of Oxyphor G2 and PpIX.

Both Oxyphor G2 and PpIX can be effectively excited with red light at a wavelength around 632 nm. This allows simultaneous excitation within a single measurement volume. The emission peaks are well separated without spectral overlap. Therefore, in principle, these spectral properties are excellently suited for simultaneous excitation and separate detection of the two phosphors. The intravascular localization of Oxyphor G2 combined with the mitochondrial localization of PpIX therefore enables simultaneous measurement of $\mu PO_2$ and $mitoPO_2$ (figure 3).

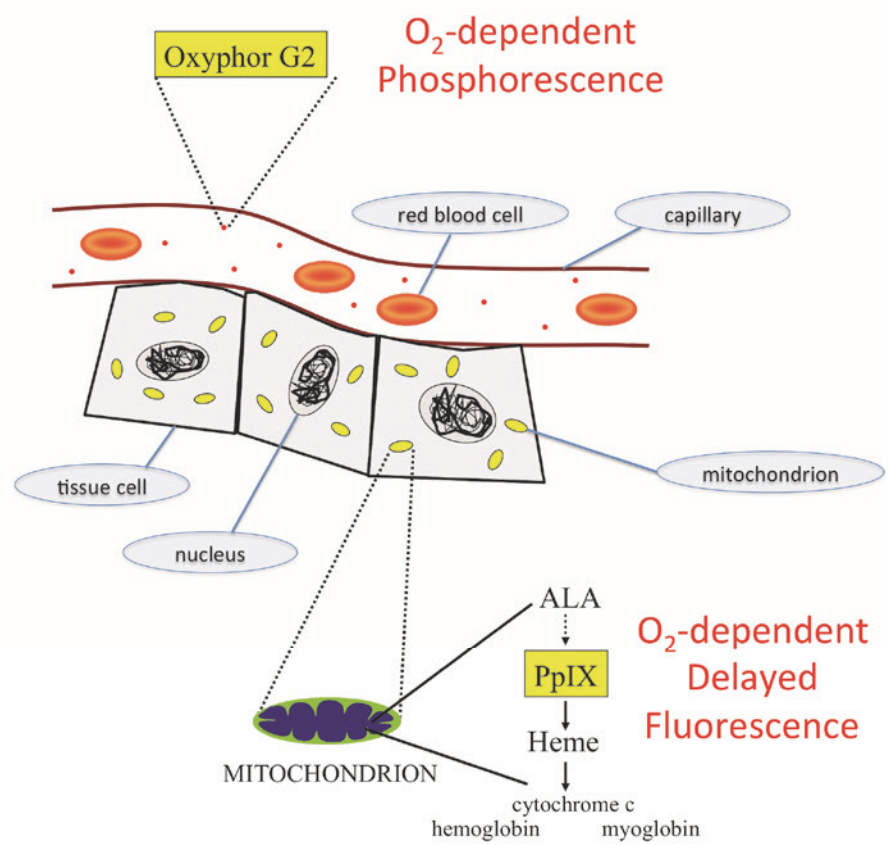


**Figure 3.** Schematic representation of the measuring concept. Oxyphor G2 is directly injected into the bloodstream and is used as microvascular oxygen probe by means of oxygen-dependent quenching of phosphorescence. PpIX is induced in the mitochondria by administration of its precursor ALA and is used as mitochondrial oxygen probe by means of oxygen-dependent quenching of delayed fluorescence.

DELAY LUMINESCENCE SETUP

A schematic drawing of the experimental setup is shown in figure 4. A compact computer-controlled tunable laser (Opolette 355-I, Opotek, Carlsbad, CA, USA), providing pulses with a specified duration of 4-10 ns and typically 2-4 mJ/pulse over the tunable range of 410 to 670 nm, was used as excitation source. The laser was coupled into a Fiber Delivery System (Opotek, Carlsbad, CA, USA) consisting of 50 mm planoconvex lens, X-Y fibermount and a 2 meter fiber with a core diameter of 1000 µm. This fiber was coupled to the excitation branch of a bifurcated reflection probe (FCR-7IR400-2-ME, Avantes b.v., Eerbeek, The Netherlands) by an In-Line Fiber Optic Attenuator (FOA-Inline, Avantes b.v., Eerbeek, The Netherlands). The light output of the excitation branch was set at 200 µJ/pulse as

measured by a FieldMate laser power meter with PowerMax PS19 measuring head (Coherent Inc., Santa Clara, CA, USA). The emission branch of the reflection probe was coupled to a bifurcated fiber assembly (Model 77533, Newport, Irvine, CA, USA), which acted as splitter for the two detection channels.

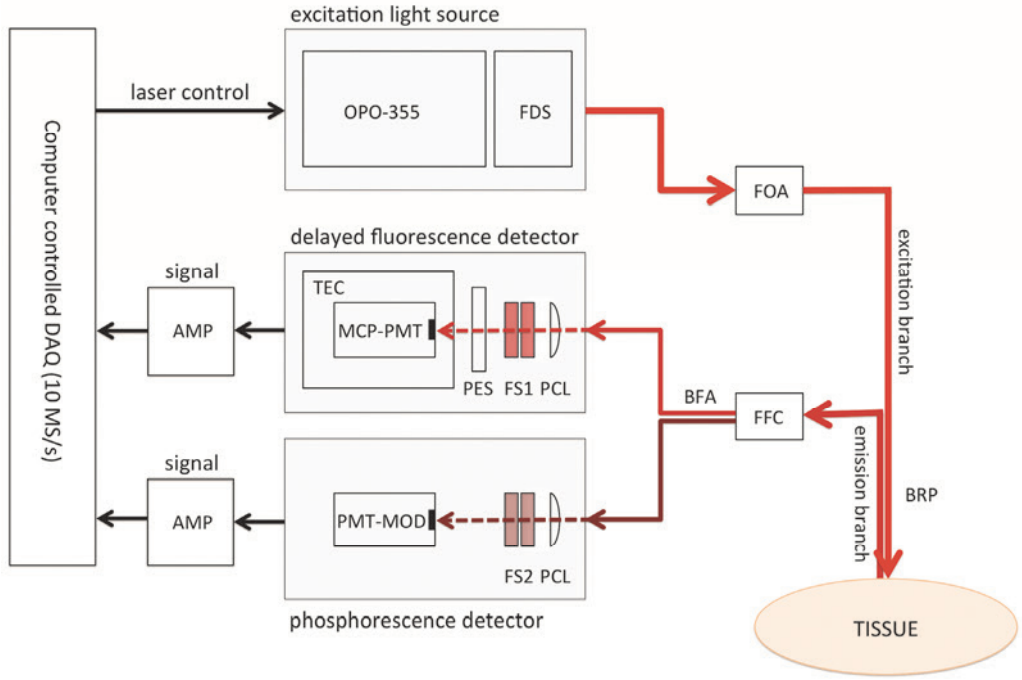


**Figure 4.** Schematic drawing of the experimental setup. OPO-355: Opolette 355-I, FDS: Fiber Delivery System, FOA: Fiber Optic Attenuator, BFP: Bifurcated Reflection Probe, FFC: Fiber to Fiber Coupling, BFA: Bifurcated Fiber Assembly, PCL: Plano Convex Lens, FS1 & FS2: Filter Sets, PES: Protective Electronic Shutter, MCP-PMT: Micro Channel Plate Photomultiplier Tube, TEC: Thermo Electric Cooling, PMT-MOD: Photomultiplier Module, AMP: Amplifier, DAQ: Data Acquisition.

The PpIX signal was detected by a gated microchannel plate photomultiplier tube (MCP-PMT R5916U series, Hamamatsu Photonics, Hamamatsu, Japan). The MCP-PMT was custom adapted with an enhanced red-sensitive photocathode having a quantum efficiency of 24% at 650 nm. The MCP-PMT was mounted on a gated socket assembly (E3059-501, Hamamatsu Photonics, Hamamatsu, Japan) and cooled to –30 °C by a thermoelectric cooler (C10373, Hamamatsu Photonics, Hamamatsu, Japan). The MCP-PMT was operated at a voltage in the range of 2300V-3000V by a regulated high-voltage DC power supply (C4848-02, Hamamatsu Photonics, Hamamatsu, Japan). One branch of the bifurcated fiber (splitter) was fit into an Oriel Fiber Bundle Focusing Assembly (Model 77799, Newport, Irvine, CA, USA) which was coupled to the MCP-PMT by an in-house built optics consisting of a filter-holder, a plano convex lens (BK-7, OptoSigma, Santa Ana, CA,

USA) with focal length of 90 mm and an electronic shutter (04 UTS 203, Melles Griot, Albuquerque, NM, USA). The shutter was controlled by an OEM Shutter Controller Board (59 OSC 205, Melles Griot, Albuquerque, NM, USA) and served as protection for the PMT, which was configured for the "normally on" mode. The PpIX emission light was filtered by a combination of a 590 nm longpass filter (OG590, Newport, Irvine, CA, USA) and a broadband (675 ± 25 nm) bandpassfilter (Omega Optical, Brattleboro, VT, USA).

The Oxyphor G2 signal was detected by a photomultiplier module with gate function (H10304-20-NN, Hamamatsu Photonics, Hamamatsu, Japan). The second branch of the bifurcated fiber (splitter) was fit into an Oriel Fiber Bundle Focusing Assembly (Model 77799, Newport, Irvine, CA, USA) which was coupled to the PMT-module by an in-house built optics consisting of a filter-holder, a plano convex lens (BK-7, OptoSigma, Santa Ana, CA, USA) with focal length of 90 mm. The Oxyphor G2 emission light was filtered by a combination of a 715 nm longpass filter (RG715, Newport, Irvine, CA, USA) and a 790 ± 20 nm bandpassfilter (Omega Optical, Brattleboro, VT, USA).

The output currents of the photomultipliers were voltage-converted by in-house built amplifiers with an input impedance of 440 ohm, 400 times voltage amplification and a bandwidth around 20 Mhz. Data-acquisition was performed by a PC-based data-acquisition system containing a 10 MS/s simultaneous sampling data-acquisition board (NI-PCI-6115, National Instruments, Austin, TX). The amplifiers were coupled to the DAQ-board by a BNC interface (BNC-2090A, National Instruments, Austin, TX). The data-acquisition ran at a rate of 10 mega samples per second and 64 laser pulses (repetition rate 20 Hz) were averaged prior to analysis. Control of the setup and analysis of the data was performed with software written in LabView (Version 8.6, National Instruments, Austin, TX, USA).

ANALYSIS OF DELAY LUMINESCENCE

In case of non-homogeneous oxygen tension the delayed luminescence signal can in general be described by an integral over an exponential kernel:

$$y(t) = \int_0^t \exp(-\lambda t) f(\lambda) d\lambda \qquad (2)$$

where f(λ) denotes the spectrum of reciprocal lifetimes within the finite data set y(t). Mono-Exponential Analysis (MEA) in generally overestimates the average lifetime and

consequently underestimates the $PO_2$ within the sample volume [11]. A much better estimation of the average $PO_2$ and an indication of its heterogeneity can be obtained by the approach described by Golub et al. [20]. They demonstrated that the heterogeneity in oxygen pressure could be analyzed by fitting distributions of quencher concentration to the delayed luminescence data. Corresponding to their work, the fitting function for a simple rectangular distribution with a mean $PO_2$ $Q_m$ and a $PO_2$ range from $Q_m - \delta$till $Q_m + \delta$ is:

$$Y_R = \exp\left(-\left(k_0 + k_q Q_m\right)t\right) \bullet \frac{\sinh(k_q \delta t)}{k_q \delta t} \tag{3}$$

where Y(t) is the normalized delayed fluorescence data, $k_0$ is the first-order rate constant for delayed fluorescence decay in the absence of oxygen, $k_q$ is the quenching constant and $\delta$ is half the width of the rectangular distribution. In terms of quenching constants and the Stern-Volmer relationship, equation 3 can be rewritten as:

$$Y_R = \exp\left(-\left(\frac{1}{\tau_0} + k_q \left\langle PO_2 \right\rangle\right)t\right) \bullet \frac{\sinh(k_q \delta t)}{k_q \delta t} \tag{4}$$

where $<PO_2>$ is the mean $PO_2$ within the sample volume and $\tau_0$ the lifetime in the absence of oxygen. The standard deviation ($\sigma$) can be retrieved from $\delta$ by:

$$\sigma = \frac{\delta}{\sqrt{3}} \tag{5}$$

This approach was successfully used by our group in phosphorescence lifetime measurements [11]. Recently we demonstrated that the approach is also useful for delayed fluorescence lifetime measurements in the case of complex underlying lifetime distributions [17]. Analysis of the delayed luminescence signals by means of equations 3-4 is referred to as the Rectangular Distribution Method (RDM).

Analysis of the photometric signals, by means of MEA and RDM, was performed with software written in LabView (Version 8.6, National Instruments, Austin, TX, USA), using the Marquart-Levenberg non-linear fit procedure.

ANALYSIS OF INFLUENCE OF NOISE

Signal-to-noise ratio (SNR) in time domain lifetime measurements is commonly defined as the ratio of maximal signal amplitude (at the start of the decay) to the maximum signal of the noise (peak-to-peak). The negative effects of noise on the accuracy of the measurement are inversely related to the lifetime. Therefore, the presence of noise especially degrades measurement accuracy at higher $PO_2$ levels.

Because the quenching constants of PpIX and Oxyphor G2 are not the same, the effect of noise on the accuracy of $\mu PO_2$ and $mitoPO_2$ measurements differs. We analyzed the relationship between measurement accuracy, $PO_2$ and SNR of the two channels by means of computer simulations. In steps of 10 mmHg, over a $PO_2$ range of 0-300 mmHg, we simulated delayed fluorescence and phosphorescence traces. SNR was varied by adding different amounts of Poisson distributed noise to the simulated decays (SNR 5, 10, 20 and 50). The $PO_2$ was calculated back from the noisy signal by lifetime analysis. The noise-induced error was calculated as the absolute difference between simulated $PO_2$ and recovered $PO_2$. We performed 500 simulation runs per $PO_2$ step and defined the potential noise-induced error as the maximum error occurring during these 500 runs.

MEASUREMENT OF SPECTRAL PROPETIES

Absorption spectra were recorded using a Hitachi U-3000 Spectrophotometer (Hitachi High-Technologies Corporation, Tokyo, Japan). Emission spectra were recorded using a Hitachi F-4500 Fluorescence Spectrophotometer (Hitachi High-Technologies Corporation, Tokyo, Japan). Both Oxyphor G2 and PpIX were dissolved in phosphate buffered saline containing 4% bovine serum albumin (Sigma-Aldrich, St. Louis, MO, USA) to a final concentration of 10 µM. Emission spectra were recorded after deoxygenating the sample by flushing with nitrogen.

ANIMAL PREPARATION

The experimental protocol was approved by the Animal Research Committee of the ErasmusMC - University Medical Center Rotterdam. Animal care and handling were performed in accordance with the guidelines for Institutional and Animal Care and Use Committees (IACUC) and done by trained staff of the Erasmus Experimental Animal Facility.

A total of 15 male Wistar rats (Charles River, Wilmington, MA) with a bodyweight of 275-325 gram were used. Rats received either a combination of 200 mg/kg 5-aminolevulinic acid (ALA, Sigma-Aldrich, St. Louis, MO, USA) and 0.4 mg/kg Oxyphor G2 (Oxygen Enterprises, Philadelphia, PA, USA) (n = 10) or only Oxyphor G2 (n = 5). In order to ensure an optimal mitochondrial PpIX concentration, ALA was administered by intraperitoneal injection 2.5 hours before start of experimental procedures. Animals were anesthetized by an intraperitoneal injection of a mixture of Ketamine (90 mg/kg, Alfasan, Woerden, The Netherlands), Medetomidine (0.5 mg/kg, Sedator Eurovet Animal Health BV, Bladel, The Netherlands) and Atropine (0.05 mg/kg, Centrofarm Services BV, Etten-Leur, The Netherlands). A continuous intravenous infusion of Ketamine (50 mg/kg/hr) was used for maintaining anesthesia. A tracheotomy was performed prior to starting mechanical ventilation. Mechanical ventilation, using a Babylog 8000 ventilator (Dräger, Dräger Medical Netherlands BV, Zoetermeer, The Netherlands), was controlled and adjusted on end-tidal $PCO_2$ (~ 35 mmHg).

A catheter (sterilized 0.9 mm diameter polyethylene catheter) was inserted in the right jugular vein for intravenous administration of anesthetics, Oxyphor G2 and fluids (0.9% NaCl, 5 mL $kg^{-1}$ $h^{-1}$). A similar catheter was placed in the right carotid artery to monitor arterial blood pressure (MAP) using a Powerlab 8/30 data-acquisition system with LabChart Pro (ADInstruments, Bella Vista NSW, Australia). This catheter was also used for taking arterial blood gases. The animal was placed onto a heating pad and body temperature was rectally measured and kept around 37 °C.

A midline laparotomy was performed to gain access to the liver for measuring $\mu PO_2$ and $mitoPO_2$. Before infusion of Oxyphor G2, 20 minutes prior to the start of the actual oxygen measurements, signals were recorded for examination of cross talk between the channels. This was repeated after administration of Oxyphor G2. Measurements were performed in dimmed light, after assuring proper positioning of the reflection probe. ALA was dissolved in phosphate buffered saline (PBS) and adjusted to pH 7.4 prior to injection. Oxyphor G2 was dissolved in PBS (1.25 mg/ml) as stock solution.

Variations in inspired oxygen fraction ($FiO_2$) were made during the protocol at set time points by mixtures of oxygen and nitrogen. Instrumentation and Oxyphor G2 administration were performed while breathing 40% oxygen (0.4 $FiO_2$). After first measurements at 0.4 $FiO_2$, $FiO_2$ was set to 1.0 and after a stabilization period of 20 min the second measurements were performed. Then $FiO_2$ was set to 0.2 and again after a

stabilization period of 20 min the third measurements were performed. In the time control group (n = 5) $FiO_2$ was set at 0.4 during the entire experiment. At the end of the experimental protocol animals were euthanized by an overdose of Euthasol (ST Farma, Raamsdonksveer, The Netherlands).

STATISTICAL ANALYSIS

Data are expressed as mean ± standard deviation (s.d.) unless stated otherwise. Repeated-measures analysis of variance, one-way ANOVA with Bonferroni posttest, was used to analyze the effect of changes in $FiO_2$ on physiological parameters. Two-way ANOVA for repeated measurements with Bonferroni posttest was used to analyze differences between $\mu PO_2$ and $mitoPO_2$ at the various $FiO_2$ settings. $P < 0.05$ was considered significant.

**RESULTS**

In order to measure signals of different porphyrins simultaneously, it is mandatory that the readings do not mutually interfere. The wide spectral separation of the emissions of PpIX and Oxyphor G2, 690 nm and 790 nm respectively, indicate this should be possible to achieve. Indeed, as is shown in figure 5, there was no interference of the two signals. Injection of ALA induced a clear delayed fluorescence signal in the 690 nm channel, indicating buildup of mitochondrial PpIX within the liver. In contrast, ALA administration did not induce any signal in the 790 nm channel. While injection of Oxyphor G2 induced a readily measurable phosphorescence signal at 790 nm, it was not detectable in the 690 nm channel. In both channels a faint decaying signal was observed in the absence of porphyrins. This background was not oxygen-sensitive and most probably originated from the glass in the fiber optic. Overall this background accounted to less than 5% of the total signal and no background corrections were made in the signal analysis.

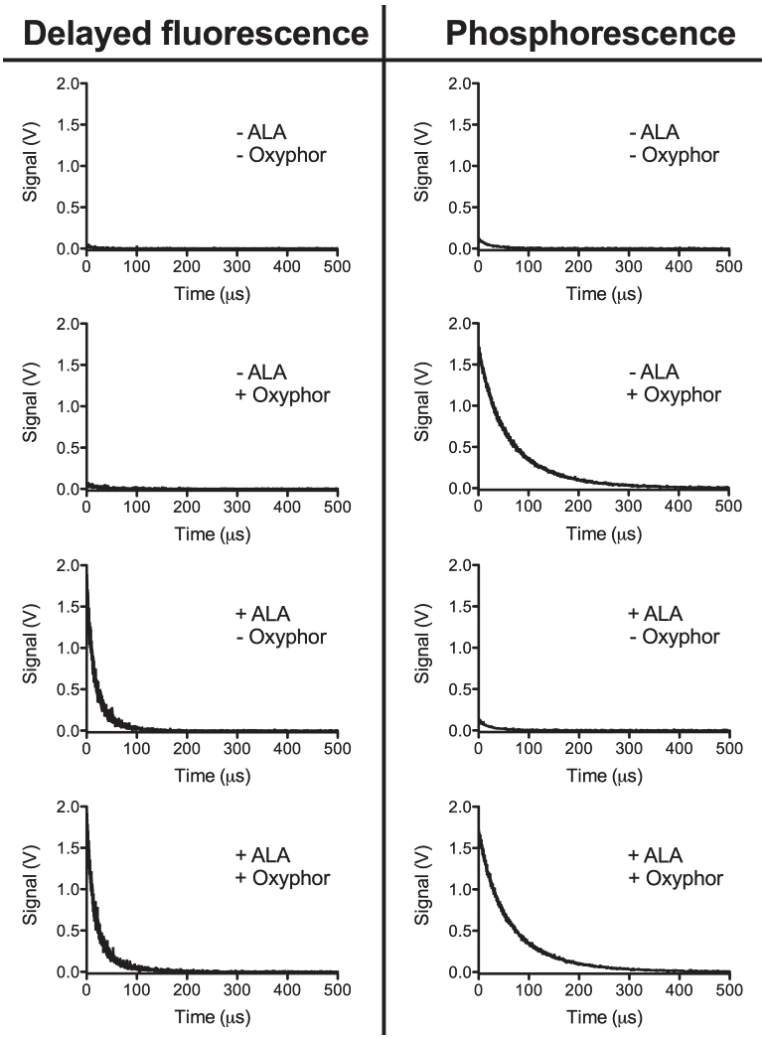


**Figure 5** Signals obtained from both channels with and without various combinations of probes. Delayed fluorescence at 690 nm and phosphorescence at 790 nm simultaneously measured after excitation at 632 nm. ALA: 200 mg/kg 5-aminolevulinic acid, Oxyphor: 0.4 mg/kg Oxyphor G2.

Noise is inevitably present in real signals and generally has a negative effect on the accuracy of measurements. Because the quenching constants for $\mu PO_2$ and $mitoPO_2$ differ, the dynamic range of measure lifetimes differs between the channels. Interpretation of simultaneous measurements could be hampered by inter channel differences in noise sensitivity. Therefore we analyzed the relationship between accuracy, $PO_2$ and SNR by means of computer simulations (figure 6). It is evident that both channels behave differently, with the delayed fluorescence measurement being more sensitive to the deleterious effects of noise. However, in practice, SNR > 20 is readily achieved for both

PpIX and Oxyphor G2. In that case, the noise-induced potential error in both channels is below 2% over a large $PO_2$ range.

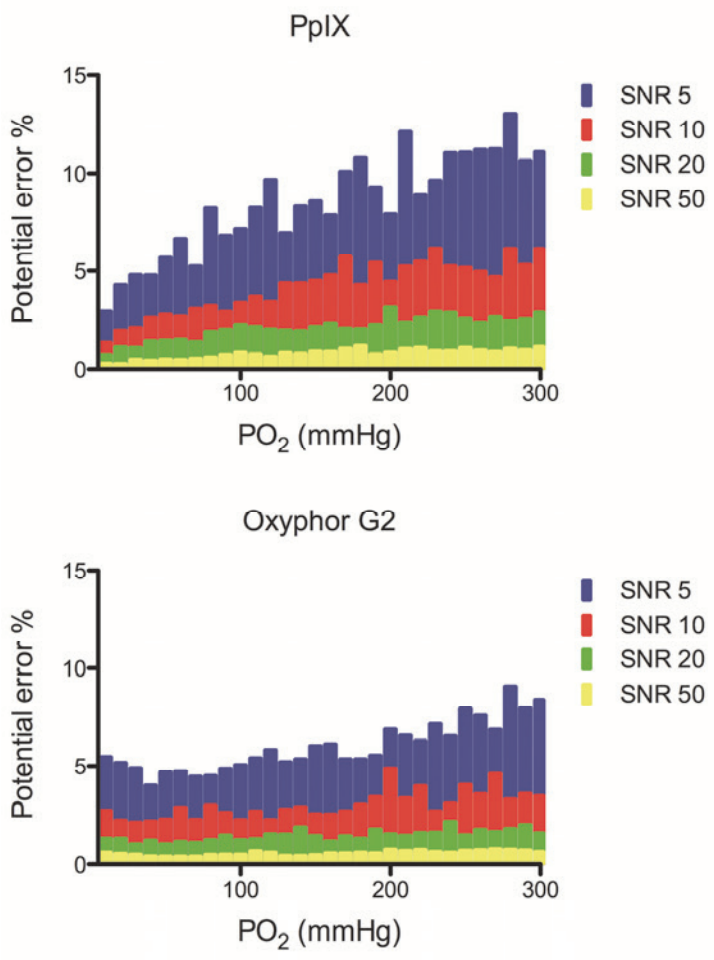


**Figure 6** Noise-induced potential error in $PO_2$ retrieval as result of the presence of noise in delayed fluorescence (upper panel) and phosphorescence (lower panel) signals. SNR: signal-to-noise ratio.

In general, the oxygen tension in tissue is non-homogeneous because of the existence of oxygen gradients as a result of oxygen consumption and diffusion. Delayed luminescence of oxygen-sensitive probes is therefore not decaying mono-exponentially but the photometric signals contain lifetime distributions. Figure 7 shows an example of a phosphorescence trace from Oxyphor G2 measured in rat liver at 0.4 $FiO_2$ (= 40% oxygen). Mono-exponential analysis (MEA) resulted in a poor fit and, compared to the rectangular distribution method (RDM), resulted in a relatively long phosphorescence lifetime. In the case of MEA the lifetime was 96.8 µs, corresponding to a $\mu PO_2$ of 23.4 mmHg. The RDM

resulted in a lifetime of 69.8 µs, corresponding to an average $\mu PO_2$ of 38.2 mmHg. The remaining small difference between data and RDM curve fit at early times reflects the fact that a rectangular distribution is only an estimation of the real oxygen distribution.

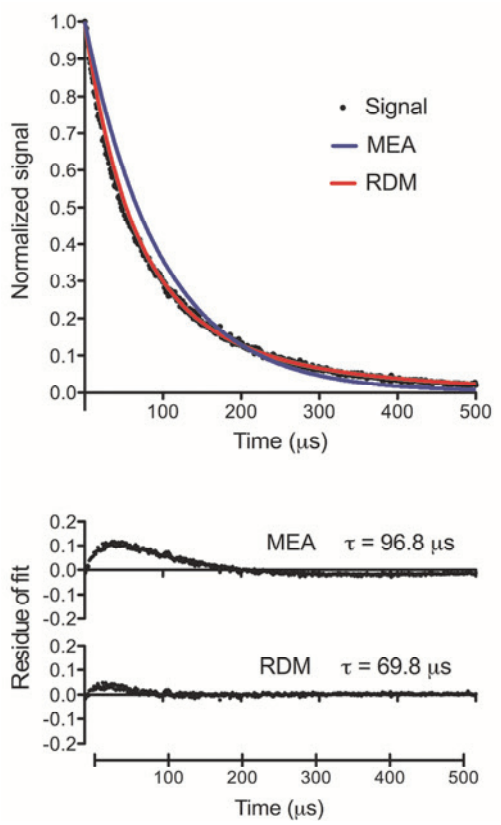


**Figure 7.** Example of two different fit procedures on a phosphorescence signal measured in *in vivo* rat liver at 0.4 $FiO_2$. Raw phosphorescence decay data and the corresponding curves of two fit procedures (upper panel). Residue of fit (difference between data and fit) for both fit procedures and the obtained phosphorescence lifetimes. MEA, mono-exponential analysis; RDM, rectangular distribution method.

An example of a simultaneous measurement of PpIX delayed fluorescence and Oxyphor G2 phosphorescence is shown in Figure 8. Both signals showed clear oxygen-sensitivity, with the lifetime becoming visually longer at a lower inspired oxygen fraction. The lifetimes of PpIX delayed fluorescence were 17.9 µs at 1.0 $FiO_2$ and 39.4 µs at 0.2 $FiO_2$, corresponding to an average mito$PO_2$ of 65.8 mmHg and 29.1 mmHg respectively. The lifetimes of Oxyphor G2 phosphorescence were 44.1 µs at 1.0 $FiO_2$ and 59.9 µs at 0.2 $FiO_2$, corresponding to an average $\mu PO_2$ of 69.2 mmHg and 47.0 mmHg respectively.

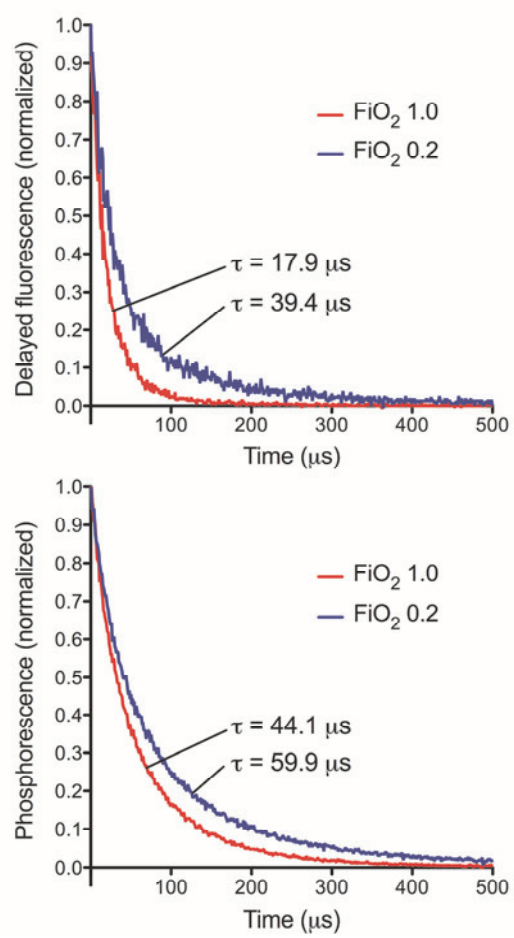


**Figure 8** Examples of delayed luminescence data measured at two different inspired oxygen fractions ($FiO_2$). Delayed fluorescence from PpIX (upper panel) and phosphorescence from Oxyphor G2 (lower panel). Lifetimes were obtained by RDM analysis.

Simultaneous measurements of liver mito$PO_2$ and µ$PO_2$ at three $FiO_2$ steps were performed in a series of 5 rats. An overview of physiological variables is given in Table 1. Arterial $PO_2$, as measured by bloodgas analysis, significantly differed between the $FiO_2$ steps, being approximately 5 times higher at 1.0 $FiO_2$ compared to 0.2 $FiO_2$. From the other variables only the MAP at 0.2 $FiO_2$ is significantly lower than MAP at 0.4 and 1.0 $FiO_2$. End-tidal $CO_2$ and temperature were actively controlled by ventilation and external heating. Heart rate and hemoglobin concentration were stable during the $FiO_2$ steps.

Figure 9 shows the results of the simultaneous measurements of mito$PO_2$ and µ$PO_2$ at various $FiO_2$ settings. Both mito$PO_2$ and µ$PO_2$ increased at higher $FiO_2$, and there were

significant differences between 0.2 $FiO_2$ and 1.0 $FiO_2$ and between 0.4 $FiO_2$ and 1.0 $FiO_2$. Furthermore, at all $FiO_2$ settings the average $mitoPO_2$ was a little lower than the average $\mu PO_2$ but only at 1.0 $FiO_2$ this difference was statistically significant. The standard deviation, as a measure of heterogeneity obtained from the RDM, was significantly higher for $\mu PO_2$ compared to $mitoPO_2$ at all $FiO_2$ settings. At 1.0 $FiO_2$ the heterogeneity in $\mu PO_2$ was significantly higher compared to the heterogeneity in $\mu PO_2$ at 0.2 $FiO_2$. In the time control group at 0.4 $FiO_2$ $\mu PO_2$ and $mitoPO_2$ and their heterogeneity were stable over time and similar to the experimental group at 0.4 $FiO_2$.

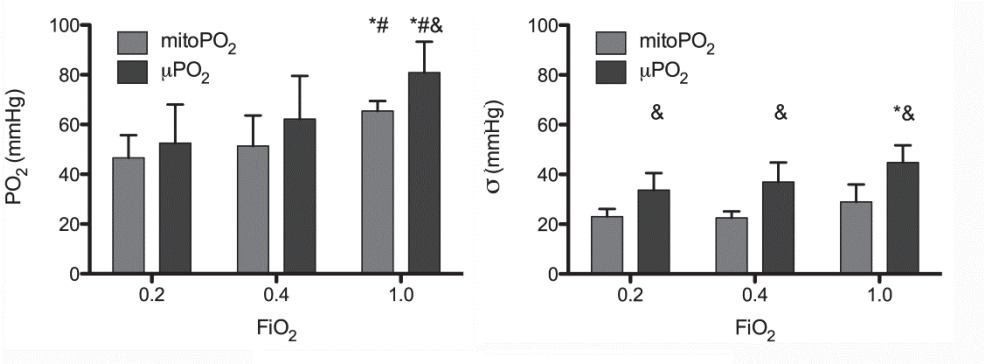


**Figure 9** Microvascular and mitochondrial $PO_2$ in rat liver at different $FiO_2$ values. Average $PO_2$ as obtained by RDM analysis (upper panel) and corresponding standard deviation (lower panel). Significantly different compared to (*) 0.2 $FiO_2$, (#) 0.4 $FiO_2$ and (&) $mitoPO_2$.

## DISCUSSION AND CONCLUSION

In this work, we present a method to simultaneously measure oxygen tension in the mitochondria and microcirculation within intact living tissue. The method is based on a combination of oxygen-dependent quenching of delayed fluorescence of ALA-enhanced mitochondrial PpIX and oxygen-dependent quenching of phosphorescence of the exogenous dye Oxyphor G2. We comprehensively describe a time-domain based measurement system consisting of a tunable pulsed laser and two gated red-sensitive photomultipliers. The measurement equipment is fiber-based and can be easily used in (patho)physiological studies in small and large experimental animals. We demonstrate that the *in vivo* measured signals of PpIX and Oxyphor G2 do not interfere and that SNR ≥ 20 reduces noise-induced inaccuracy of both channels below 2%. Furthermore, we provide data of the first simultaneous measurements of $mitoPO_2$ and $\mu PO_2$, measured in rat liver

in vivo during ventilation with various inspired oxygen fractions. To analyze the complex photometric signals we used RDM analysis, which provides the mean and standard deviation of the $PO_2$ in the measurement volume.

Our view on tissue oxygenation has gradually changed over years with the advent of novel technology to measure oxygen in tissues. Oxygen is supplied from blood to the tissues by passive diffusion and the site for oxygen exchange is the microcirculation. Although classically the capillary network was identified as the most likely site for oxygen to leave the bloodstream, a more modern view is that oxygen has the ability to diffuse from any microvessel along a large enough oxygen gradient [26]. Surrounding the microcirculation and in between the tissue cells is the interstitial space. Recent studies in resting skeletal muscle have indicated the existence of only a small gradient between microvessels and interstitium [27, 28]. The intracellular $PO_2$ and its influence on metabolism *in vivo* remains the most difficult to measure. Measurements of intracellular $PO_2$ have mostly been indirect, e.g. via measurement of myoglobin saturation [29]. Only recently it has become possible to measure directly $PO_2$ in mitochondria of living intact tissue [18, 19].

Since mitochondria are the oxygen consuming and energy producing organelles of cells, the development of a technique to measure mito$PO_2$ removes the last hurdle in our ability to comprehensively measure tissue oxygenation. Especially in combination with microvascular $PO_2$ measurements it might be possible to gain direct insight in oxygen gradients and oxygen consumption. We previously used a combination of endogenously enhanced PpIX en Oxyphor G2 to measure, in cell suspensions, mito$PO_2$ and extracellular $PO_2$ in culture medium [16]. These measurements were performed in cuvettes with separate devices that, unfortunately, could not be integrated into a useful *in vivo* measurement system. Therefore, we developed a dedicated fiber-based setup that allows simultaneous measurement of mito$PO_2$ and $\mu PO_2$ in intact tissue using PpIX and Oxyphor G2.

In the current study we focused on the rat liver, since we have extensively evaluated the mito$PO_2$ measurements in this type of tissue [19]. The measured mito$PO_2$ values in the current study are very similar to our previously reported results. In light of the fact that intracellular $PO_2$ is generally expected to be low (several mmHg) as a result of mitochondrial oxygen consumption, we were surprised to find such high mito$PO_2$. However, mito$PO_2$ values were well in the range of reported tissue $PO_2$ values measured by micro oxygen electrodes [30]. In our current study we can directly compare our mito$PO_2$ measurements with the well-established phosphorescence lifetime technique.

This direct comparison learns that only a small difference between mito$PO_2$ and $\mu PO_2$ exists in liver. This latter is not surprising due to the anatomical structure of the liver, with very close proximity of tissue cells to blood and overall high blood supply. Furthermore, our findings fit well in the current view that tissue $PO_2$ might be much higher than classically reported with invasive techniques [31]. Indeed, a recent study using minimally invasive 19F MRI in a rat model found tissue $PO_2$ levels well above 50 mmHg in several organs including liver [32]. The standard deviation in $\mu PO_2$ obtained from the RDM analysis is larger than that for the mito$PO_2$. This is most likely due to the size of the reflection probe. The measurement volume likely contains multiple microvessels that represent heterogenous $PO_2$.

Overall, our study shows that implementation of the technique to measure simultaneously $\mu PO_2$ and mito$PO_2$ by oxygen-dependent delayed luminescence is feasible, based on a combination of exogenous Oxyphor G2 and endogenous PpIX. With ongoing evaluation of the use of the mito$PO_2$ technique in other organs and tissues it is expected that this approach will greatly contribute to further our understanding of oxygen transport and oxygen metabolism in health and disease.

**ACKNOWLEDGEMENTS**

This work was financially supported by the Young Investigator Grant 2009 (awarded to E.G.M.) from the Dutch Society of Anesthesiology. The authors thank Jacqueline Voorbeijtel and Patricia Specht for their expert biotechnical help. The authors thank dr. G.A. Koning and the Laboratory of Experimental Surgical Oncology of the ErasmusMC for help with the spectral measurements.

**CONFLICT OF INTEREST STATEMENT**

E.G.M is founder and shareholder of Photonics Healthcare B.V., a company aimed at making the delayed fluorescence lifetime technology available to a broad public. Photonics Healthcare B.V. holds the exclusive licenses to several patents regarding this technology, filed and owned by the Academic Medical Center in Amsterdam and the Erasmus Medical Center in Rotterdam, The Netherlands.

**REFERENCES**


1. Springett, R. and H.M. Swartz, *Measurements of oxygen in vivo: overview and perspectives on methods to measure oxygen within cells and tissues.* Antioxidants & redox signaling, 2007. **9**(8): p. 1295-301.
2. Lubbers, D.W. and H. Baumgartl, *Heterogeneities and profiles of oxygen pressure in brain and kidney as examples of the pO2 distribution in the living tissue.* Kidney international, 1997. **51**(2): p. 372-80.
3. Sinaasappel, M., et al., *PO2 measurements in the rat intestinal microcirculation.* The American journal of physiology, 1999. **276**(6 Pt 1): p. G1515-20.
4. Swartz, H.M. and R.B. Clarkson, *The measurement of oxygen in vivo using EPR techniques.* Physics in medicine and biology, 1998. **43**(7): p. 1957-75.
5. Swartz, H.M. and J. Dunn, *The difficulties in comparing in vivo oxygen measurements: turning the problems into virtues.* Advances in experimental medicine and biology, 2005. **566**: p. 295-301.
6. Vanderkooi, J.M., et al., *An optical method for measurement of dioxygen concentration based upon quenching of phosphorescence.* The Journal of biological chemistry, 1987. **262**(12): p. 5476-82.
7. Rozhkov, V., D. Wilson, and S. Vinogradov, *Phosphorescent Pd porphyrindendrimers: tuning core accessibility by varying the hydrophobicity of the dendritic matrix.* Macromolecules, 2002. **35**: p. 1991-1993.
8. Vinogradov, S.A., L.W. Lo, and D.F. Wilson, *Dendritic plyglutamic porphyrins: probing porphyrin protection by oxygen-dependent quenching of phosphorescence.* Chemistry - A European Journal, 1999. **5**: p. 1338-1347.
9. Dunphy, I., S.A. Vinogradov, and D.F. Wilson, *Oxyphor R2 and G2: Phosphors for measuring oxygen by oxygen-dependent quenching of phosphorescence.* Analytical Biochemistry, 2002. **310**(2): p. 191-198.
10. Poole, D.C., et al., *Measurement of muscle microvascular oxygen pressures: Compartmentalization of phosphorescent probe.* Microcirculation, 2004. **11**(4): p. 317-326.
11. Johannes, T., E.G. Mik, and C. Ince, *Dual-wavelength phosphorimetry for determination of cortical and subcortical microvascular oxygenation in rat kidney.* Journal of applied physiology, 2006. **100**(4): p. 1301-10.
12. Vinogradov, S.A., et al., *A method for measuring oxygen distributions in tissue using frequency domain phosphorometry.* Comparative biochemistry and physiology. Part A, Molecular & integrative physiology, 2002. **132**(1): p. 147-52.

13. Ziemer, L.S., et al., *Oxygen distribution in murine tumors: characterization using oxygen-dependent quenching of phosphorescence.* Journal of applied physiology, 2005. **98**(4): p. 1503-10.
14. Johannes, T., et al., *Iloprost preserves renal oxygenation and restores kidney function in endotoxemia-related acute renal failure in the rat.* Critical care medicine, 2009. **37**(4): p. 1423-32.
15. Johannes, T., et al., *Influence of fluid resuscitation on renal microvascular PO2 in a normotensive rat model of endotoxemia.* Critical care, 2006. **10**(3): p. R88.
16. Mik, E.G., et al., *Mitochondrial PO2 measured by delayed fluorescence of endogenous protoporphyrin IX.* Nature methods, 2006. **3**(11): p. 939-45.
17. Harms, F.A., et al., *Oxygen-dependent delayed fluorescence measured in skin after topical application of 5-aminolevulinic acid.* Journal of biophotonics, 2011: p. doi: 10.1002/jbio.201100040. [Epub ahead of print].
18. Mik, E.G., et al., *Mitochondrial oxygen tension within the heart.* Journal of molecular and cellular cardiology, 2009. **46**(6): p. 943-51.
19. Mik, E.G., et al., *In vivo mitochondrial oxygen tension measured by a delayed fluorescence lifetime technique.* Biophysical journal, 2008. **95**(8): p. 3977-90.
20. Golub, A.S., et al., *Analysis of phosphorescence in heterogeneous systems using distributions of quencher concentration.* Biophysical journal, 1997. **73**(1): p. 452-65.
21. Johannes, T., E.G. Mik, and C. Ince, *Nonresuscitated endotoxemia induces microcirculatory hypoxic areas in the renal cortex in the rat.* Shock, 2009. **31**(1): p. 97-103.
22. Mik, E.G., T. Johannes, and C. Ince, *Monitoring of renal venous PO2 and kidney oxygen consumption in rats by a near-infrared phosphorescence lifetime technique.* American journal of physiology. Renal physiology, 2008. **294**(3): p. F676-81.
23. Poulson, R., *The enzymic conversion of protoporphyrinogen IX to protoporphyrin IX in mammalian mitochondria.* The Journal of biological chemistry, 1976. **251**(12): p. 3730-3.
24. Fukuda, H., A. Casas, and A. Batlle, *Aminolevulinic acid: from its unique biological function to its star role in photodynamic therapy.* The international journal of biochemistry & cell biology, 2005. **37**(2): p. 272-6.
25. van den Boogert, J., et al., *5-Aminolaevulinic acid-induced protoporphyrin IX accumulation in tissues: pharmacokinetics after oral or intravenous administration.* Journal of photochemistry and photobiology. B, Biology, 1998. **44**(1): p. 29-38.

26. Pittman, R.N., *Oxygen gradients in the microcirculation.* Acta physiologica, 2011. **202**(3): p. 311-22.
27. Wilson, D.F., et al., *Measuring oxygen in living tissue: intravascular, interstitial, and "tissue" oxygen measurements.* Advances in experimental medicine and biology, 2011. **701**: p. 53-9.
28. Wilson, D.F., et al., *Oxygen pressures in the interstitial space and their relationship to those in the blood plasma in resting skeletal muscle.* Journal of applied physiology, 2006. **101**(6): p. 1648-56.
29. Mole, P.A., et al., *Myoglobin desaturation with exercise intensity in human gastrocnemius muscle.* The American journal of physiology, 1999. **277**(1 Pt 2): p. R173-80.
30. van Wagensveld, B.A., et al., *Intrahepatic tissue pO2 during continuous or intermittent vascular inflow occlusion in a pig liver resection model.* European surgical research. Europaische chirurgische Forschung. Recherches chirurgicales europeennes, 1998. **30**(1): p. 13-25.
31. Wilson, D.F., *Quantifying the role of oxygen pressure in tissue function.* American journal of physiology. Heart and circulatory physiology, 2008. **294**(1): p. H11-3.
32. Liu, S., et al., *Quantitative tissue oxygen measurement in multiple organs using (19) F MRI in a rat model.* Magnetic resonance in medicine : official journal of the Society of Magnetic Resonance in Medicine / Society of Magnetic Resonance in Medicine, 2011.

# CHAPTER 3

# *Validation of the Protoporphyrin IX - Triplet State Lifetime Technique for mitochondrial oxygen measurements in the skin*

Floor A. Harms[1], Sander I.A. Bodmer[1], Nicolaas J. H. Raat[1], Robert J. Stolker[1] and Egbert G. Mik[1,2]

1 Department of Anesthesiology, Laboratory of Experimental Anesthesiology, Erasmus MC - University Medical Center Rotterdam, Rotterdam, The Netherlands

2 Department of Intensive Care, Erasmus University Medical Center Rotterdam, 's-Gravendijkwal 230, 3015 CE Rotterdam, The Netherlands

**Short title:** Validation of mitochondrial $PO_2$ on skin.

Published in: Optics Letters, 2012. **37**(13): p. 2625-7

**ABSTRACT**

Mitochondrial oxygen tension can be measured in vivo by means of oxygen-dependent quenching of delayed fluorescence of protoporphyrin IX (PpIX). Here we demonstrate that mitochondrial $PO_2$ (mito$PO_2$) can be measured in the skin of a rat after topical application of the PpIX precursor 5- aminolevulinic acid (ALA). Calibration of mito$PO_2$ measurements was done by comparison with simultaneous measurements of the cutaneous microvascular $PO_2$ This was done under three different conditions: in normal skin tissue, in nonrespiration skin tissue due to the application of cyanide, and in anoxic skin tissue after the ventilation with 100% nitrogen. The results of this study show that it is feasible to measure the mito$PO_2$ after the topical application of ALA cream by means of the PpIX–triplet state lifetime technique.

**LETTER**

The intracellular partial oxygen pressure ($PO_2$) influences cellular functions. Not only because oxygen plays a major role in the oxidative phosphorylation [1], but also because of its regulating role in cellular growth, metabolism, and gene expression [2, 3]. Several methods have been developed and used over the years to estimate intracellular oxygenation in vivo [4]. However, each of the available methods has its limitations. They are either invasive, locally destructive, semiquantitative, indirect, measure in an unknown tissue compartment, or are not feasible for clinical use because of toxicity [5].

Recently we introduced the protoporphyrin IX-triplet state lifetime technique (PpIX-TSLT). The PpIX-TSLT overcomes part of the above-mentioned limitations, enabling oxygen measurements by means of the oxygendependent optical properties of the 5-aminolevulinic acid (ALA) induced protoporphyrin IX (PpIX) [6]. It is the first technique that allows measuring mitochondrial $PO_2$ (mito$PO_2$) in living cells, and it can be applied in vivo [7, 8]. The mitochondria are the energy producing organelles of cells that require oxygen to function, making the mitochondria the most desired place to measure oxygen. Other major advantages of PpIX-TSLT are that the technique is quantitative, leaves tissues intact, and is applicable in man [9]. Current implementations of PpIX-TSLT measure the delayed fluorescence lifetime to determine the triplet state lifetime [6-9].

Oxygen-dependent quenching of delayed fluorescence in rat and human skin has been observed after topical application of 2.5% 5-ALA cream [9]. ALA is a precursor of PpIX, and

topical administration of ALA causes accumulation of PpIX inside the mitochondria of the epidermal cells [10]. Dermal application of ALA allows convenient use of PpIX-TSLT in humans. However, in order to enable reliable cutaneous mito$PO_2$ measurements and pave the way for clinical use of PpIX-TSLT as a monitoring technique, the signal needs to be calibrated first. Calibrations of PpIX-TSLT have been performed in cultured cells [6], liver and heart [7,8]. Our aim was to validate the previously determined calibration constants for application on the skin.



Photo-excitation with a pulse of light (510 nm) results in population of the first excited triplet state ($T_1$). Quenching of $T_1$ by oxygen causes the triplet state lifetime, and therefore the delayed fluorescence lifetime, to be oxygen-dependent. The lifetime is quantitatively related to the partial oxygen pressure ($PO_2$) by the Stern–Volmer relationship:

$$PO_2 = \frac{\frac{1}{\tau} - \frac{1}{\tau_0}}{k_q} \qquad (1)$$

where $\tau$ is the measured decay time, $\tau 0$ is the decay time at an oxygen pressure of zero and $k_q$ is the quenching constant.

The Stern - Volmer equation describes the relationship between the $PO_2$ and the lifetime in case of a homogeneous oxygen distribution. Due to non- uniformities in oxygen pressure, a more reliable estimation of the oxygen pressure during *in vivo* conditions is made by the Rectangular Distribution Method (RDM) [11]:

$$Y_R = \exp\left(-\left(\frac{1}{\tau_0} + k_q \langle PO_2 \rangle\right) t\right) \cdot \frac{\sin h\left(k_q \, \delta t\right)}{k_q \, \delta t} \qquad (2)$$

where $\langle PO_2 \rangle$ is mean $PO_2$ within the sample volume and $\tau 0$ is the lifetime in the absence of oxygen.

The calibration constants of $\tau 0$ and $k_q$ have been previously determined. For liver a $\tau 0$ = 0.8 ± 0.1 ms and $k_q$ = 832 ± 25 $mmHg^{-1}s^{-1}$ was obtained [8], while for the heart a $\tau 0$ = 0.8 ms and $k_q$ = 826 ± 51 $mmHg^{-1}$ $s^{-1}$ was found [7]. These similar values suggest that the calibration constants are independent of tissue type. A calibration procedure as described for heart and liver is not applicable in skin; therefore we thought of another procedure to

validate the previously found calibration constants. To this end we simultaneously measured cutaneous mitoPO$_2$ and microvascular oxygen tension (μPO$_2$) in rats.

The μPO$_2$ measurements were based on the oxygen dependent quenching of phosphorescence of the near infrared phosphor Oxyphor G2, a water-soluble phosphorescent dye that is injected into the circulation where it binds to albumin and is confined to the circulation [12-14]. The spectral properties of Oxyphor G2 and PpIX are very favorable because of their widely separated emission band (~800 nm for Oxyphor G2 and ~690 nm for PpIX).

This property allows it to measure the mitoPO$_2$ and μPO$_2$ simultaneously, without cross talk between the two signals [15]. The used setup was essentially the same as described previously [15].

We used pulsed excitation light with a wavelength of 510 nm, and an absorption peak of PpIX. The duration of a light pulse was 4–10 ns, and the light output at the end of the measurement probe was 200 μJ/pulse. The absorption maxima of Oxyphor G2 are 440 and 632 nm. Despite the fact that Oxyphor G2 does not have an absorption peak at 510 nm, it showed adequate phosphorescence after excitation with 510 nm (Figure. 1).

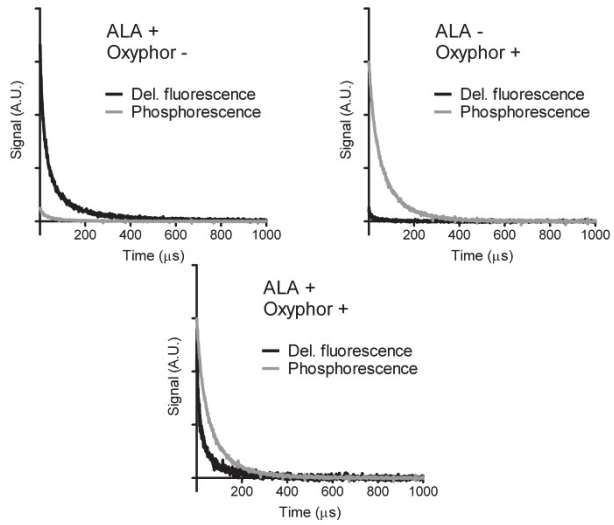


**Figure 1.** Various combination of the signals with and without oxyphor or protoporphyrin IX (PpIX). Delay fluorescence at 690 nm and phosphorescence at 790 nm simultaneously measured after excitation at 510nm.

The simultaneous oxygen measurements were performed in nine male Wistar rats. Animal handling and instrumentation were done as described in detail elsewhere [9]. The rats were anesthetized and mechanically ventilated. A mixture of hydrophilic cremor lanette (Lanettecrème I FNA, Bipharma, Weesp, The Netherlands) with 2.5% 5-ALA (Sigma-Aldrich, St. Louis, Missouri) was applied on the abdominal skin of the rat and was covered with an adhesive film (IV 3000 Smith and Nephew Medical Ltd., Hull, UK). The ALA cream was left in place for a period of three hours in order to enhance mitochondrial PpIX. Twenty minutes before the start of the measurements, 0.4 mg⁄kg Oxyphor G2 (Pdmeso-tetra-(4-carboxyphenyl)-tetrabenzoporphyrin, Oxygen Enterprises, Philadelphia, USA) was injected.

To prevent tissue contamination with atmospheric oxygen, the abdomen was covered with a gas barrier film (Parafilm "M"®, American National CanTM, Chicago, Illinois).

The first simultaneous oxygen measurements were performed in normal skin tissue, randomly at three different inspired oxygen fractions ($FiO_2$), by mixtures of oxygen and nitrogen. There was a 10-minute stabilization period between every $FiO_2$ step. During the different $FiO_2$ steps of 0.21, 0.4, and 1.0, the arterial oxygen pressure (art. $PO_2$) varied from 77 ± 3 mmHg to 191 ± 8 and 455 ± 17 mmHg, respectively. The results of the simultaneous measurements show a clear correlation between the $\mu PO_2$ and $mitoPO_2$ (Figure. 2). There was a mean oxygen gradient between the microvessels and the mitochondria ($\Delta PO_2$) of 25 ± 7.6 mmHg. A similar $PO_2$ gradient has been reported between the intravascular and interstitial compartments and is probably caused by the oxygen consumption in the mitochondria [16]. To eliminate the $\Delta PO_2$ mitochondrial respiration was blocked by the local application of 2% potassium cyanide (Sigma-Aldrich, St. Louis, Missouri) mixed with hydrophilic cremor lanette. Cyanide ions ($CN^-$) bind with high affinity to the mitochondrial cytochrome c oxidase, thereby almost irreversibly blocking its activity. As a result, the electron transport in the enzyme chain of oxidative phosphorylation and subsequently mitochondrial ATP production and oxygen can no longer be metabolized by the mitochondria [17]. Ten minutes after the local application of cyanide, the same measurements were performed in the nonrespiring tissue. The results of the measurements show a shortened lifetime in both signals that are corresponding to an increased $\mu PO_2$ and $mitoPO_2$. A delayed fluorescence lifetime <10 µs was measured during the ventilation steps with $FiO_2$ 0.4 and 1.0. Such short lifetimes are corresponding to nonphysiological high oxygen levels, and the current setup is not able to accurately calculate these lifetimes [8]. Because we are mainly interested in the physiological $PO_2$ range, we present the mean $\mu PO_2$ and $mitoPO_2$ in respiring and nonrespiring tissue during

the ventilation of a $FiO_2$ of 0.21 (Fig. 3). In contrast to respiring mitochondria, $\mu PO_2$ and $mitoPO_2$ were not significantly different in the nonrespiring mitochondria. The disappearance of a diffusion gradient between the $PO_2$ measurements is consistent with blocked mitochondrial oxygen consumption [6]. This result also indicates that the quenching constant ($k_q$) that was previously determined in heart and liver was also accurate for $mitoPO_2$ measurements in the skin.

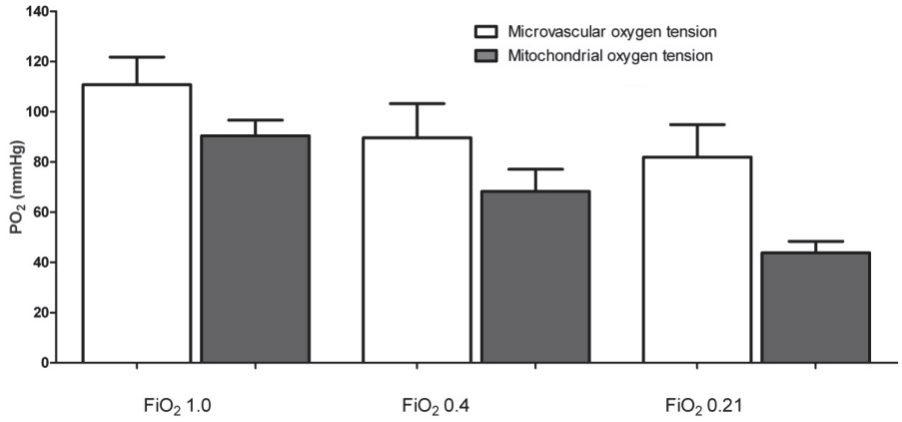


**Figure 2.** A stepwise reduction in inspired oxygen fraction ($FiO_2$) resulted in a decline in microvascular oxygen tension and mitochondrial oxygen tension. Data are presented as means ± SEM; n = 9

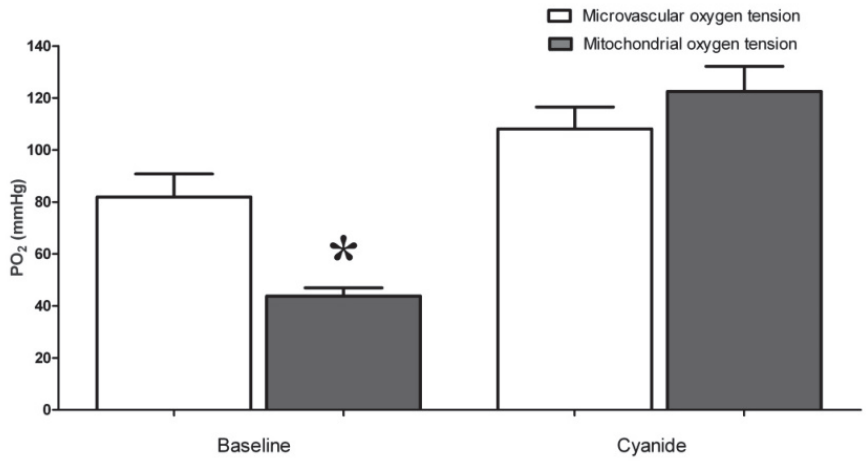


**Figure 3**. Mean oxygen tension during an inspired oxygen fraction ($FiO_2$) of 0.21 in respiring (baseline) and nonrespiring tissue (cyanide) due to the local application of cyanide. Results show a decreased gap between microvascular oxygen tension and mitochondrial oxygen tension. Data are presented as mean ± SEM; n = 9. *P < 0.05 versus mean baseline mitochondrial oxygen tension.

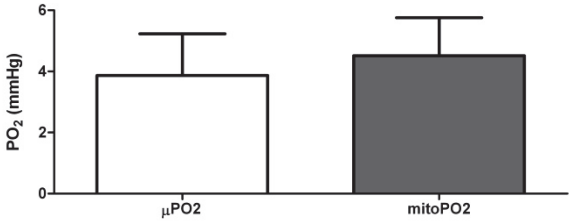


**Figure 4.** Oxygen tension ($PO_2$) in skin tissue during nitrogen ventilation. There is nonsignificant difference between microvascular oxygen tension ($\mu PO_2$) and mitochondrial oxygen tension ($mitoPO_2$). Data are presented as means ± SEM; n =4.



To test the calibration constants at the low end of the $PO_2$ range, we induced hypoxia by ventilating the rats with nitrogen for 2 min. The $\mu PO_2$ and $mitoPO_2$ dropped to 3.8 ± 1 and 4.5 ± 1 mmHg, respectively (Figure 4). This is in agreement with the tissue oxygenation that van de Laan et al. measured after nitrogen ventilation [18]. The longest delayed fluorescence lifetime measured in vivo during anoxic ventilation was 0.2 ms. However, this is not the true $\tau 0$ since we did not reach complete anoxia on the tissue level. Since the $\Delta PO_2$ between the two signals is not significantly different from zero, the previously determined $\tau 0$ appears also to be accurate for the skin.

This study presents the validation of the quenching constants for the $mitoPO_2$ measurements in the skin. The power of the technique relies on the robust lifetime technology, which allows in vivo measurement in different skin types with different optical properties without the need for recalibration. Another clear advantage of the PpIX- TSLT is that it overcomes most limitations of the existing methods for measuring tissue oxygenation. Since the technique is based on the presence of the endogenously synthesized PpIX, no tissue destruction is required and oxygen is measured at a defined and important cellular compartment, the mitochondria.

The topical application of ALA is a safe method that is widely used in the treatment of, for example, benign skin lesions [18]. In photodynamic therapy, patients do barely experience side effects related to the light dose. Only repeated measurements of the PpIX-TSLT would result in an equivalent light dose used in photodynamic therapy. For this reason we expect minimum safety issues in bringing the PpIX-TSLT technique to applications in humans.

Overall, our study shows that it is feasible to measure the $mitoPO_2$ in the skin after the topical application of ALA cream by means of the PpIX-TSLT.

The authors thank Jacqueline Voorbeijtel and Patricia Specht for their expert biotechnical help. This research is financially supported by a Life Sciences Pre-Seed Grant (grant no. 40-41300-98-9037) from the Netherlands Organization for Health Research and Development (ZonMW).

**REFERENCES**

1. Mitchell, P. and J. Moyle, *Chemiosmotic hypothesis of oxidative phosphorylation.* Nature, 1967. **213**(5072): p. 137-9.
2. Rissanen, E., H.K. Tranberg, and M. Nikinmaa, *Oxygen availability regulates metabolism and gene expression in trout hepatocyte cultures.* Am J Physiol Regul Integr Comp Physiol, 2006. **291**(5): p. R1507-15.
3. Zhou, L., et al., *Divergent effects of extracellular oxygen on the growth, morphology, and function of human skin microvascular endothelial cells.* J Cell Physiol, 2000. **182**(1): p. 134-40.
4. Springett, R. and H.M. Swartz, *Measurements of oxygen in vivo: overview and perspectives on methods to measure oxygen within cells and tissues.* Antioxid Redox Signal, 2007. **9**(8): p. 1295-301.
5. Wagner, P.D., *Muscle intracellular oxygenation during exercise: optimization for oxygen transport, metabolism, and adaptive change.* Eur J Appl Physiol, 2012. **112**(1): p. 1-8.
6. Mik, E.G., et al., *Mitochondrial PO2 measured by delayed fluorescence of endogenous protoporphyrin IX.* Nat Methods, 2006. **3**(11): p. 939-45.
7. Mik, E.G., et al., *Mitochondrial oxygen tension within the heart.* J Mol Cell Cardiol, 2009. **46**(6): p. 943-51.
8. Mik, E.G., et al., *In vivo mitochondrial oxygen tension measured by a delayed fluorescence lifetime technique.* Biophys J, 2008. **95**(8): p. 3977-90.
9. Harms, F.A., et al., *Oxygen-dependent delayed fluorescence measured in skin after topical application of 5-aminolevulinic acid.* J Biophotonics, 2011. **4**(10): p. 731-9.
10. de Bruijn, H.S., et al., *Microscopic localisation of protoporphyrin IX in normal mouse skin after topical application of 5-aminolevulinic acid or methyl 5-aminolevulinate.* J Photochem Photobiol B, 2008. **92**(2): p. 91-7.
11. Golub, A.S., et al., *Analysis of phosphorescence in heterogeneous systems using distributions of quencher concentration.* Biophys J, 1997. **73**(1): p. 452-65.

12. Bodmer, S.I., et al., *Microvascular and mitochondrial PO(2) simultaneously measured by oxygen-dependent delayed luminescence.* J Biophotonics, 2012. **5**(2): p. 140-51.
13. Dunphy, I., S.A. Vinogradov, and D.F. Wilson, *Oxyphor R2 and G2: phosphors for measuring oxygen by oxygen-dependent quenching of phosphorescence.* Anal Biochem, 2002. **310**(2): p. 191-8.
14. Johannes, T., E.G. Mik, and C. Ince, *Dual-wavelength phosphorimetry for determination of cortical and subcortical microvascular oxygenation in rat kidney.* J Appl Physiol (1985), 2006. **100**(4): p. 1301-10.
15. Wilson, D.F., et al., *Measuring oxygen in living tissue: intravascular, interstitial, and "tissue" oxygen measurements.* Adv Exp Med Biol, 2011. **701**: p. 53-9.
16. Clausen, T., et al., *Induced mitochondrial failure in the feline brain: implications for understanding acute post-traumatic metabolic events.* Brain Res, 2001. **908**(1): p. 35-48.
17. van der Laan, L., et al., *NADH videofluorimetry to monitor the energy state of skeletal muscle in vivo.* J Surg Res, 1998. **74**(2): p. 155-60.
18. Ibbotson, S.H., *Adverse effects of topical photodynamic therapy.* Photodermatol Photoimmunol Photomed, 2011. **27**(3): p. 116-30.

# CHAPTER 4

# Cutaneous respirometry by dynamic measurement of mitochondrial oxygen tension for monitoring mitochondrial function *in vivo*

Floor A. Harms[1], Wilhelmina J. Voorbeijtel[1], Sander I.A. Bodmer[1], Nicolaas J.H. Raat[1], Egbert G. Mik[1,2]

1 Department of Anesthesiology, Laboratory of Experimental Anesthesiology, Erasmus MC – University Medical Center Rotterdam, 's-Gravendijkwal 230, 3015 CE Rotterdam, The Netherlands

2 Department of Intensive Care, Erasmus MC – University Medical Center Rotterdam, 's-Gravendijkwal 230, 3015 CE Rotterdam, The Netherlands

**Short title:** Cutaneous respirometry for monitoring mitochondrial function *in vivo*

Published in: Mitochondrion, 2013. 13(5): p. 507-14

**ABSTRACT**

Progress in diagnosis and treatment of mitochondrial dysfunction in chronic and acute disease could greatly benefit from techniques for monitoring of mitochondrial function *in vivo*. In this study we demonstrate the feasibility of *in vivo* respirometry in skin. Mitochondrial oxygen measurements by means of oxygen-dependent delayed fluorescence of protoporphyrin IX are shown to provide a robust basis for measurement of local oxygen disappearance rate (ODR). The fundamental principles behind the technology are described, togheter with an analysis method for retrievel of respirometry data. The feasibility and reproducibility of this clinically useful approach are demonstrated in a series of rats.

**INTRODUCTION**

Mitochondrial dysfunction has been associated with the aging process [1] and a variety of human disorders, such as cardiovascular [2] and neurodegenerative diseases [3, 4]. Mitochondrial dysfunction has also been recognized as an important factor in acute critical illness, like sepsis and septic shock [5-8]. Over recent years, mitochondria have become an interesting target for drug therapy, and the research field aimed at “Targeting Mitochondria” is active and expanding [9]. However, because of the central role of mitochondria in energy metabolism and cellular survival, pharmacological intervention on the mitochondrial level might prove to have serious side effects. Such side effects will potentially result in a small therapeutic window for future drugs. Therefore, the ability to monitor mitochondrial function for diagnosis, treatment effects, and the occurrence of side effects in patients might be of great benefit. For these reasons, there is real need for the development of methods for monitoring *in vivo* mitochondrial function at the bedside.

Most of the available methods to assess the respiratory chain of the mitochondria *in vivo* are based on semi-quantitative measurements of mitochondrial NADH, FAD or the redox state of cytochrome oxidase. For example, the optical properties of NADH allow assessment of *in vivo* mitochondrial redox state by means of NADH fluorescence [10-12]. A drawback of *in vivo* NADH fluorimetry is that the fluorescence signal not only depends on the redox state but is also affected by other factors, like hemoglobin levels, leading to artifacts [13]. Another widely used method is near infrared spectroscopy (NIRS). NIRS enables continuous monitoring of variations in hemoglobin oxygenation and in the redox

state of cytochrome c oxidase. Unfortunately, recovery of the cytochrome oxidase signal from NIRS data remains controversial [14]. Like the problems with NADH fluorimetry, NIRS is influenced by tissue-specific effects, such as the wavelength dependence of the optical path length and changes in light scattering [15, 16].

Alternatively, measuring the local oxygen disappearance rate (ODR) gives insight into the metabolic activity of oxidative phosphorylation, as proposed by Davies and Grendell in 1962 [17]. The ODR was measured by the decrease in tissue $PO_2$, with respect to time following cessation of blood flow. The local ODR is a function of several factors including oxygen supply from oxyhemoglobin trapped in the capillaries, metabolic consumption and diffusivity parameters. Until the late 80's a lot of studies using ODR were done [18-20], but finally the further development of the ODR-based oxygen consumption measurements stopped due to technical limitations [21]. These limitations were imposed by the use of oxygen electrodes. These electrodes cause local tissue destruction, consume oxygen, and have a relatively slow response time [18].



The progress in techniques to measure tissue $PO_2$ opened the opportunity for new developments in the ODR measurements [21]. An excellent example of this is an optical technique based on oxygen-dependent quenching of phosphorescence, originally developed by Vanderkooi and Wilson in the late 1980s [22]. This technique relies on the injection of metallo-porphyrin dyes in experimental animals. It allows for the measurement of $PO_2$ in the microcirculation or interstitium, depending on the site of injection [23-25]. The $PO_2$ can be calculated from the phosphorescence decay kinetics and, once calibrated, phosphorescence lifetime measurements do not require recalibration [26]. Recently, Golub et al. used this optical method for measuring local tissue $VO_2$, in microscope-based respirometry in spinotrapezium muscle [21].

As an alternative to the use of injectable exogenous oxygen-sensitive dyes, the Protoporphyrin IX - Triplet State Lifetime Technique (PpIX-TSLT) [27] was introduced. PpIX-TSLT enables oxygen measurements by means of the oxygen-dependent optical properties of protoporphyrin IX. Application of 5-aminolevulinic acid (ALA) leads to mitochondrial accumulation of endogenously synthesized protoporphyrin IX. PpIX-TSLT is the first technique that allows measurements of the mitochondrial $PO_2$ (mito$PO_2$) in living cells. Importantly, it can be applied *in vivo* [28-30] and, because the technology relies on lifetime instead of intensity measurements, it is insensitive to changes in tissue optical properties.

PpIX-TSLT can be effectively used after topical application of ALA, for example in skin [28]. The technique can be applied in man, and the use of PpIX-TSLT for measuring mitochondrial ODR has been proposed as a potential clinical monitoring technique for mitochondrial function [31]. Combining steady-state mito$PO_2$ measurements with the principles of ODR measurements can provide useful information about the mitochondrial oxygenation, oxygen consumption and oxygen affinity of the mitochondrial respiratory chain. In this study, we explore the possibility of mitochondrial oxygen consumption measurements in skin using the PpIX-TSLT technique. We describe the fundamental principles behind the technology and a working implementation of the technique for ODR measurements. Furthermore, we provide a method for analysis of delayed-fluorescence-based ODR data and demonstrate the feasibility and reproducibility of our method in rats.

## METHODS

### PRINCIPLE OF MITO$PO_2$ MEASUREMENTS

The background of the PpIX-TSLT is described in detail elsewhere [27, 30]. In short, PpIX is the final precursor of heme in the heme biosynthetic pathway. PpIX is synthesized in the mitochondria, and administration of ALA substantially enhances the PpIX concentration (Figure 1A). Since the conversion of PpIX to heme is a rate-limiting step, administration of ALA causes accumulation of PpIX inside the mitochondria. PpIX possesses a triplet state that reacts strongly with oxygen, making its lifetime oxygen-dependent. Population of the first excited triplet state occurs upon photo-excitation with a pulse of light, and causes the emission of red delayed fluorescence. The delayed fluorescence lifetime is related to mito$PO_2$ (Figure 1B) according to the Stern- Volmer equation:

$$mitoPO_2 = \left(1/\tau - 1/\tau_0\right)/k_q \qquad (1)$$

in which $\tau$ is the measured delayed fluorescence lifetime, $k_q$ is the quenching constant and $\tau_0$ is the lifetime at zero oxygen. In case of a non-homogenous oxygen distribution inside the measurement volume, a reliable estimation of the average $PO_2$ can be made by the Rectangular Distribution Method (RDM) [32, 33].

$$Y(t) = Y_0 \exp\left[-\left(1/\tau_0 + k_q\left\langle mitoPO_2\right\rangle\right)t\right]\sinh\left(k_q \delta t\right)/k_q \delta t \qquad (2)$$

where Y(t) is the delayed fluorescence signal, t is the time from the beginning of the delayed fluorescence decay, $Y_0$ is the initial signal intensity at t = 0, <mitoPO$_2$> is the average mitochondrial oxygen tension and ? is the half-width of the $PO_2$ distribution.

Calibrations of PpIX-TSLT have been performed in cultured cells [27], rat liver [30] and rat heart [29]. *In vivo* values for the quenching constants have been found to be $k_q$ = 830 $mmHg^{-1}s^{-1}$ and $\tau_0$ = 0.8 ms. In a previous study we demonstrated that administration of 2.5% ALA cream induces oxygen-dependent delayed fluorescence in skin [28]. Recently, the quenching constants were validated for such use of PpIX-TSLT in skin tissue [34], which is the basis of the PpIX-TSLT implementation in this study.



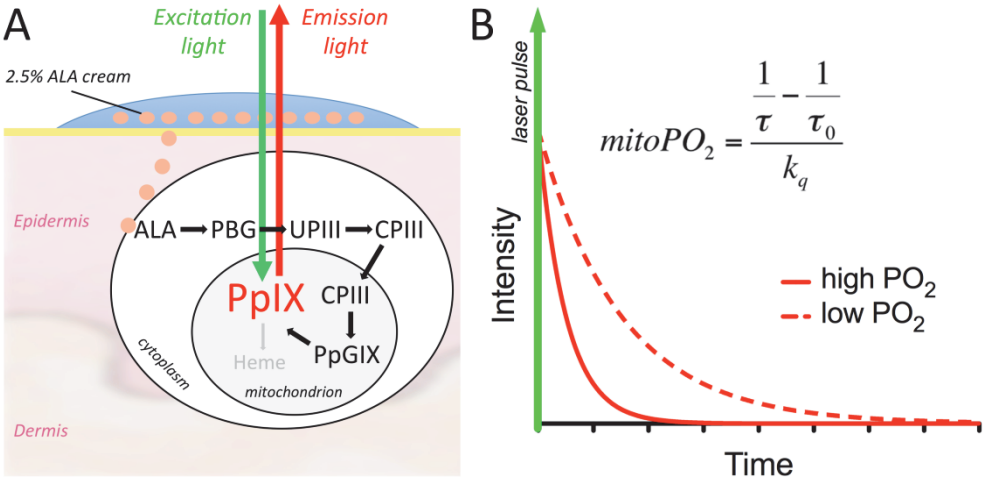


**Figure 1.** Background of the Protoporphyrin IX - Triplet State Lifetime Technique. Panel A shows the principle by which ALA administration enhances mitochondrial PpIX levels. Panel B shows the principle of measuring mitochondrial $PO_2$ by means of oxygen-dependent delayed fluorescence of PpIX, using pulsed excitation with green (510 nm) light. The delayed fluorescence lifetime is oxygen-dependent according to the Stern-Volmer equation, in which $k_q$ is the quenching constant and $\tau_0$ is the lifetime at zero oxygen. ALA, 5-aminolevulinic acid; PBG, porphobilinogen; UPIII, urporphyrinogen III; CPIII, coporporphyrinogen III; PpGIX, protoporphyrinogen IX and PpIX, protoporphyrin IX.

DELAY LUMINESCENCE SETUP

A compact computer-controlled tunable laser (Opolette 355-I, Opotek, Carlsbad, CA, USA), providing pulses with a specified duration of 4–10 ns and typically 2–4 mJ/pulse over the tunable range of 410 to 670 nm, was used as excitation source. The laser was coupled into a Fiber Delivery System (Opotek, Carlsbad, CA, USA) consisting of 50 mm planoconvex lens, X–Y fibermount and a 2 m fiber with a core diameter of 1000 µm. This fiber was

coupled to a custom made reflection probe by an In-Line Fiber Optic Attenuator (FOA-Inline, Avantes b.v., Eerbeek, The Netherlands). The reflection probe consisted of two 1000 µm fibers with a length of 2 m (P1000-2-VIS-NIR, Ocean Optics, Dunedin, FL, USA) mounted at the common end into a stainless steel holder with a separation of 1 mm between the fibers. The common end of the reflection probe consisted of an aluminium rod with a length of 5 cm and a diameter of 10 mm. The light output of the excitation branch was measured by a FieldMate laser power meter with PowerMax PS19 measuring head (Coherent Inc., Santa Clara, CA, USA). The PpIX signal was detected by a gated microchannel plate photomultiplier tube (MCP-PMT R5916U series, Hamamatsu Photonics, Hamamatsu, Japan).

The MCP-PMT was custom adapted with an enhanced red-sensitive photocathode having a quantum efficiency of 24% at 650 nm. The MCP-PMT was mounted on a gated socket assembly (E3059-501, Hamamatsu Photonics, Hamamatsu, Japan) and cooled to -30$^{o}$C by a thermoelectric cooler (C10373, Hamamatsu Photonics, Hamamatsu, Japan). The MCP-PMT was operated at a voltage in the range of 2000–2700V by a regulated high-voltage DC power supply (C4848-02, Hamamatsu Photonics, Hamamatsu, Japan). The emission branch of the reflection probe was fit into an Oriel Fiber Bundle Focusing Assembly (Model 77799, Newport, Irvine, CA, USA) which was coupled to the MCP-PMT by an in-house built optics consisting of a filter-holder, a plano convex lens (BK-7, OptoSigma, Santa Ana, CA, USA) with focal length of 90 mm and an electronic shutter (04 UTS 203, Melles Griot, Albuquerque, NM, USA). The shutter was controlled by an OEM Shutter Controller Board (59 OSC 205, Melles Griot, Albuquerque, NM, USA) and served as protection for the PMT, which was configured for the “normally on” mode. The PpIX emission light was filtered by a combination of a 590 nm longpass filter (OG590, Newport, Irvine, CA, USA) and a broadband (675 -25 nm) bandpassfilter (Omega Optical, Brattleboro, VT, USA).

The output current of the photomultiplier was voltage-converted by an in-house built amplifier with an input impedance of 440 ohm, 400 times voltage amplification and a bandwidth around 20 Mhz. Data-acquisition was performed by a PC-based data acquisition system containing a 10 MS/s simultaneous sampling data-acquisition board (NI-PCI-6115, National Instruments, Austin, TX). The amplifier was coupled to the DAQ-board by a BNC interface (BNC-2090A, National Instruments, Austin, TX). The data-acquisition ran at a rate of 10 mega samples per second. Control of the setup was performed with software written in LabView (Version 8.6, National Instruments, Austin, TX, USA).

PRINCIPLE OF OXYEN DISAPPEARANCE RATE MEASUREMENTS

Oxygen-dependent delayed fluorescence was induced in skin at the measurement site by local administration of 2.5% ALA cream [28]. Above the measurement site, the reflection probe was mounted on a height adjustable construction providing different settings of the probe distances to the skin. Local occlusion of the microcirculation in the skin was obtained by local pressure with the measurement probe. This simple procedure reliably created stop-flow conditions and induced measurable oxygen disappearance due to cessation of microvascular oxygen supply and ongoing cellular oxygen consumption. Mito$PO_2$ was measured before and during application of pressure at an interval of 1Hz and using 1 laser pulse per measurement. The principle of ODR measurements is shown in Figure 2.



The mito$PO_2$, in the following analysis simply denoted as $PO_2$, inside a measurement volume $V_m$ reflects the balance between oxygen consumption inside $V_m$ and oxygen inflow into $V_m$. Total oxygen consumption consists of tissue oxygen consumption and the additional oxygen consumption induced by the measuring procedure. Under conditions of normal blood flow and steady state oxygen supply-demand, $PO_2$ is constant and oxygen inflow is dependent on microcirculatory oxygen delivery. During no-flow conditions, induced by application of external pressure on $V_m$, microcirculatory oxygen delivery is halted and $PO_2$ inside $V_m$ will drop due to oxygen consumption. Because of gradually increasing $PO_2$ difference between $V_m$ and the surrounding tissue, oxygen starts to diffuse into $V_m$. The rate of $PO_2$ change within $V_m$ during stop-flow is therefore described by:

$$dPO_2(t)/dt = -VO_2(t) - OCM(t) + DOI(t) \quad (3)$$

where $dPO_2(t)/dt$ is the rate of oxygen disappearance at a certain time point t, $VO_2(t)$ is the tissue oxygen consumption, $OCM(t)$ is the Oxygen Consumption by the Measurement and $DOI(t)$ is the Diffusive Oxygen Influx into $V_m$.

$VO_2(t)$ is oxygen-dependent and, according to Michaelis-Menten kinetics, can be described as:

$$VO_2(t) = \left(V_{max} \cdot PO_2(t)\right) \Big/ \left(P_{50} + PO_2(t)\right) \quad (4)$$

where $V_{max}$ is the not supply-dependent maximal tissue oxygen consumption and $P_{50}$ is the $PO_2$ at which cellular oxygen consumption is reduced to 1/2 $V_{max}$. $PO_2(t)$ denotes the $PO_2$ in the measurement volume at time point t.

Oxygen influx into $V_m$ from the surrounding tissue, $DOI(t)$, is proportional to the $PO_2$ difference ($\Delta PO_2$) between $V_m$ and its boundaries. Assuming the surrounding tissue remains at the initial $PO_2$ value $PO_2(t_0)$ and $PO_2(t)$ in the measurement volume decreases, $DOI(t)$ can be written as:

$$DOI(t) = Z\left(\Delta PO_2(t)\right) = Z\left(PO_2(t_0) - PO_2(t)\right) \quad (5)$$

where Z is the inflow coefficient, $\Delta PO_2(t)$ is the $PO_2$ difference between measurement volume and surrounding tissue, $PO_2(t_0)$ is the initial oxygen tension. Substitution of equations 4 and 5 in equation 3 yields:

$$dPO_2(t)/dt = \left(V_{\max} \cdot PO_2(t)\right)/\left(P_{50} + PO_2(t)\right) - OCM(t) - Z\left(PO_2(t_0) - PO_2\right) \quad (6)$$

Since the autoconsumption by the method is occurring per flash [35], $OCM(t)$ is actually not a continuous but a discrete function. Let $P_n$ denote the measured $PO_2$ after flash number $n$, then the autoconsumption can be written as [21]:

$$OCM(P_n) = KP_n \quad (7)$$

where $K$ is the so called autoconsumption coefficient. Substitution of equation 5 in the discrete form of equation 4 and adopting the notation previously used by Golub et al. [21] yields:

$$dP_n/d_n = -\left(V_{\max} \cdot P_n\right)/\left(P_{50} + P_n\right) - KP_n + Z(P_0 - P_n) \quad (8)$$

In this equation, $P_n$ is the measured $PO_2$ after excitation flash number $n$, $P_0$ is the mean $PO_2$ before stop-flow and $dP_n/dn$ is the rate of oxygen disappearance. In non-respiring tissue $P_n$ can be explicitly written as:

$$Pn = \left(P_0 / \left(K + Z\right)\right)\left[Z + K\exp(-(K+Z)n)\right] \quad (9)$$

Using equation 9 as fitting model for ODC recorded in non-respiring tissue allows estimation of factors *Z* and *K*.

The autoconsumption coefficient *K* depends on the concentration of PpIX in $V_m$ and the excitation energy [35]. The overall effect of OCM on the retrieved parameters from ODC data also depends on the excitation frequency and total number of flashed needed to record adequate data. If the experimental setting allows minimizing excitation energy and frequency to such extend that OCM is negligible over the timecourse of a measurement the autoconsumption part can be omitted from the analysis. Furthermore, if $P_0 >> P_{50}$ the initial slope of the ODC is a direct measurement of $V_{max}$. Under these circumstances $P_{50}$ and *Z* can be retrieved from experimental ODC by fitting the following equation:

$$dP_n / d_n = -\left(V_0 \cdot P_n\right) / \left(P_{50} + P_n\right) + Z\left(P_0 - P_n\right) \quad (10)$$

where $mitoVO_2$ is the slope of the ODC determined from the linear part of the curve directly after the beginning of tissue compression.

SIGNAL PROCESSING AND DATA ANALYSIS

Signal processing was performed with custom-made software written in LabView (Version 8.6, National Instruments, Austin, TX, USA). Delayed fluorescence lifetimes were retrieved from photometric signals by RDM analysis according to equation 2, using the Marquart-Levenberg non-linear fit procedure standard available in LabView. Oxygen disappearance curves were analyzed by fitting equations 9 or 10 to the data using a numerical approach. A Runge-Kutta representation of the equations was fitted on ODCs by constrained nonlinear optimization using sequential quadratic programming standard available in LabView.

Data are expressed as mean ± standard error (SE) unless stated otherwise. Data analysis and data presentation were performed with GraphPad Prism (Version 5, GraphPad Software Inc., San Diego, CA, USA).

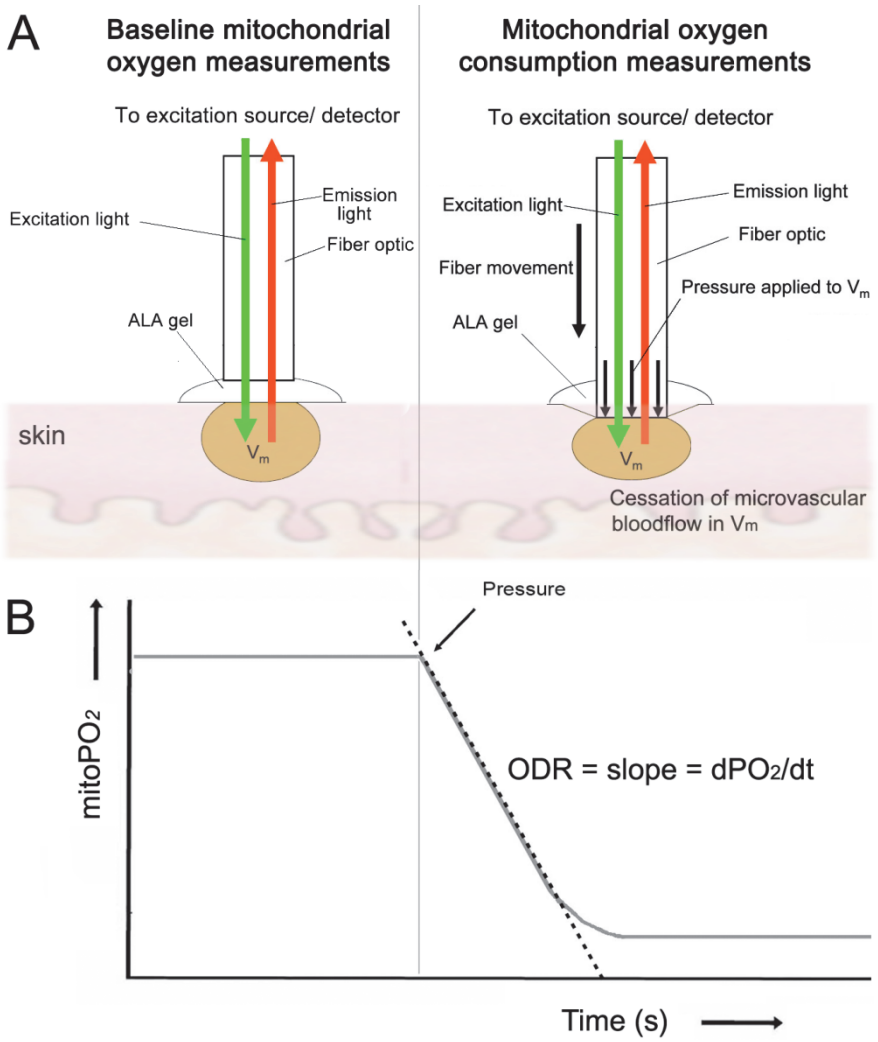


**Figure 2.** Principles of respirometry in skin by PpIX-TSLT. Panel A shows schematically the baseline mitoPO$_2$ measurement and the principle of respirometry by pressure-induced cessation of microvascular blood flow. Panel B shows the theoretical time-course of mitoPO$_2$ during an ODR measurement.

ANIMAL PREPARATION

The protocol was approved by the Animal Research Committee of the Erasmus MC - University Medical Center Rotterdam. Animal care and handling were performed in accordance with the guidelines for Institutional and Animal Care and Use Committees.

A total of 11 male Wistar rats (Charles River, Wilmington, MA, USA, body weight 280-350 g) were used in this study. The animals were anesthetized by an intraperitoneal injection of a mixture of ketamine 90 mg kg$^{-1}$ (Alfasan, Woerden, The Netherlands), medetomidine

0.5 mg $kg^{-1}$ (Sedator Eurovet Animal Health BV, Bladel, The Netherlands), and atropine 0.05 mg $kg^{-1}$ (Centrofarm Services BV, Etten-Leur, The Netherlands).

Mechanical ventilation was performed via tracheotomy. Ventilation was adjusted on end-tidal $PCO_2$, keeping the arterial $PCO_2$ between 35 and 45 mmHg. A polyethylene catheter (PE50, outer diameter 0.9 mm) was inserted into the right jugular vein for intravenous administration of fluids. Arterial blood pressure and heart rate were monitored with a similar catheter in the left femoral artery. Every hour analysis of arterial blood gas was done and cardiac output was measured by thermodilution with the thermistor inserted in the right carotid artery. Ketamine (50 mg $kg^{-1}$ $h^{-1}$) and crystalloid solution (Ringer lactate, 5 mL $kg^{-1}h^{1}$) were infused intravenously for maintaining anaesthesia and fluid balance. Body temperature was rectally measured and kept at 38 ± 0.5 °C by means of a heating pad.



EXPERIMENTAL PROCEDURES

PpIX concentration was enhanced by topical application of 2.5% ALA cream. A mixture of hydrophilic cremor lanette (Lanettecreme I FNA, Bipharma, Weesp, The Netherlands) and 2.5% 5-aminolevulinic acid (Sigma-Aldrich, St. Louis, MO, USA) was prepared just before use and administered topically on the abdominal skin after hair removal. The latter was accomplished by shaving and use of hair removal cream (Veet, Reckitt Benckiser Co., Slough, UK). The exposed skin was covered with an adhesive film (IV 3000 Smith and Nephew Medical Ltd., Hull, UK) to avoid oxygen diffusion from surrounding air. To prevent premature exposure of PpIX to light, the area was covered with aluminium foil. In three hours sufficient PpIX was converted to start the mito$PO_2$ measurements.

The ODR measurements were performed in 8 rats by repeated mito$PO_2$ measurements (one flash every second), recorded 10 seconds before, during, and 20 seconds after an 80 seconds compression period. Compression was induced by local pressure with the measurement probe, blocking the oxygen supply by a temporary occlusion of the microvessels. After flow arrest in the microvessels, the mito$PO_2$ drops due to oxygen consumption in the mitochondria. The mitochondrial $dPO_2/dt$ was analyzed according to section 2.3.

In a separate group of rats (n=3), ODR was determined in non-respiring skin tissue. The latter was accomplished by the mitochondrial blocker 2% potassium cyanide (Sigma-Aldrich, St. Louis, MO, USA) mixed in a hydrophilic cremor lanette. The potassium cyanide cream was locally applied at the abdominal skin of the rats for a period of ten minutes.

The pilot experiment in human skin was voluntarily performed on the sternum of the principal investigator (E.G.M.). A small aliquot of 2.5% ALA-cream was topically applied under adhesive foil and protected from light for 3 hours prior to start of measurement.

**RESULTS**

Topical application of ALA to the abdominal skin of rats induced readily detectable delayed fluorescence signals, of which the lifetime kinetics could be analyzed according to equation 2 (Figure 3A). Baseline mitoPO$_2$ values were typically around 60 mmHg and application of pressure to the skin instantaneously caused prolonging of the delayed fluorescence lifetime. The latter indicated disappearance of mitochondrial oxygen due to cessation of oxygen supply and ongoing oxygen consumption. Release of pressure was accompanied by instantaneous rise in mitochondrial oxygen levels. MitoPO$_2$ after pressure release typically showed a transient overshoot compared to baseline values, likely due to a local hyperemic response (Figure 3B). Eventually mitoPO$_2$ restored to baseline and repeated measurements at 15 minutes intervals at the same spot gave reproducible results over a prolonged time period, arguing against occurrence of cellular or mitochondrial damage due to pressure and irradiation.

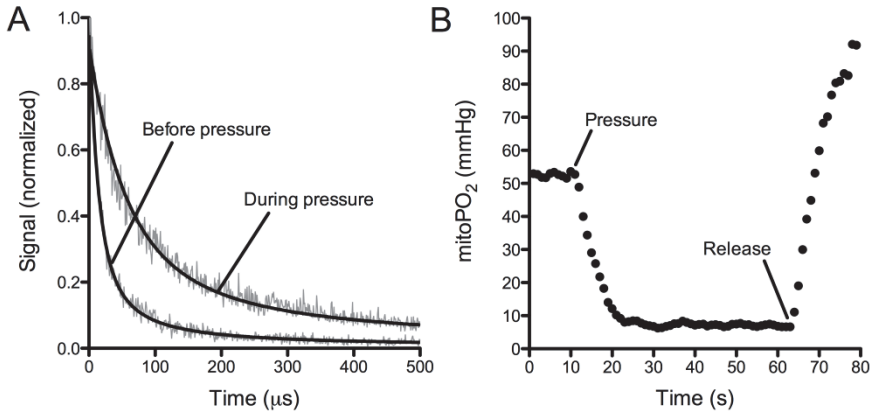


**Figure 3.** Panel A shows examples of delayed fluorescence signals and corresponding RDM analysis (solid lines), before application of pressure with the measuring probe (t = 16.6 μs) and just before release of pressure (t = 93.4 μs). Panel B shows a typical example of an ODR experiment in the abdominal skin of a rat.

As explained in section 2.3, ODR is not only determined by cellular oxygen consumption, but can also be influenced by the autoconsumption (OCM) of the PpIX-TSLT (K) and the

oxygen inflow from the surrounding tissue (Z). The OCM is caused by a well-known phenomenon, called photoconsumption [36]. Due to this phenomenon every excitation pulse consumes a small part of the dissolved oxygen, which potentially can results in a significant overestimation of cellular oxygen consumption [21]. We tested whether OCM would significantly influence ODR in our experimental situation, using an excitation energy of 250 µJ/pulse and a repetition frequency of 1 Hz. Figure 4A shows ODR measurements in non-respiring tissue after topical application of cyanide. No oxygen disappearance due to photoconsumption was measurable at relatively high mitoPO$_2$ induced by blockage of oxygen consumption. OCM is oxygen-dependent according to equation 7, making its potential effects even less in real ODR measurements. These results indicated that ODR curves measured with our setup, using the tested pulse energy and measurement frequency, could be analyzed without explicitly taking OCM into account.



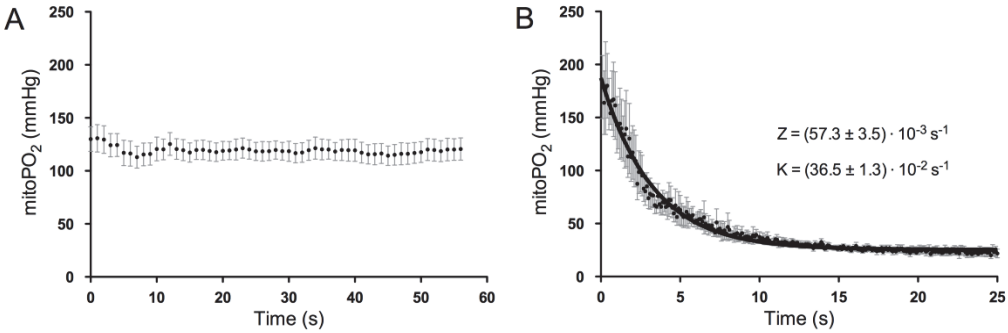


**Figure 4.** Panel A shows the time-course of mitoPO$_2$ during measurements in non-respiring skin tissue using standard experimental settings (n = 3). Panel B shows effects of OCM, measured in non-respiring skin tissue using excessive excitation (n = 3). The solid line is the fit according to equation 9.

To determine the potential effects of Diffusive Oxygen Influx (DOI) in our measurements, we estimated inflow coefficient Z using the approach of Golub et al. [21]. Again, ODR measurements were performed in non-respiring tissue. However, in order to induce significant OCM, excessive excitation was used and the excitation frequency was increased 10-fold to 10 Hz. Due to the increased amount of excitation light, OCM was detectable and the time-course of mitoPO$_2$ is shown in figure 4B. Under the described experimental conditions, Z was determined to be $(57.3 \pm 3.5)\cdot 10^{-3}$ s$^{-1}$ by fitting of equation 9 to the obtained ODC.

While OCM is a factor that can, to a certain extent, be controlled and minimized by choosing appropriate experimental conditions, DOI depends on the interaction between the measuring probe and the tissue. Since skin composition depends on anatomical location and is not the same for all individuals, Z is likely to fluctuate considerably. Instead

of using a fixed value for Z, fitting of Z on ODCs as extra parameter could take such fluctuations into account. Determining $mitoVO_2$ directly from the initial slope of the ODC (Figure 5A) reduced the number of unknown parameters in the fitting procedure (equation 10) to 3. Figure 5B shows an example of fitting equation 10 to an ODC. Values of $mitoPO_2$, $P_{50}$ and Z were determined by the fitting procedure, $mitoVO_2$ and $P_{eq}$ were determined separately. $P_{eq}$ is the steady-state $mitoPO_2$ at which cellular oxygen consumption and diffusive oxygen influx are in equilibrium. The value of Z (0.059 $s^{-1}$) retrieved from this ODC obtained in respiring tissue was in excellent agreement with the value of Z measured in non-respiring tissue.

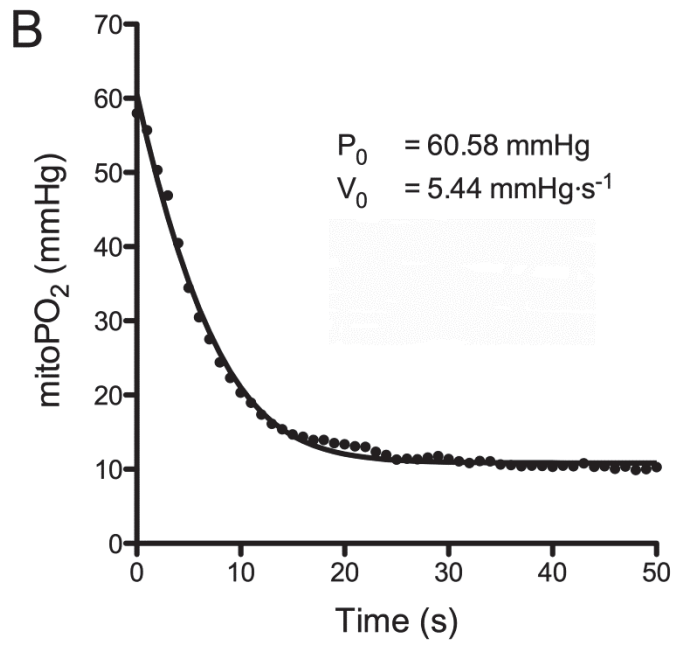


**Figure 5**. Typical example of in vivo respirometry. $mitoVO_2$ was determined from the linear part of the ODC at the start of tissue compression (Panel A). Peq is the steady state mitoPO2 at which oxygen consumption is balanced by diffusive oxygen inflow. Panel B demonstrates application of the Michaelis-Menten-based fitting model according to equation 10. $P_0 = mitoPO_2$, $v_0 = mitoVO_2$

We performed experiments in a series of 8 rats in order to test the feasibility and reproducibility of our method and gain insight in the means and variances of parameters $mitoPO_2$, $mitoVO_2$, $P_{50}$ and Z. Table 1 shows the values for macro hemodynamic parameters and provides measured blood gas values. All rats were hemodynamically stable, well ventilated with 40% oxygen and showed no signs of systemic hypoperfusion as witnessed by a low serum lactate level. Mitochondrial $PO_2$ measurements and in vivo

respirometry could be performed in all animals without technical difficulties. A total of 24 ODC were measured, at four different regions on the abdominal skin. Figure 6 gives an impression of the inter- and intra-animal variability of mito$VO_2$ and $P_{50}$. Shown are the results of the 4 abdominal measurements in the individual animals. The complete respirometry data are shown in Table 2. These data show that in vivo respirometry by PpIX-TSLT is feasible and provides reproducible results with low variance in all assessed parameters.

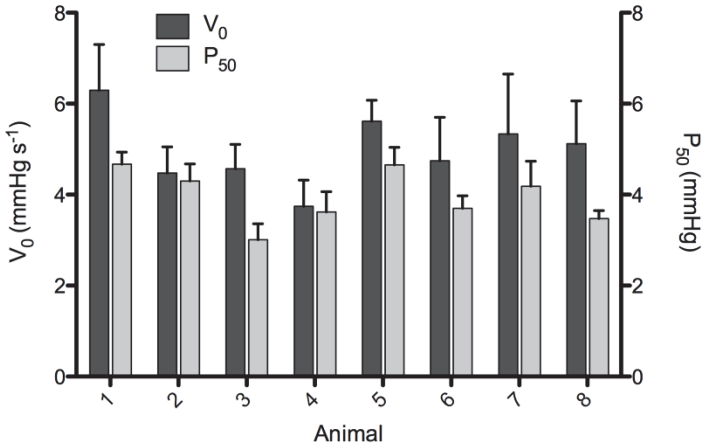


**Figure 6**. Average mito$VO_2$ and P50 obtained by in vivo respirometry in four distinct locations in the abdominal skin of 8 individual rats. $V_0$ = mito$VO_2$

| Parameter | Mean ± SE (8) |
|---|---|
| CO (ml/min) | 158 ± 33 |
| MAP (mmHg) | 77 ± 6 |
| HR (bpm) | 243 ± 11 |
| Lactate (mmol/L) | 1.06 ± 0.10 |
| pH | 7.32 ± 0.02 |
| $aPO_2$ (mmHg) | 196 ± 11 |
| $aPCO_2$ (mmHg) | 39.8 ± 2.5 |

Values are means ± SE (number of animals)

**Table 1.** Systemic parameters of the experimental animals. CO, cardiac output; MAP, mean arterial pressure; HR, heart rate; $aPO_2$, arterial $PO_2$; $aPCO_2$, arterial $PCO_2$.

| Parameter | Mean ± SE (8) |
|---|---|
| $P_0$ (mmHg) | 59.4 ± 1.4 |
| $V_0$ (mmHg $s^{-1}$) | 4.99 ± 0.27 |
| $P_{50}$ (mmHg) | 3.95 ± 0.21 |
| Z ($s^{-1}$) | 0.099 ± 0.008 |

Values are means ± SE (number of animals)

**Table 2.** Average parameters obtained by *in vivo* respirometry in rat abdominal skin.
$P_0$ = mitoPO$_2$ $V_0$ = mitoVO$_2$.

Since our ultimate goal is to develop a method for bedside monitoring of mitochondrial function in patients, we performed a pilot experiment in human skin to demonstrate that our technique can be extended to use in man. Oxygen-dependent delayed fluorescence was readily detectable 3 hours after ALA administration. Figure 7 shows an ODC measured in skin overlying the sternum of the volunteer.

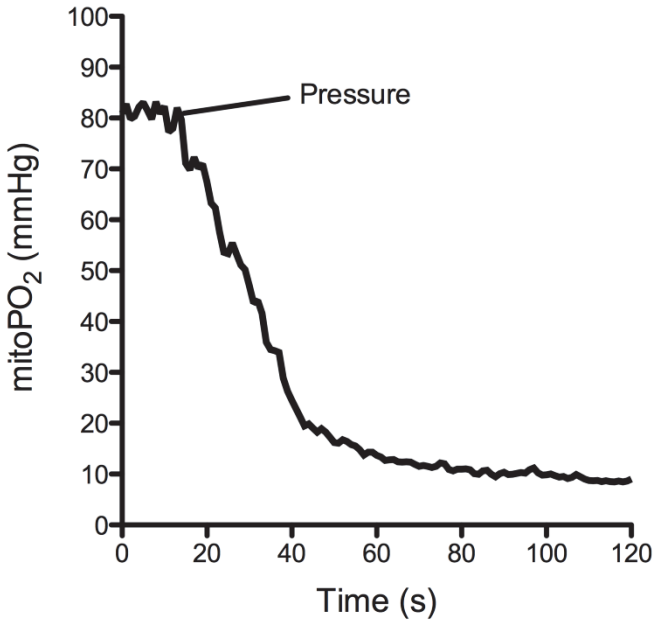


**Figure 7.** Pilot experiment on the sternum of a volunteer, 3 hours after topical administration of ALA-cream.

## DISCUSSION

In this work, we present a novel approach for measuring local tissue oxygen consumption in skin. It is based on a combination of an optical technique for measuring mito$PO_2$ with a non-invasive and robust method for measuring ODR. Mito$PO_2$ is measured by means of PpIX-TSLT in a small tissue volume. This tissue volume is small enough to allow cessation of microvascular blood flow by application of local pressure with the measuring probe. Dynamic measurement of changes in mito$PO_2$ enables recording of ODC and subsequent analysis allows recovery of parameters Mito$PO_2$, mito$VO_2$, $P_{50}$ and Z. Interestingly, oxygen consumption was completely abolished by application of cyanide, indicating that the method allows mitochondrial respirometry *in vivo*. The used implementation of PpIX-TSLT is based on topical application of ALA-cream to the skin and can be used in man. This paves the way for development of a clinical technique for monitoring mitochondrial respiration.



In current clinical practice oxygen consumption can be measured by Fick's principle, combining data on the regional blood flow and arterial-venous oxygen content difference [37]. Fick's principle can be applied to either the whole body, in which the blood flow represents cardiac output, or to an individual organ, in which organ blood flow is used. The measurement of cardiac output and organ flow and the methodology to determined blood $O_2$ contents can be subject to larger measurement errors what can implicate significant measurement errors [38, 39]. Therefore, the obtained data are not a reliable representation of mitochondrial respiration and Fick's principle is not often used for clinical decision-making.

A more direct and local approach was developed in the 70's and 80' and was based on the disappearance of oxygen during macrohemodynamic cessation of blood flow, for example used in brain cortex [40, 41]. Unfortunately, these early implementations of ODR measurements had both conceptual and technical limitations. For example, occlusion of large blood vessels or cardiac arrest causes pooling of blood in the tissue, which makes measurements highly dependent on hemoglobin content in the tissue. Independence of hemoglobin-bound oxygen could only be achieved by perfusion with hemoglobin free solutions or by keeping the tissue oxygen levels well above 100 mmHg [18, 20, 42]. In contrast, creating stop-flow conditions by applying local pressure to tissue, as used in our approach, causes extrusion of blood from the microvessels in the measurement volume [21], reducing the influence of hemoglobin on the ODC. Another drawback of the classical method was caused by the use of microelectrodes, which causes technical limitations, like

local tissue damage, movement artifacts and oxygen consumption by the tip of the electrode. Recent attempts using the old principles of macrohemodynamic occlusion have been made using modern technology like near-infrared spectroscopy [43] and oxygen-sensitive optodes [44]. While nowadays the technical limitations of oxygen electrodes can be largely overcome, pooling of blood and the interference of hemoglobin-bound oxygen remains a problem.

Using local microvascular occlusion, as an alternative to total body circulatory arrest or occlusion of large blood vessels, is a way to solve the problem of blood pooling. This was recently demonstrated by microscope-based respirometry in muscle [21], combining a topically applied oxygen-sensitive phosphorescent dye with arrest of microvascular blood flow by local pressure on the tissue. Unfortunately, due to reliance on an exogenously administered metallo-porphyrin dye, this approach is not applicable in man. In our current study, we demonstrate that PpIX-TSLT, for measuring mitochondrial oxygen tension *in vivo*, can be combined with the principles of the local ODR technique. In principle, this new embodiment of ODR measurements enables the development of tools to clinically monitor parameters of mitochondrial function, like mitochondrial oxygenation and oxygen consumption. Using a Michaelis-Menten-based model, taking into account the influence of diffusive oxygen influx, we were able to measure parameters mito$PO_2$, mito$VO_2$ and $P_{50}$ with good reproducibility.
The value for mito$VO_2$ in rat skin is comparable to the result previously reported for resting skeletal muscle [21], being 4.99 ± 0.27 mmHg/s and 3.37 ± 0.35 mmHg $s^{-1}$ respectively. It is important to recognize that these values deviate an order of magnitude from results obtained by 'classical' ODR measurements, in which oxygen disappearance takes typically tens of seconds [41] to even minutes [45]. It is likely that the diminished influences of blood pooling and hemoglobin content account to these differences. The value for $P_{50}$ measured in skin is in agreement with values obtained by phosphorescence quenching in suspensions of isolated cells [46, 47]. However, these studies show that intact cells have a higher $P_{50}$ than isolated mitochondria due to diffusion limited oxygen supply. Therefore, more research is needed in order to understand the factors contributing to $P_{50}$ *in vivo* and investigate whether $P_{50}$ is a robust parameter for monitoring *in vivo* mitochondrial function.

PpIX-TSLT-based ODR in skin allows topical application of ALA and makes the technique applicable in man. Furthermore, the choice for the skin allows the measurement of cutaneous mitochondrial ODR without the influence of the initial $PO_2$. In de past, this influence has made the interpretation of ODR data as an estimation of local tissue oxygen

consumption difficult. For example, Reneau and Halsey [20], Gaab et al. [19] and more recently Nematbakhsh et al. [44] showed a correlation between the initial $PO_2$ and the $dPO_2/dt$ calculated from the ODR in brain or kidney of rats, rabbits and gerbils, suggesting that the oxygen supply is regulated by the metabolic demand. This regulation of the oxygen consumption is a well know phenomenon in tissues like brain, heart, skeletal muscle and liver, with the skin being a notable exception [48].

## CONCLUSION

Our results show the feasibility of cutaneous respirometry by a combination of PpIX-TSLT and local tissue compression. Enabling measurement of the oxygen disappearance rate in skin at the level of the mitochondria, the technique is quantitative, robust and provides information about mitochondrial parameters like $mitoPO_2$, $mitoVO_2$ and $P_{50}$. We expect that clinical implementation of the method will greatly contribute to our understanding of mitochondrial function and oxygen metabolism in health and disease. For example, this technique could be useful for evaluation of dermal drugs, guiding of systemic mitochondrial therapy and monitoring of mitochondrial function in critically ill patients.



## ACKNOWLEDGEMENTS

This work was financially supported by a Life Sciences Pre-Seed Grant (grant no 40-41300-98-9037) from the Netherlands Organization for Health Research and Development (ZonMW).

## CONFLICT OF INTEREST STATEMENT

Dr. E.G. Mik is founder and shareholder of Photonics Healthcare B.V., a company aimed at making the delayed fluorescence lifetime technology available to a broad public. Photonics Healthcare B.V. holds the exclusive licenses to several patents regarding this technology, filed and owned by the Academic Medical Center in Amsterdam and the Erasmus Medical Center in Rotterdam, The Netherlands.

**REFERENCES**


1. Navarro, A. and A. Boveris, *The mitochondrial energy transduction system and the aging process.* Am J Physiol Cell Physiol, 2007. **292**(2): p. C670-86.
2. Ballinger, S.W., *Mitochondrial dysfunction in cardiovascular disease.* Free Radic Biol Med, 2005. **38**(10): p. 1278-95.
3. Schapira, A.H. and M. Gegg, *Mitochondrial contribution to Parkinson's disease pathogenesis.* Parkinsons Dis, 2011. **2011**: p. 159160.
4. Schmitt, K., et al., *Insights into mitochondrial dysfunction: aging, amyloid-beta, and tau-A deleterious trio.* Antioxid Redox Signal, 2012. **16**(12): p. 1456-66.
5. Brealey, D., et al., *Mitochondrial dysfunction in a long-term rodent model of sepsis and organ failure.* American Journal of Physiology - Regulatory Integrative and Comparative Physiology, 2004. **286**(3 55-3): p. R491-R497.
6. Fink, M.P., *Cytopathic hypoxia. Is oxygen use impaired in sepsis as a result of an acquired intrinsic derangement in cellular respiration?* Crit Care Clin, 2002. **18**(1): p. 165-75.
7. Galley, H.F., *Oxidative stress and mitochondrial dysfunction in sepsis.* British Journal of Anaesthesia, 2011. **107**(1): p. 57-64.
8. Gellerich, F.N., et al., *Impaired energy metabolism in hearts of septic baboons: Diminished activities of complex I and complex II of the mitochondrial respiratory chain.* Shock, 1999. **11**(5): p. 336-341.
9. . in *ISANH Conferences*. 2011. Berlin: 2nd World Congress on Targeting Mitochondria.
10. Chance, B., et al., *Basic principles of tissue oxygen determination from mitochondrial signals.* Adv Exp Med Biol, 1973. **37A**: p. 277-92.
11. Ince, C., J.M. Coremans, and H.A. Bruining, *In vivo NADH fluorescence.* Adv Exp Med Biol, 1992. **317**: p. 277-96.
12. Mayevsky, A. and E. Barbiro-Michaely, *Use of NADH fluorescence to determine mitochondrial function in vivo.* Int J Biochem Cell Biol, 2009. **41**(10): p. 1977-88.
13. Mayevsky, A. and G.G. Rogatsky, *Mitochondrial function in vivo evaluated by NADH fluorescence: from animal models to human studies.* Am J Physiol Cell Physiol, 2007. **292**(2): p. C615-40.
14. Matcher, S.J., et al., *Performance comparison of several published tissue near-infrared spectroscopy algorithms.* Anal Biochem, 1995. **227**(1): p. 54-68.
15. Boushel, R. and C.A. Piantadosi, *Near-infrared spectroscopy for monitoring muscle oxygenation.* Acta Physiol Scand, 2000. **168**(4): p. 615-22.
16. Kakihana, Y., et al., *Brain oxymetry in the operating room: current status and future directions with particular regard to cytochrome oxidase.* J Biomed Opt, 2008. **13**(3): p. 033001.
17. Davies, P.W. and R.G. Grenell, *Metabolism and function in the cerebral cortex under local perfusion, with the aid of an oxygen cathode for surface measurement of cortical oxygen consumption.* J Neurophysiol, 1962. **25**: p. 651-83.
18. Buerk, D.G., et al., *Interpretation of oxygen disappearance curves measured in blood perfused tissues.* Adv Exp Med Biol, 1986. **200**: p. 151-61.

19. Gaab, M.R., B. Poch, and V. Heller, *Oxygen tension, oxygen metabolism, and microcirculation in vasogenic brain edema.* Adv Neurol, 1990. **52**: p. 247-56.
20. Reneau, D.D. and J.H. Halsey, Jr., *Interpretation of oxygen disappearance rates in brain cortex following total ischaemia.* Adv Exp Med Biol, 1977. **94**: p. 189-98.
21. Golub, A.S., M.A. Tevald, and R.N. Pittman, *Phosphorescence quenching microrespirometry of skeletal muscle in situ.* Am J Physiol Heart Circ Physiol, 2011. **300**(1): p. H135-43.
22. Vanderkooi, J.M. and D.F. Wilson, *A new method for measuring oxygen concentration in biological systems.* Adv Exp Med Biol, 1986. **200**: p. 189-93.
23. Johannes, T., et al., *Iloprost preserves renal oxygenation and restores kidney function in endotoxemia-related acute renal failure in the rat.* Crit Care Med, 2009. **37**(4): p. 1423-32.
24. Johannes, T., et al., *Influence of fluid resuscitation on renal microvascular PO2 in a normotensive rat model of endotoxemia.* Crit Care, 2006. **10**(3): p. R88.
25. Wilson, D.F., et al., *Measuring oxygen in living tissue: intravascular, interstitial, and "tissue" oxygen measurements.* Adv Exp Med Biol, 2011. **701**: p. 53-59.
26. Mik, E.G., et al., *Excitation pulse deconvolution in luminescence lifetime analysis for oxygen measurements in vivo.* Photochem Photobiol, 2002. **76**(1): p. 12-21.
27. Mik, E.G., et al., *Mitochondrial PO2 measured by delayed fluorescence of endogenous protoporphyrin IX.* Nat Methods, 2006. **3**(11): p. 939-45.
28. Harms, F.A., et al., *Oxygen-dependent delayed fluorescence measured in skin after topical application of 5-aminolevulinic acid.* J Biophotonics, 2011. **4**(10): p. 731-9.
29. Mik, E.G., et al., *Mitochondrial oxygen tension within the heart.* J Mol Cell Cardiol, 2009. **46**(6): p. 943-51.
30. Mik, E.G., et al., *In vivo mitochondrial oxygen tension measured by a delayed fluorescence lifetime technique.* Biophys J, 2008. **95**(8): p. 3977-90.
31. Mik, E.G., *Methods and devices for assessment of mitochondrial function.* 2009: US 2011/0182825 A1.
32. Golub, A.S., et al., *Analysis of phosphorescence in heterogeneous systems using distributions of quencher concentration.* Biophys J, 1997. **73**(1): p. 452-65.
33. Bodmer, S.I., et al., *Microvascular and mitochondrial PO(2) simultaneously measured by oxygen-dependent delayed luminescence.* J Biophotonics, 2012. **5**(2): p. 140-51.
34. Harms, F.A., et al., *Validation of the protoporphyrin IX-triplet state lifetime technique for mitochondrial oxygen measurements in the skin.* Opt Lett, 2012. **37**(13): p. 2625-7.
35. Golub, A.S. and R.N. Pittman, *PO2 measurements in the microcirculation using phosphorescence quenching microscopy at high magnification.* Am J Physiol Heart Circ Physiol, 2008. **294**(6): p. H2905-16.
36. Mitra, S. and T.H. Foster, *Photochemical oxygen consumption sensitized by a porphyrin phosphorescent probe in two model systems.* Biophys J, 2000. **78**(5): p. 2597-605.
37. Pittman, R.N., 2011.
38. Marson, F., et al., *Correlation between oxygen consumption calculated using Fick's method and measured with indirect calorimetry in critically ill patients.* Arq Bras Cardiol, 2004. **82**(1): p. 77-81, 72-6.

39. Smithies, M.N., et al., *Comparison of oxygen consumption measurements: indirect calorimetry versus the reversed Fick method.* Crit Care Med, 1991. **19**(11): p. 1401-6.
40. Leniger-Follert, E., *Direct determination of local oxygen consumption of the brain cortex in vivo.* Pflugers Arch, 1977. **372**(2): p. 175-9.
41. Nair, P.K., D.G. Buerk, and J.H. Halsey, Jr., *Comparisons of oxygen metabolism and tissue PO2 in cortex and hippocampus of gerbil brain.* Stroke, 1987. **18**(3): p. 616-22.
42. Whalen, W.J., et al., *Cat carotid body: oxygen consumption and other parameters.* J Appl Physiol, 1981. **50**(1): p. 129-33.
43. Gomez, H., et al., *Characterization of tissue oxygen saturation and the vascular occlusion test: influence of measurement sites, probe sizes and deflation thresholds.* Crit Care, 2009. **13 Suppl 5**: p. S3.
44. Nematbakhsh, M., et al., *Local maximum oxygen disappearance rate has limited utility as a measure of local renal tissue oxygen consumption.* Journal of Pharmacological and Toxicological Methods, 2010. **61**(3): p. 297-303.
45. Pareznik, R., et al., *Changes in muscle tissue oxygenation during stagnant ischemia in septic patients.* Intensive Care Med, 2006. **32**(1): p. 87-92.
46. Robiolio, M., W.L. Rumsey, and D.F. Wilson, *Oxygen diffusion and mitochondrial respiration in neuroblastoma cells.* Am J Physiol, 1989. **256**(6 Pt 1): p. C1207-13.
47. Rumsey, W.L., et al., *Cellular energetics and the oxygen dependence of respiration in cardiac myocytes isolated from adult rat.* J Biol Chem, 1990. **265**(26): p. 15392-402.
48. Wolff, C.B., *Normal cardiac output, oxygen delivery and oxygen extraction.* Adv Exp Med Biol, 2007. **599**: p. 169-82.

# CHAPTER 5

# *Non-invasive monitoring of mitochondrial oxygenation and respiration in critical illness using a novel technique*

Floor A. Harms[1], Sander I.A. Bodmer[1], Wilhelmina J. Voorbeijtel[1], Nicolaas J.H. Raat[1], Egbert G. Mik[1,2]

1 Department of Anesthesiology, Laboratory of Experimental Anesthesiology, Erasmus University Medical Center Rotterdam, 's-Gravendijkwal 230, 3015 CE Rotterdam, The Netherlands

2 Department of Intensive Care, Erasmus University Medical Center Rotterdam, 's-Gravendijkwal 230, 3015 CE Rotterdam, The Netherlands

**Short title:** Monitoring of mitochondria in critical illness

Submitted for publication

**ABSTRACT**

**Objective:** Although mitochondrial dysfunction is proposed to be involved in the pathophysiology of sepsis, conflicting results are reported. Variation in the methods used to assess mitochondrial function might contribute to this controversy. A non-invasive method for monitoring mitochondrial function *in vivo* might help overcome the technical limitations of measurements in tissue biopsies. Therefore, this study explores the possibility of *in vivo* monitoring of mitochondrial oxygen tension ($mitoPO_2$) and oxygen consumption ($mitoVO_2$) in an endotoxin-induced septic animal model. Both parameters were determined in skin by means of the protoporphyrin IX-triplet state lifetime technique (PpIX-TSLT).

**Design:** Prospective, randomized animal study.

**Setting:** University laboratory.

**Methods:** Adult male Wistar rats (n=28) were anesthetized and mechanically ventilated.

**Interventions:** A 5-aminolevulinic acid (ALA) cream was applied to the abdominal skin of rats to induce endogenous protoporphyrin IX (PpIX) in the mitochondria. Pulsed green light was used to excite PpIX, of which the lifetime of the emitted delayed fluorescence depends on $mitoPO_2$. Oxygen consumption was determined by repeated $mitoPO_2$ measurements while locally blocking oxygen supply by applying pressure with the measurement probe. Kinetic aspects of the drop in $mitoPO_2$ were recorded during 60 s of skin compression. Mitochondrial respiration was derived from the slope of the $mitoPO_2$ oxygen disappearance curve. Animals were assigned to a control group (no treatment), or to receive lipopolysaccharide without fluid resuscitation (LPS-) or lipopolysaccharide plus fluid resuscitation (LPS+). Sepsis was induced by intravenous LPS injection (1.6 mg/kg during 10 min), fluid resuscitation was performed by continuous infusion of a colloid solution, 7 ml $kg^{-1}$ $h^{-1}$ (Voluven) and a 2-ml bolus of the same colloid solution. Measurements were made before and 3 h after induction of sepsis.

**Measurements and Results:** At baseline (t0) all rats were hemodynamically stable without systemic signs of hypoperfusion. After LPS induction (t1), significant ($p<0.05$) hemodynamic changes were observed in both LPS groups. At t0, $mitoPO_2$ and $mitoVO_2$ were 59 ± 1 mmHg, 64 ± 3 mmHg, 68 ± 4 mmHg and 5.0 ± 0.3 mmHg $s^{-1}$, 5.3 ± 0.5 mmHg $s^{-1}$, 5.7 ± 0.5 mmHg $s^{-1}$ in the control, LPS+ and LPS- groups, respectively; at t1 these values were 58 ± 5 mmHg, 50 ±2.3 mmHg, 30 ± 3.3 mmHg and 4.5 ± 0.5 mmHg $s^{-1}$, 3.3 ± 0.3 mmHg $s^{-1}$, 1.8 ± 0.3 mmHg $s^{-1}$, respectively. At t1, only $mitoPO_2$ showed a significant difference between the controls and LPS-. In contrast, at t1 both LPS groups showed a significantly lower $mitoVO_2$ compared to controls**.**

**Conclusion:** These data show the feasibility to monitor alterations in mitochondrial oxygen consumption *in vivo* by PpIX-TSLT in an endotoxin-induced septic rat model. As PpIX-TSLT can also be used in humans, these results may contribute to the development of a clinical device to monitor mitochondrial function in the critically ill.

## INTRODUCTION

Sepsis and septic shock are life-threatening disorders with a high mortality rate of 30-60% [1]. The pathophysiology of sepsis is multifactorial and complex. Consequently, the treatment of severe sepsis and septic shock requires extensive knowledge and often reaches the limits of possibilities in the intensive care unit. Part of the current treatment of sepsis is aimed at safeguarding or restoring oxygen supply to tissue cells by early aggressive administration of intravenous fluids, and the use of inotropic and vasoactive agents. Early aggressive resuscitation in sepsis is known to modulate inflammation [2] and improve microvascular perfusion [3], even though the clinical outcome is not always improved [4-6]. Therefore, the management of sepsis remains a challenge despite advances in both monitoring and treatment.

Mitochondrial dysfunction is suggested to be a key issue in the pathophysiology of and recovery from sepsis [7, 8]. In the case of mitochondrial dysfunction, optimization of the macro- and microcirculation alone is not likely to result in improved aerobic cell metabolism. This might explain why treatment focused on adequate tissue perfusion and oxygenation does not always lead to a better prognosis. Despite many studies on the role of mitochondrial dysfunction in sepsis over the last 40 years, clear evidence for the underlying mechanism is still lacking [9]. Whereas some authors report decreased mitochondrial oxygen consumption in sepsis [9-12] others found an unchanged [13] or even improved [14-18] mitochondrial function under similar circumstances.

Most knowledge on mitochondrial dysfunction in sepsis is derived from animal experiments using isolated mitochondria from tissue biopsies [8, 10, 19], providing detailed insight into the function of the respiratory chain. However, measurements in isolated mitochondria may not reflect the *in vivo* situation. This is due to the possible loss of essential metabolites during mitochondrial isolation and disruption of the normal interactions of the organelle with the cytoskeleton [20]. Such experimental limitations may partly explain the controversial reports on mitochondrial dysfunction in sepsis [9]. In

addition, the use of different methods to measure mitochondrial oxygen consumption, different models of sepsis, a long or short duration of sepsis, and different target organs may also contribute to the lack of a clear pattern [21]. Therefore, in their review, Jeger et al. concluded that: "*…in order to get a better understanding about mitochondrial dysfunction in sepsis a valid non-invasive method to monitor mitochondrial function in vivo would be necessary"* [9].

The technique developed to measure mitochondrial $PO_2$ (mito$PO_2$), by means of the protoporphyrin IX-triplet state lifetime technique (PpIX-TSLT)[22, 23] provides new opportunities to monitor mitochondrial function *in vivo*. PpIX-TSLT enables mito$PO_2$ measurements by means of the oxygen-dependent optical properties of 5-aminolevulinic acid (ALA)-induced endogenous protoporphyrin IX (PpIX). Our group investigates mitochondrial respirometry with the aim to monitor mito$PO_2$ and mitochondrial oxygen consumption (mito$VO_2$) in skin [24-26]. PpIX-TSLT is the first technique to allow measurement of mito$PO_2$ in living cells, and can also be applied *in vivo* [23, 27]. Moreover, because it is non-invasive and safe for application in humans [28] this technique may enable clinical monitoring of mitochondrial function at the cellular level.

The present study explores the possibility to monitor *in vivo* mito$PO_2$ and mito$VO_2$ in an animal model of acute critical illness. We report on the use of PpIX-TSLT for cutaneous respirometry in healthy rats compared with rats with endotoxin-induced sepsis.

## METHODS

### PRINCIPLE OF MITO$PO_2$ MEASUREMENTS

The background of PpIX-TSLT is described in detail elsewhere [22-24, 26]. In short, PpIX is the final precursor of heme in the heme biosynthetic pathway. PpIX is synthesized in the mitochondria, and administration of ALA substantially enhances the PpIX concentration. Since the conversion of PpIX to heme is a rate-limiting step, administration of ALA causes accumulation of PpIX inside the mitochondria (Fig. 1). PpIX possesses a triplet state that reacts strongly with oxygen, making its lifetime oxygen dependent. Population of the first excited triplet state occurs upon photoexcitation with a pulse of light, and causes the emission of red delayed fluorescence. The delayed fluorescence lifetime is related to mito$PO_2$ according to the Stern-Volmer equation:

$$PO_2 = \frac{\frac{1}{\tau} - \frac{1}{\tau_0}}{k_q} \quad (1)$$

in which τ is the measured delayed fluorescence lifetime, $k_q$ is the quenching constant and $\tau_0$ is the lifetime at zero oxygen. In case of a non-homogenous oxygen distribution inside the measurement volume, a reliable estimation of the average $PO_2$ can be made by the rectangular distribution method (RDM)[29, 30]

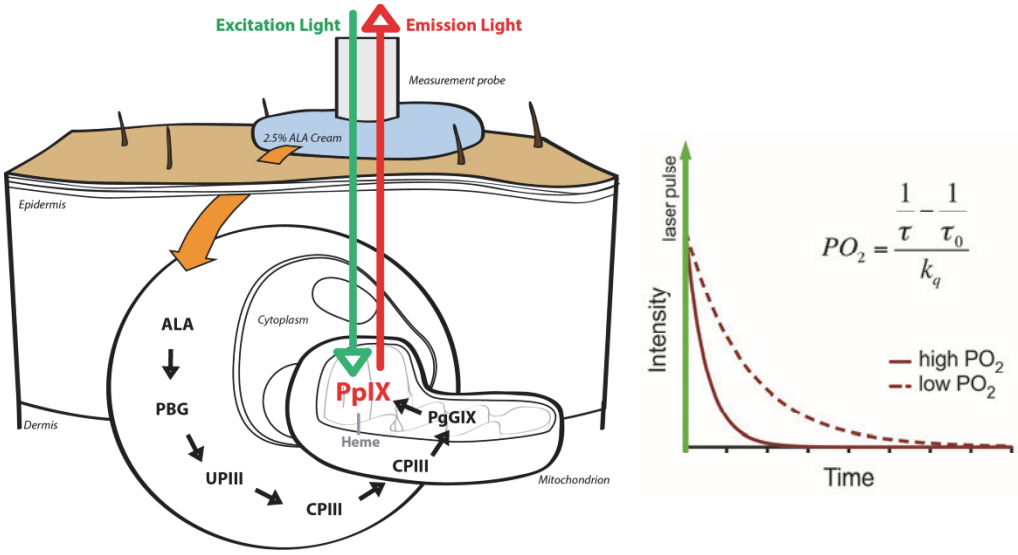


**Figure 1.** Panel A: Principle of the protoporphyrin IX-triplet state lifetime technique. The pathway by which topical ALA administration enhances mitochondrial PpIX levels and the principle of delayed fluorescence detection after an excitation pulse with green (510 nm) light. Emission light is the delayed fluorescence (red, 630-700 nm) and its lifetime is oxygen-dependent. ALA, 5-aminolevulinic acid; PBG, porphobilinogen; UPIII, urporphyrinogen III; CPIII, coporporphyrinogen III; and PpIX, protoporphyrin IX.Panel B: PpIX emits delayed fluorescence after excitation by a pulse of green (510 nm) light. The delayed fluorescence lifetime is oxygen-dependent, according to the Stern-Volmer equation (inset), in which $k_q$ is the quenching constant and $\tau_0$ is the lifetime at zero oxygen.

## PRINCIPLE OF OXYGEN CONSUMPTION MEASUREMENTS

$MitoVO_2$ is measured by the oxygen disappearance rate after local cessation of oxygen supply by pressure-induced occlusion of the microcirculation. The reflection probe was mounted above the ALA cream-treated skin with a height-adjustable stand, allowing different settings of probe-to-skin distance. Occlusion of the microcirculation in skin was obtained by local pressure with the measurement probe. This simple procedure reliably created stop-flow conditions and induced measurable oxygen disappearance rates (ODR),

due to cessation of microvascular oxygen supply and ongoing cellular oxygen consumption. Mito$PO_2$ was measured before and during application of pressure at an interval of 1 Hz, using 1 laser pulse per measurement. The principles of mito$VO_2$ measurements are shown in Figure 2. We have described these principles in detail and provided a working implementation of the technique for mito$VO_2$ measurements [26]. In that implementation, we developed a method for analysis of delayed-fluorescence-based ODR data to calculate mito$PO_2$ and mito$VO_2$ and $P_{50}$ and demonstrated the feasibility and reproducibility of our method in rats [26].

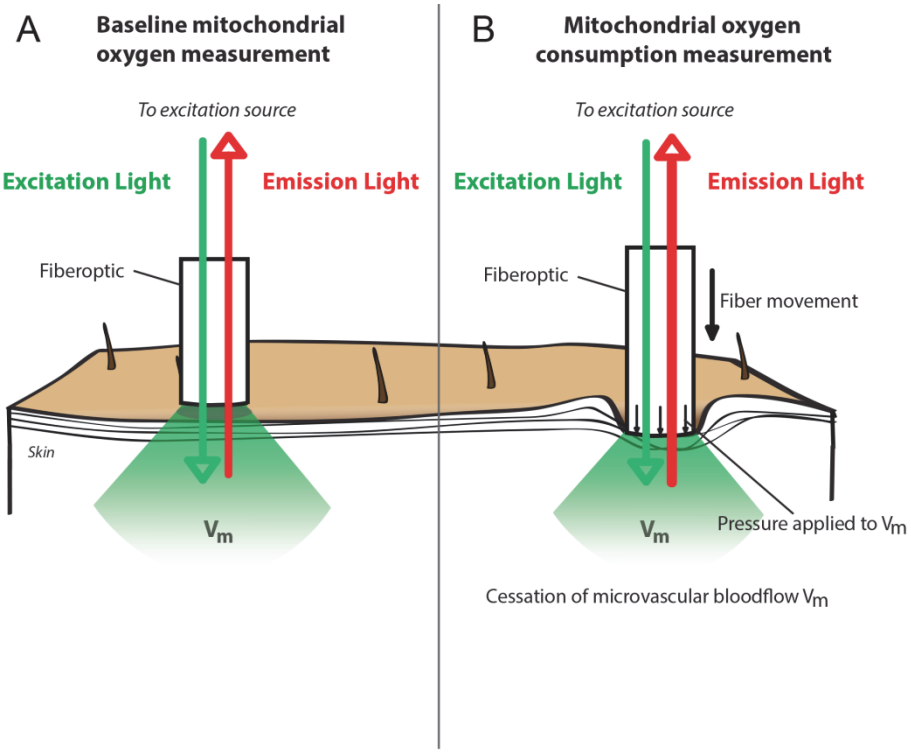


**Figure 2.** Principles of the respirometry in skin by oxygen-dependent quenching of delayed fluorescence of protoporphyrin IX. The first panel (A) shows the baseline measurement. The second panel (B) shows the principle of the pressure-induced cessation of microvascular blood flow. $V_m$, measurement volume.

## ANIMAL PREPARATION

The protocol was approved by the Animal Research Committee of the Erasmus University Medical Center Rotterdam. Animal care and handling were performed in accordance with the guidelines for Institutional and Animal Care and Use Committees.

A total of 28 male Wistar rats (mean body weight 292 g, SD ± 25.5 g) were used in this study. All animals were anesthetized by intraperitoneal injection of a mixture of ketamine

90 mg $kg^{-1}$ (Alfasan, Woerden, the Netherlands), 0.5 mg $kg^{-1}$ medetomidine (Sedator Eurovet Animal Health BV, Bladel, the Netherlands) and 0.05 mg $kg^{-1}$ atropine (Centrofarm Services BV, Etten-Leur, the Netherlands). Ketamine (50 mg $kg^{-1}$ $h^{-1}$) and crystalloid solution (Ringer's lactate, 5 ml $kg^{-1}$ $h^{-1}$) were infused intravenously to maintain anesthesia and fluid balance. Following tracheotomy, mechanical ventilation was instigated (Babylog 8000 plus; Dräger, Lubeck, Germany). Ventilation was adjusted on end-tidal $PCO_2$, keeping the arterial $PCO_2$ at 35-45 mmHg. A polyethylene catheter (outer diameter 0.9 mm) was inserted into the right jugular vein for intravenous administration of a colloid solution (Voluven 3.5 ml $kg^{-1}$ $h^{-1}$). Arterial blood pressure and heart rate were monitored with a similar catheter in the left femoral artery. Every hour we performed analysis of arterial blood gas, and measured cardiac output by thermodilution with the thermistor inserted in the right carotid artery. Body temperature was rectally measured and maintained at 38 ± 0.5°C by means of a heating pad.

EXPERIMENTAL SETUP

In all groups PpIX was induced by topical application of 2.5% ALA cream. The ALA cream was prepared by mixing hydrophilic cremor lanette (Lanettecreme I FNA, Bipharma, Weesp, the Netherlands) and 2.5% 5-aminolevulinic acid (Sigma-Aldrich, St. Louis, MO, USA) just before use. The cream was topically administered on the abdominal skin after hair removal. The latter was accomplished by shaving and subsequent use of hair removal cream (Veet, Reckitt Benckiser Co., Slough, UK). The ALA-treated skin was covered with an adhesive film to avoid evaporation. Furthermore, to prevent premature exposure of the primed skin to light, the primed area was covered with aluminum foil. After 3 h, sufficient PpIX had accumulated to commence baseline (t0) *in vivo* measurements of mito$PO_2$ and mito$VO_2$.

After measurements at t0, animals were assigned to one of three groups: lipopolysaccharide without fluid resuscitation (LPS-, n=10), LPS with resuscitation (LPS+, n=10), and an untreated control group (n=8). The LPS groups received an intravenous LPS injection (1.6 mg/kg during 10 min) (extracted from E. coli, serotype 0127:B8; Sigma-Aldrich, USA). The LPS was dissolved at a concentration of 1 mg/ml in a crystalloid solution. Three hours after infusion of LPS the oxygen measurements were repeated (t1).

In the LPS+ group fluid resuscitation was achieved by continuous infusion of a colloid solution, 7 ml $kg^{-1}$ $h^{-1}$ (Voluven, Fresenius Kabi, Bad Homburg, Germany); a 2-ml bolus of the same colloid solution was administered just before the start of the t2 measurements. Finally, in the LPS- group a 2-ml colloid fluid bolus (Voluven, Fresenius Kabi, Bad Homburg,

Germany) was given directly after t1 measurements to a achieve a late resuscitation model. The effect of this late resuscitation on mitoPO$_2$ and mitoVO$_2$ was measured directly after fluid administration (t2). Figure 3 describes the experimental setup.

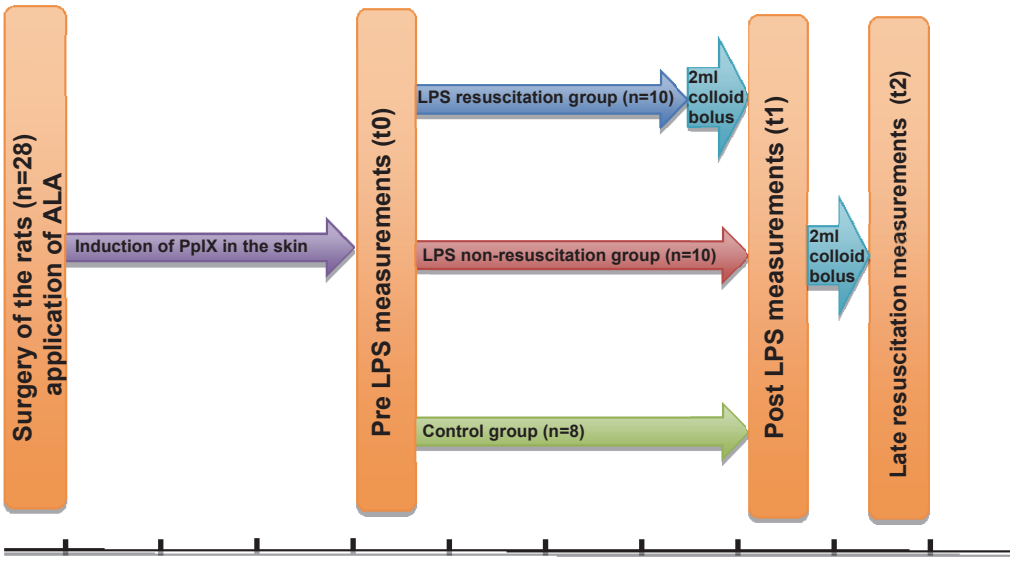


**Figure 3.** Schematic flowchart of the experimental setup. ALA, 5-aminolevulinic acid; LPS, lipopolysaccharide

STATISTICAL ANALYSIS

Statistical analyses were performed using IBM SPSS version 21 (IBM Corporation, Armonk, NY, USA). Unless stated otherwise, all values are reported as mean ± standard error (SE). Statistical significance between groups was calculated using a two-tailed Student's t-test. A paired Student's t-test was used to compare differences between measurements at t0 and t1. A p-value ≤ 0.05 was considered statistically significant.

## RESULTS

Delayed fluorescence signals were easily detected 3 h after induction with topically applied ALA. Table 1 presents data on the hemodynamic parameters of the experimental groups. At the t0 measurement all rats were hemodynamically stable without signs of hypoperfusion (reflected by low serum lactate) and there were no significant differences

between the groups. At t1, significant ($p<0.05$) changes in hemodynamics were observed in both LPS groups. In the LPS+ group macrohemodynamic parameters were preserved by means of fluid resuscitation, indicated by unchanged mean arterial blood pressure and cardiac output. In contrast, in the LPS- group macrohemodynamic parameters were compromised. Both LPS groups showed significant metabolic acidosis with increased serum lactate.

Table 1. Hemodynamic parameters of the three experimental groups.

| Parameter | Pre LPS measurements mean ± | Post LPS measurements (t1) mean ± SE |
|---|---|---|
| CONTROL group n=8 | | |
| Cardiac output, ml/min | 137 ± | 115 ± 32 |
| Mean arterial pressure, mmHg | 78 ± 4 | 66 ± 3* |
| Heart rate, bpm | 235 ± | 244 ± 12 |
| p | 7.33 ± | 7.28 ± 0.04 |
| $pCO_2$, mmHg | 39 ± 1.8 | 36 ± 2.0 |
| $pO_2$, mmHg | 201 ± 3.99 | 201 ± 6.64 |
| Lactate, mmol/L | 1.2 ± 0.15 | 1.2 ± 0.08 |
| Parameter | Pre LPS measurements mean ± | Post LPS measurements (t1) mean ± SE |
| LPS resuscitation group n=10 | | |
| Cardiac output, ml/min | 118 ± | 111 ± 36 |
| Mean arterial pressure, mmHg | 82 ± 3 | 80 ± |
| Heart rate, bpm | 240 ± 7 | 292 ± 14*† |
| p | 7.34 ± | 7.16 ± 0.02*† |
| $pCO_2$, mmHg | 36 ± 2 | 38.5 ± 2 |
| $pO_2$, mmHg | 196 ± 5 | 209 ± 3* |
| Lactate, mmol/L | 1.10 ± 0.07 | 3.87 ± 0.32*† |
| Parameter | Pre LPS measurements mean ± | Post LPS measurements (t1) mean ± SE |
| LPS non resuscitation group n=10 | | |
| Cardiac output, ml/min | 135 ± | 50 ± 19* |
| Mean arterial pressure, mmHg | 76 ± 9 | 57 ± |
| Heart rate, bpm | 247 ± | 268 ± 29 |
| p | 7.35 ± | 7.14 ± 0.01*† |
| $pCO_2$, mmHg | 35 ± 2 | 37 ± |
| $pO_2$, mmHg | 192 ± 3 | 189 ± 7 |
| Lactate, mmol/L | 1.38 ± | 4.30 ± 0.33*† |

Values are means ± SE,

* significant difference compared with baseline measurements,

† Significant difference ($p<0.05$) compared with control group.

Table 2 presents data on mito$PO_2$ and mito$VO_2$. Both parameters showed a significant decrease in the LPS-induced septic groups, whereas no differences were observed in the control group. In the LPS+ group no differences in mito$PO_2$ were observed compared with

the control group. However, in spite of normal mitoPO$_2$ values, there was a significantly decreased mitoVO$_2$ in the LPS+ group. At t1, in the LPS- group both mitoPO$_2$ and mitoVO$_2$ were significantly lower compared with values at t0. Figure 4 presents a representative example of mitochondrial consumption measurements under normal conditions (Fig. 4A) and under septic conditions without resuscitation (Fig. 4B).

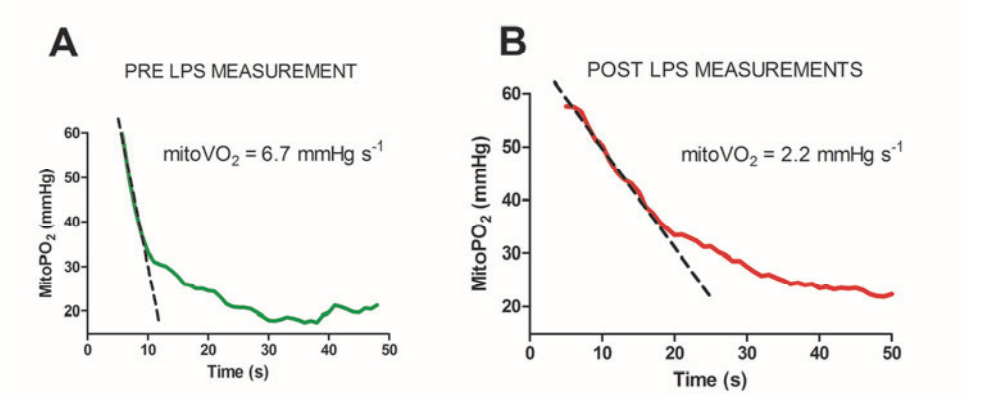


**Figure 4.** Representative example of mitocondrial oxygen consumption measurement in a rat of the non-resuscitation group. Panel A: before administation of LPS. Panel B: 3 hours after administration of LPS

Table 2. MitoPO$_2$ and mitoVO$_2$ before and after LPS induction.

| Parameter | Pre LPS measurements (t0) mean ± SE | Post LPS measurements (t1) mean ± SE |
|---|---|---|
| CONTROL group n = 8 | | |
| mitoPO$_2$, mmHg | 59 ± 1 | 58 ± 5 |
| mitoVO$_2$, mmHg s$^{-1}$ | 5.0 ± 0.3 | 4.5 ± 0.5 |
| LPS resuscitation group n = 10 | | |
| mitoPO$_2$, mmHg | 64 ± 3.0 | 50 ± 2.3 * |
| mitoVO$_2$, mmHg s$^{-1}$ | 5.3 ± 0.5 | 3.3 ± 0.3 *† |
| LPS non resuscitation group n = 10 | | |
| mitoPO$_2$, mmHg | 68 ± 4 † | 30 ± 3.3*† |
| mitoVO$_2$, mmHg s$^{-1}$ | 5.7 ± 0.51 | 1.8 ± 0.3 *† |

Values are means ± SE,
* significant difference (P<0.05) compared to baseline measurements,
† Significant difference (P<0.05) compared to control group.

Figure 5 shows mitoPO$_2$ and mitoVO$_2$ measurements in the LPS- group measured at baseline (t0), during septic conditions without fluid resuscitation (t1), and immediately after a late fluid resuscitation (t2) with a bolus of colloid. MitoPO$_2$ values measured before the stop-flow situation were generally around 65 mmHg; induction of sepsis resulted in hemodynamic changes, with a corresponding decrease in mitoPO$_2$ to values around 30 mmHg. MitoPO$_2$ recovered to baseline values after late resuscitation with a fluid bolus. Before late resuscitation, the decreased mitoVO$_2$ might be a consequence of the persisting hypoperfusion resulting in low mitoPO$_2$ values. Interestingly, however, recovery of the mitoPO$_2$ values by fluid resuscitation in the late resuscitation group also failed to result in normalization of mitoVO$_2$.

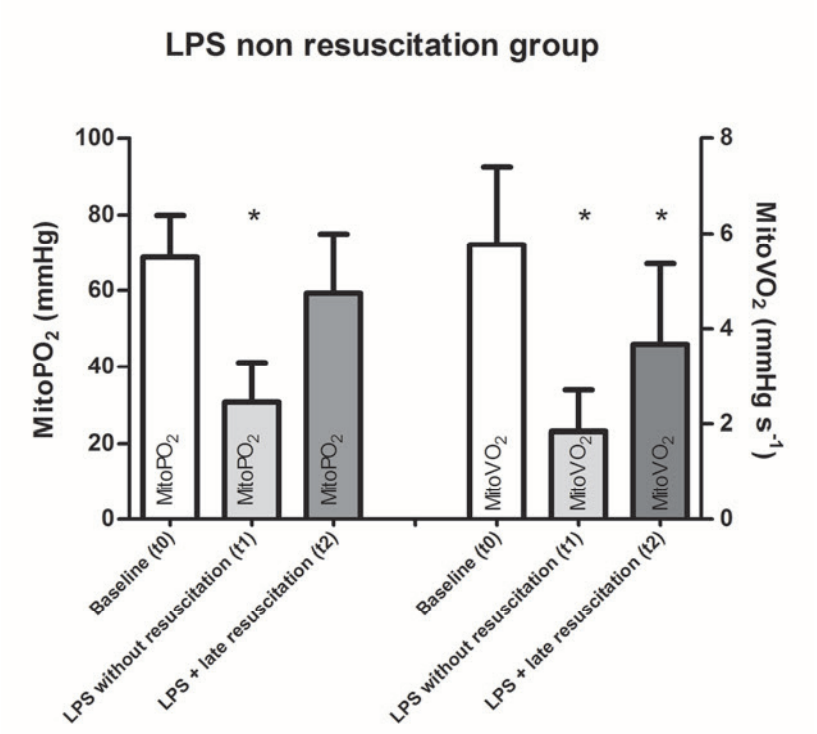


**Figure 5.** Average mitoPO$_2$ and mitoVO$_2$ in the non-resuscitation group at three time points: at baseline (t0) before the induction of sepsis, 3 h after LPS infusion (t1), and after late fluid resuscitation (t2). Data are presented as means ± SE. *significant difference compared with baseline measurements ($p<0.05$).
LPS, lipopolysaccharide; mitoPO$_2$, mitochondrial oxygen tension; mitoVO$_2$, mitochondrial oxygen consumption

**DISCUSSION**

In this acute model of LPS-induced sepsis in rats, our results support the idea that mitochondrial dysfunction contributes to the pathophysiology of sepsis, even in the absence of severe hemodynamic shock and diminished mitochondrial oxygenation. We found reduced cellular oxygen consumption after restoring tissue oxygenation to baseline levels with fluid resuscitation. Combined with the finding of increased serum lactate in the absence of shock, this clearly indicates a hampered aerobic metabolism. Importantly, these measurements were made on the cellular level *in vivo,* thereby eliminating the potential bias introduced by more invasive and destructive techniques such as mitochondrial isolation.

As expected in an animal model of induced sepsis, our LPS-induced septic rats were hemodynamically compromised with a low mean arterial pressure and cardiac output. Also, septic rats showed high lactate levels and low pH levels, and signs of metabolic acidosis, suggesting increased anaerobic metabolism. However, while the induction of sepsis without fluid resuscitation resulted in a clear decrease in both mito$PO_2$ and mito$VO_2$, fluid resuscitation resulted in other changes. Early fluid resuscitation, given to avoid the development of tissue hypoperfusion, resulted in decreased mito$VO_2$ while the mito$PO_2$ remained almost unchanged compared with the control group. Furthermore, late resuscitation by a fluid bolus almost completely restored the mito$PO_2$ to baseline values. However, in contrast to expectations based on the classical view of mitochondrial dysfunction being secondary to inadequate oxygenation, mito$VO_2$ did not recover after fluid resuscitation. Impaired mito$VO_2$, despite normal mito$PO_2$, suggests that persisting mitochondrial dysfunction plays a role in the development of sepsis. Administration of LPS in rats is known to induce complex I inhibition of the mitochondrial respiratory in heart, liver and diaphragm mitochondria [13, 31-33]. The present findings are probably based on the same principles and are likely to reflect the *in vivo* situation of this phenomenon.

In addition to the above findings, our results demonstrate that PpIX-TSLT enables monitoring of the mitochondrial function in skin. The technique provides *in vivo* information on oxygenation and oxygen consumption of the mitochondria, without the need to damage tissue for isolation of mitochondria. Therefore, our method overcomes some of the disadvantages of earlier studies on mitochondrial dysfunction in sepsis. Because PpIX-TSLT can be applied in humans it is potentially feasible for clinical monitoring. Although our implementation of PpIX-TSLT is an important step towards addressing the need for a valid non-invasive method to monitor mitochondrial function *in*

*vivo,* as proposed by Jeger et al. [9], some questions still remain. For example, the skin has to be proven to be a suitable target organ for monitoring mitochondrial function. There is evidence that the skin is one of the first organs in which signs of mitochondrial failure occurred [34, 35], in which case the skin could be an excellent early indicator for mitochondrial pathology.
The clinical relevance of our method needs additional studies which, for example, investigate the correlation between mitochondrial function in the skin and other organs.

## CONCLUSIONS

This study shows the feasibility to measure mitochondrial oxygenation and oxygen consumption in endotoxemic rats by means of cutaneous PpIX-TSLT. A decreased mito$VO_2$ in the presence of preserved or restored mito$PO_2$ suggests that mitochondrial dysfunction contributes to the metabolic failure in sepsis, even in the absence of hemodynamic shock. These results are promising in view of our aim to develop a clinical mitochondrial monitoring technique. Clinical implementation of this technique is likely to contribute to our understanding of mitochondrial dysfunction in sepsis and the development of therapeutic approaches aimed at restoring aerobic metabolism and cellular function.



## ACKNOWLEDGMENTS

The authors thank Patricia Specht for expert biotechnical help and Bart Lukkes for help with the design of Figures 1 and 2. This research is financially supported by a Life Sciences Pre-Seed Grant (grant no. 40-41300-98-9037) from the Netherlands Organization for Health Research and Development (ZonMW).

## CONFLICT OF INTEREST STATEMENT

Dr. E.G. Mik is founder and shareholder of Photonics Healthcare B.V., a company aimed at making the delayed fluorescence lifetime technology available to a broad public. Photonics Healthcare B.V. holds the exclusive licenses to several patents related to this

technology, filed and owned by the Academic Medical Center in Amsterdam and the Erasmus Medical Center in Rotterdam, the Netherlands

**REFERENCES**


1. Bakker, J., et al., *[Sepsis, a complicated syndrome with major medical and social consequences]*
   *Sepsis, een gecompliceerd syndroom met belangrijke medische en maatschappelijke consequenties.* Ned Tijdschr Geneeskd, 2004. **148**(20): p. 975-8.
2. Grocott, M.P., M.G. Mythen, and T.J. Gan, *Perioperative fluid management and clinical outcomes in adults.* Anesth Analg, 2005. **100**(4): p. 1093-106.
3. Natanson, C., et al., *Antibiotics versus cardiovascular support in a canine model of human septic shock.* Am J Physiol, 1990. **259**(5 Pt 2): p. H1440-7.
4. Ospina-Tascon, G., et al., *Effects of fluids on microvascular perfusion in patients with severe sepsis.* Intensive Care Med, 2010. **36**(6): p. 949-55.
5. Rivers, E.P., et al., *Fluid therapy in septic shock.* Curr Opin Crit Care, 2010. **16**(4): p. 297-308.
6. Hernandez, G., et al., *The holistic view on perfusion monitoring in septic shock.* Curr Opin Crit Care, 2012. **18**(3): p. 280-6.
7. Fink, M.P., *Cytopathic hypoxia. Is oxygen use impaired in sepsis as a result of an acquired intrinsic derangement in cellular respiration?* Crit Care Clin, 2002. **18**(1): p. 165-75.
8. Galley, H.F., *Oxidative stress and mitochondrial dysfunction in sepsis.* British Journal of Anaesthesia, 2011. **107**(1): p. 57-64.
9. Jeger, V., et al., *Mitochondrial function in sepsis.* Eur J Clin Invest, 2013. **43**(5): p. 532-42.
10. Brealey, D., et al., *Mitochondrial dysfunction in a long-term rodent model of sepsis and organ failure.* American Journal of Physiology - Regulatory Integrative and Comparative Physiology, 2004. **286**(3 55-3): p. R491-R497.
11. Llesuy, S., et al., *Oxidative stress in muscle and liver of rats with septic syndrome.* Free Radic Biol Med, 1994. **16**(4): p. 445-51.
12. Larche, J., et al., *Inhibition of mitochondrial permeability transition prevents sepsis-induced myocardial dysfunction and mortality.* J Am Coll Cardiol, 2006. **48**(2): p. 377-85.

13. Vanasco, V., et al., *The oxidative stress and the mitochondrial dysfunction caused by endotoxemia are prevented by alpha-lipoic acid.* Free Radic Res, 2008. **42**(9): p. 815-23.
14. Kantrow, S.P., et al., *Oxidative metabolism in rat hepatocytes and mitochondria during sepsis.* Arch Biochem Biophys, 1997. **345**(2): p. 278-88.
15. Kozlov, A.V., et al., *Opposite effects of endotoxin on mitochondrial and endoplasmic reticulum functions.* Biochem Biophys Res Commun, 2007. **352**(1): p. 91-6.
16. Dawson, K.L., E.R. Geller, and J.R. Kirkpatrick, *Enhancement of mitochondrial function in sepsis.* Arch Surg, 1988. **123**(2): p. 241-4.
17. Markley, M.A., A. Pierro, and S. Eaton, *Hepatocyte mitochondrial metabolism is inhibited in neonatal rat endotoxaemia: effects of glutamine.* Clin Sci (Lond), 2002. **102**(3): p. 337-44.
18. Takeyama, N., et al., *Altered hepatic mitochondrial fatty acid oxidation and ketogenesis in endotoxic rats.* Am J Physiol, 1990. **259**(4 Pt 1): p. E498-505.
19. Crouser, E.D., et al., *Endotoxin-induced mitochondrial damage correlates with impaired respiratory activity.* Crit Care Med, 2002. **30**(2): p. 276-84.
20. Villani, G. and G. Attardi, *In vivo control of respiration by cytochrome c oxidase in human cells.* Free Radic Biol Med, 2000. **29**(3-4): p. 202-10.
21. Singer, M., *Mitochondrial function in sepsis: acute phase versus multiple organ failure.* Crit Care Med, 2007. **35**(9 Suppl): p. S441-8.
22. Mik, E.G., et al., *In vivo mitochondrial oxygen tension measured by a delayed fluorescence lifetime technique.* Biophys J, 2008. **95**(8): p. 3977-90.
23. Mik, E.G., et al., *Mitochondrial PO2 measured by delayed fluorescence of endogenous protoporphyrin IX.* Nat Methods, 2006. **3**(11): p. 939-45.
24. Harms, F.A., et al., *Validation of the protoporphyrin IX-triplet state lifetime technique for mitochondrial oxygen measurements in the skin.* Opt Lett, 2012. **37**(13): p. 2625-7.
25. Harms, F.A., et al., *Oxygen-dependent delayed fluorescence measured in skin after topical application of 5-aminolevulinic acid.* J Biophotonics, 2011. **4**(10): p. 731-9.
26. Harms, F.A., et al., *Cutaneous respirometry by dynamic measurement of mitochondrial oxygen tension for monitoring mitochondrial function in vivo.* Mitochondrion, 2013. **13**(5): p. 507-14.
27. Mik, E.G., et al., *Mitochondrial oxygen tension within the heart.* J Mol Cell Cardiol, 2009. **46**(6): p. 943-51.

28. Mik, E.G., *Measuring Mitochondrial Oxygen Tension: From Basic Principles to Application in Humans.* Anesth Analg, 2013, Anesth Analg, 2013. **117(**4): p. 834-46.
29. Golub, A.S., et al., *Analysis of phosphorescence in heterogeneous systems using distributions of quencher concentration.* Biophys J, 1997. **73**(1): p. 452-65.
30. Bodmer, S.I., et al., *Microvascular and mitochondrial PO(2) simultaneously measured by oxygen-dependent delayed luminescence.* J Biophotonics, 2012. **5**(2): p. 140-51.
31. Kopprasch, S., et al., *Energy state, glycolytic intermediates and mitochondrial function in the liver during reversible and irreversible endotoxin shock.* Biomed Biochim Acta, 1989. **48**(9): p. 653-9.
32. Suliman, H.B., et al., *Lipopolysaccharide induces oxidative cardiac mitochondrial damage and biogenesis.* Cardiovasc Res, 2004. **64**(2): p. 279-88.
33. Vanasco, V., et al., *Endotoxemia impairs heart mitochondrial function by decreasing electron transfer, ATP synthesis and ATP content without affecting membrane potential.* J Bioenerg Biomembr, 2012. **44**(2): p. 243-52.
34. Fischer, M., et al., *Skin function parameters in intensive-care patients.* Skin Res Technol, 2005. **11**(4): p. 268-71.
35. Fischer, M., T. William, and J. Wohlrab, *Skin diseases in intensive care medicine.* J Dtsch Dermatol Ges, 2009. **7**(2): p. 108-15.

# CHAPTER 6

# *In vivo* monitoring of alterations in mitochondrial oxygen consumption

Mark A. Wefers Bettink[1], Floor A. Harms[1], Nicolaas J.H. Raat[1], Egbert G. Mik[1,2]

1 Department of Anesthesiology, Laboratory of Experimental Anesthesiology, Erasmus University Medical Center Rotterdam, 's-Gravendijkwal 230, 3015 CE Rotterdam, The Netherlands

2. Department of Intensive Care, Erasmus University Medical Center Rotterdam, 's-Gravendijkwal 230, 3015 CE Rotterdam, The Netherlands

**Short title:** Monitoring mitochondrial oxygen consumption in vivo

Published in: J clin monit comput, 2014, in press

**ABSTRACT**

**Objective:** To further validate *in vivo* mitochondrial oxygen consumption measurements with the protoporphyrin IX-triplet state lifetime technique (PpIX-TSLT) by demonstrating lipopolysaccharide (LPS)-induced inhibition of mitochondrial complex I in a rat model.
**Design:** Prospective, randomized animal study.
**Setting:** University hospital laboratory.
**Subjects:** Adult male Wistar rats (n=48).
**Interventions:** Mitochondrial function was assessed by PpIX-TSLT at two time points in 5 different groups. Animals (n=8 per group) were assigned to either a time control (TC), a succinate control (SC), a LPS (LPS --), a LPS with fluid resuscitation (LPS +-) or a LPS with fluid resuscitation and succinate group (LPS ++). LPS was infused at a rate of 12 mg/kg during 30 min. Two hours prior to LPS succinate (0.67M in saline, 5 ml/kg) was given. When applicable, fluid resuscitation (5 ml/kg/h) was started after LPS infusion.
**Measurements and Main Results:** Three hours after LPS infusion, a significant decline in mito$PO_2$ from 62 ± 9 mmHg to 40 ± 12 mmHg was measured in the LPS -- group. In the other LPS groups, fluid resuscitation prevented tissue hypoperfusion resulting in an almost unchanged mito$PO_2$ compared to baseline. Nevertheless, a significant decrease in mito$VO_2$ was observed in the LPS -- and LPS +- groups. Activation of complex II of the mitochondrial electron chain by succinate, restored mito$VO_2$ to baseline values.
**Conclusions:** These data show that PpIX-TSLT can detect the known effect of LPS on complex I of the mitochondrial respiratory chain. Therefore, we conclude that PpIX-TSLT allows *in vivo* measurement of mito$VO_2$ in skin and enables non-invasive monitoring of alterations in the parameters of mitochondrial function.

**INTRODUCTION**

Mitochondrial dysfunction is suggested to play a major role in the development of organ failure in sepsis [1]. Although the presence of pathophysiological changes in mitochondrial function in sepsis are well described [2], the role of mitochondrial dysfunction in sepsis remains controversial [3]. Decreased [4, 5], increased [6-8] and unchanged [9] mitochondrial oxygen consumption have been found under septic conditions. These conflicting results might be partly explained by the different techniques used to assess mitochondrial function [3]. The most common *ex vivo* techniques are oxygen consumption measurements using oxygen electrodes [10], such as high-resolution respirometry [11].

These *ex vivo* techniques measure in suspensions of isolated cells and mitochondria, or small tissue biopsies and may, therefore, not adequately reflect the *in vivo* situation [3]. A non-invasive *in vivo* measurement technique to monitor mitochondrial function would be of considerable value.

An innovative method to monitor mitochondrial function *in vivo* has been developed and evaluated in our laboratory [12]. The protoporphyrin IX-triplet state lifetime technique (PpIX-TSLT) enables measurement of mitochondrial oxygen tension (mito$PO_2$) in living cells and tissues [13, 14]. Further development of this technique currently allows the detection of mito$PO_2$ and mitochondrial oxygen consumption (mito$VO_2$) in the skin *in vivo* [12, 15, 16].

We have shown the possibility to measure *in vivo* the endotoxin-induced decline in mito$VO_2$ using PpIX-TSLT for cutaneous measurements in lipopolysaccharide (LPS)-treated rats (Chapter 5 of this thesis). Administration of LPS selectively inhibits complex I of the mitochondrial electron transport chain [17]. After inhibition of complex I, electron transfer will be more dependent on complex II and succinate as electron donor. The substrate succinate is used in classical respirometry to study mitochondrial oxygen consumption linked to electron flow through complex II [18]. In isolated mitochondria, the addition of succinate resulted in an increase in mitochondrial oxygen consumption in sepsis [18].



While endotoxin-induced inhibition of complex I has typically been demonstrated in mitochondria isolated from muscle biopsies, we aim to develop a non-invasive technique for monitoring mitochondrial function. For this purpose, we chose the skin as target organ since application of PpIX-TSLT on skin is also feasible in humans [7]. Mitochondrial alterations in oxygen consumption in the skin also reflect other tissues (Chapter 7 of this thesis). The present study aimed to further validate this cutaneous approach. For this, we hypothesized that administration of succinate in LPS-treated endotoxemic rats will reverse endotoxin-induced reduction of cutaneous mitochondrial respiration. In other words, PpIX-TSLT should be able to detect partial inhibition of complex I. Here validation of *in vivo* mito$VO_2$ measurements in rat skin was performed by administration of succinate under endotoxemic conditions.

## MATERIAL AND METHODS

### SUBJECTS AND PREPARATION

The experimental protocol (DEC 129-12-11) was approved by the Animal Research Committee of the Erasmus University Medical Centre Rotterdam. Animal care and handling were performed in accordance with the guidelines for Institutional and Animal Care and Use Committees.

For this study, 40 male Wister rats (Charles River, the Netherlands; body weight 280-350 g) were used. Anesthesia was induced by intraperitoneal injection of a mixture of ketamine 90 mg $kg^{-1}$ (Alfasan, Woerden, the Netherlands), medetomidine 0.5 mg $kg^{-1}$ (Sedator, Eurovet Animal Health BV, Bladel, the Netherlands) and atropine 0.05 mg $kg^{-1}$ (Centrofarm Services BV, Etten-Leur, the Netherlands). Tracheotomy was performed to enable mechanical ventilation. Ventilator settings were adjusted on end-tidal $PCO_2$, keeping the arterial $CO_2$ partial pressure at 35-45 mmHg; the inspired oxygen concentration was set at 40%. The right jugular vein was catheterized with a polyethylene 0.9 mm catheter for intravenous fluid administration. The left femoral artery was catheterized to monitor arterial blood pressure and heart rate, and for hourly blood gas analysis. Cardiac output was measured by a thermodilution method with a thermistor inserted in the right carotid artery. Anesthesia and fluid balance were maintained by continuous infusion of ketamine (50 mg $kg^{-1}$ $h^{-1}$), a crystalloid (Ringer's lactate, B. Braun Melsungen AG, Melsungen, Germany) and a synthetic colloid solution (2.5 mL $kg^{-1}$ $h^{-1}$) (Voluven®, Fresenius Kabi, Bad Homburg, Germany). Body temperature was measured rectally and maintained at 38 ± 0.5°C by means of a heating pad.

### EXPERIMENTAL PROCEDURES

Abdominal hair was removed by shaving followed by application of hair removal cream (Veet, Reckitt Benckiser Co., Slough, UK) for about 5 min. PpIX was induced by affixing a freshly prepared 2.5% 5-aminolevulinic acid (ALA) (Sigma-Aldrich, St. Louis, MO, USA) in hydrophilic cremor lanette (Lanettecreme I FNA, Bipharma, Weesp, the Netherlands). The ALA affixed skin was covered with an adhesive film to avoid oxygen diffusion from the surrounding. The skin was covered with aluminum foil to protect PpIX from light exposure. As determined previously, sufficient PpIX should be converted within 3 h after ALA application [16]. Mito$PO_2$ and mito$VO_2$ measurements were performed at 3 (T0) and 6 (T1) h after ALA application.

The 40 rats were randomly divided into 5 groups (8 rats/group); two control groups consisting of a time control group (TC) and a control group receiving succinate (SC). Three

LPS-induced endotoxemic groups consisting of a group in which only LPS was given (LPS -), a LPS group receiving fluid resuscitation (LPS+-), and a LPS group receiving fluid resuscitation and succinate (LPS++). Fluid resuscitation (Voluven®, 5 ml*kg$^{-1}$*h$^{-1}$) was given to prevent hemodynamic shock and a decline in mitoPO$_2$. Succinate dimethyl ester (Brunschwig Chemie, Amsterdam, the Netherlands, 5 ml*kg$^{-1}$*h$^{-1}$) was infused 2 h prior to the LPS infusion in the SC and LPS ++ groups. For the remaining groups, the 0.67 M succinate solution was exchanged for saline at the same rate.

In all three LPS groups endotoxemia was induced by intravenous LPS injection (lipopolysaccharide from E.Coli 0127:B8, Sigma-Aldrich, St. Louis, MO, USA). After recording baseline values (T0), a solution of 2 mg/ml LPS was infused during 30 min. Fluid resuscitation was performed by doubling the maintenance colloid infusion directly after LPS application and by an additional fluid bolus of 1 ml during 10 min prior to T1. The timeline of the experiment is shown in Figure 1.

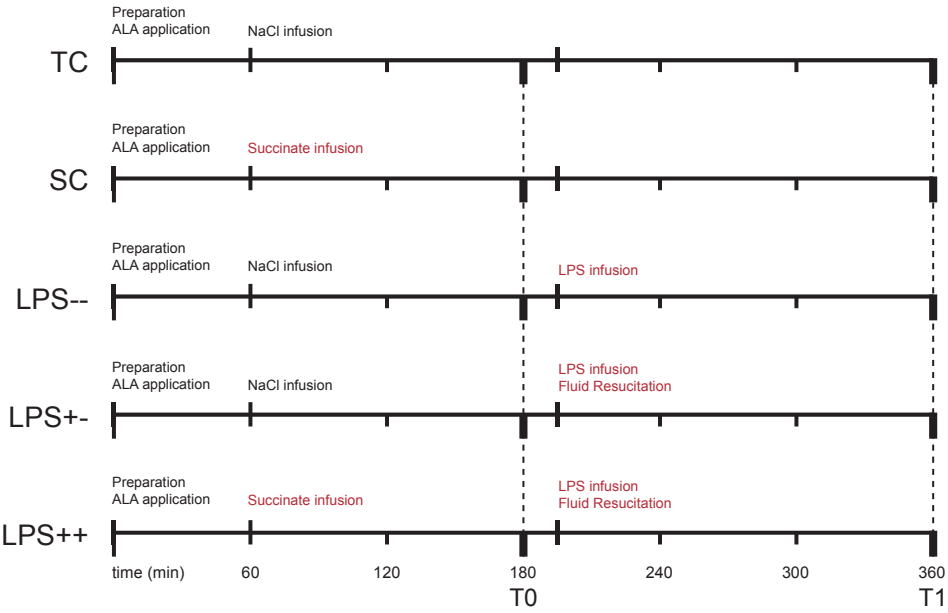


**Figure 1.** Schematic timeline of the experimental protocol. TC; time control, SC; succinate control, LPS --; endotoxemia, LPS +-; endotoxemia with fluid resuscitation, LPS ++; endotoxemia with fluid resuscitation and succinate. ALA; 5- aminolevulinic acid, LPS; lipopolysaccharide, T0 and T1 are the time points of mitoPO$_2$ and mitoVO$_2$ measurement.

PRINCIPLE OF MITO$PO_2$ MEASUREMENTS

The background of the PpIX-TSLT is described in detail elsewhere [13, 14]. In short, PpIX is the final precursor of heme in the heme biosynthetic pathway. PpIX is synthesized in the mitochondria, and administration of ALA substantially enhances the PpIX concentration. PpIX possesses a triplet state that reacts strongly with oxygen, making its lifetime oxygen-dependent. Population of the first excited triplet state occurs upon photoexcitation with a pulse of light, and causes the emission of red delayed fluorescence. The delayed fluorescence lifetime is related to the mito$PO_2$ according to the Stern-Volmer equation:

$$mitoPO_2 = \left(1/\tau - 1/\tau_0\right)/k_q \quad (1)$$

in which $\tau$ is the measured delayed fluorescence lifetime, $k_q$ is the quenching constant and $\tau_0$ is the lifetime at zero oxygen. In case of a non-homogenous oxygen distribution inside the measurement volume, a reliable estimation of the average $PO_2$ can be made by the rectangular distribution method (RDM) [19, 20]. In the present study the latter was used for fitting the delayed fluorescence signals.

PRINCIPLE OF MITO$VO_2$ MEASUREMENTS

Mito$VO_2$ is measured by the oxygen disappearance rate after local occlusion of the oxygen supply. The reflection probe was mounted on a height-adjustable construction, above the ALA-treated skin, providing different settings of the probe distances to the skin. Local occlusion of the microcirculation in the skin was obtained by local pressure with the measurement probe. This simple procedure created reliably stop-flow conditions and induced measurable oxygen disappearance rates, due to cessation of microvascular oxygen supply and ongoing cellular oxygen consumption. Mito$PO_2$ was measured before and during application of pressure at an interval of 1Hz and using 1 laser pulse per measurement. We have described the fundamental principles behind the technology and have provided a working implementation of the technique for mito$VO_2$ measurements *in vivo* [12] and a method to calculate mito$VO_2$ from the mito$PO_2$ kinetics:

$$dP_n/d_n = -(V_0 \cdot P_n)/(P_{50} + P_n) + Z(P_0 - P_n) \quad (2)$$

In this equation, $P_n$ is the measured $PO_2$ after excitation flash number $n$, $P_0$ is the mean $PO_2$ before stop-flow, $dP_n/d_n$ is the rate of oxygen disappearance and Z in the inflow coefficient for oxygen diffusion from the surrounding tissue into the measuring volume.

### STATISTICAL ANALYSIS

Data are expressed as means with standard deviation (SD), unless stated otherwise. A paired t-test was used to detect intergroup differences. Two-way ANOVA with Bonferoni post-test was used to detect intragroup differences. Normality was tested by Q-Q analysis and the Shapiro-Wilk test. A p-value $< 0.05$ was considered statistically significant.

## RESULTS

### HEMODYNAMIC PARAMETERS

Table 1 presents data on hemodynamic parameters of the experimental groups. At baseline (T0) all rats were hemodynamically stable and no significant difference was observed between the groups. Three hours after LPS infusion (T1), significant ($p<0.05$) hemodynamic changes were observed in the LPS groups, reflected by an elevation in serum lactate levels and a decrease in mean arterial blood pressure (MAP). In the LPS + - group tissue hypoperfusion was avoided by means of fluid resuscitation; this resulted in an increase in cardiac output and in an unchanged MAP.

### MITO$PO_2$ MEASUREMENTS

The application of ALA increased the amount of PpIX in the mitochondria to measurable levels, in accordance with previous experiments [16]. This increase in PpIX levels enabled measurement of mito$PO_2$ on abdominal rat skin 3 h after application of ALA. At baseline, a mito$PO_2$ value around 60 mmHg was observed in all experimental groups. At T1, a significant decline in mito$PO_2$ from 62 ± 9 mmHg to 40 ± 12 mmHg was measured in the LPS -- group. In the other LPS groups, fluid resuscitation prevented tissue hypoperfusion resulting in almost unchanged oxygen values compared to baseline (Figure 2a). The intra-individual changes in mito$PO_2$ are presented in Figure 2b.

**Table 1: Hemodynamic parameters**

| | T0 | T1 |
|---|---|---|
| **MAP (Torr)** | | |
| TC | 107±8 | 90±11 |
| SC | 97±15 | 80±7 |
| LPS -- | 100±12 | 73±15 * |
| LPS +- | 102±11 | 81±13 |
| LPS ++ | 103±10 | 71±4 * |
| **Cardiac Output (ml/min)** | | |
| TC | 153±58 | 140±56 |
| SC | 145±62 | 135±55 |
| LPS -- | 158±26 | 102±59 |
| LPS +- | 165±34 | 148±46 |
| LPS ++ | 126±35 | 100±39 |
| **Heart Rate (bpm)** | | |
| TC | 263±19 | 290±13 |
| SC | 258±16 | 267±11 |
| LPS -- | 267±20 | 294±30 |
| LPS +- | 276±16 | 306±16 |
| LPS ++ | 259±15 | 305±15 |
| **Lactate (mmol/L)** | | |
| TC | 1,2±0,2 | 1,0±0,2 |
| SC | 1,0±0,2 | 1,0±0,2 |
| LPS -- | 1,2±0,3 | 2,5±0,9 * |
| LPS+- | 1,4±0,5 | 2,2±0,8 ** |
| LPS ++ | 1,2±0,1 | 2,5±0,7 * |

Values are means ± SE,

* = P<0.05 compared to TC; ** = P<0.001 compared to TC

TC, time control; SC, succinate control; LPS --, endotoxemia

LPS +-, endotoxemia + fluid resuscitation; LPS ++,

endotoxemia + fluid resuscitation + succinate

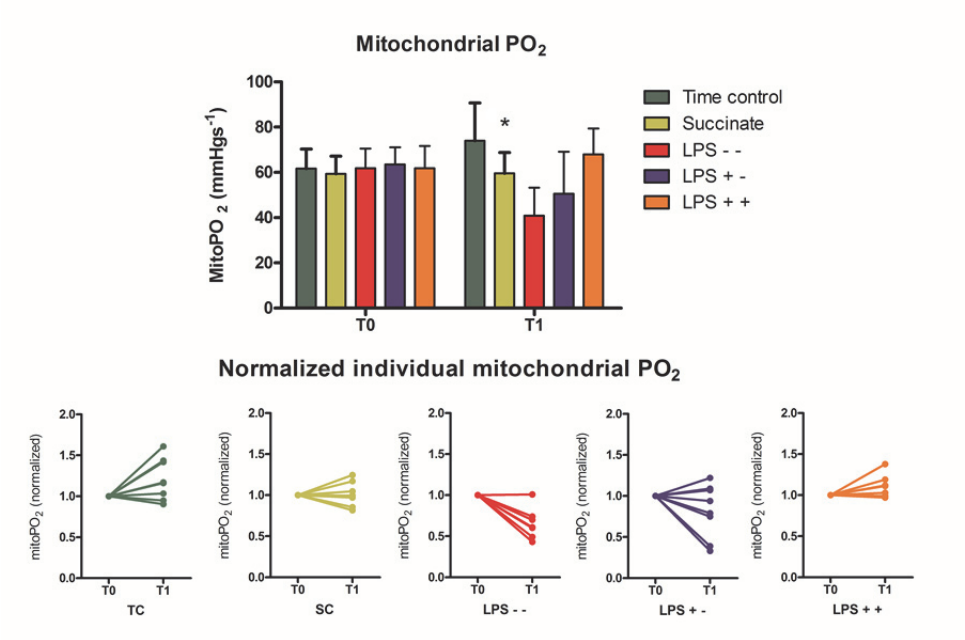


**Figure 2.** Panel A: Mito$PO_2$ at T0 and T1 in the different experimental groups. Panel B: Percentage change in mito$PO_2$. TC; time control, SC; succinate control, LPS --; endotoxemia, LPS +-; endotoxemia with fluid resuscitation, LPS ++; endotoxemia with fluid resuscitation and succinate administration, LPS; lipopolysaccharide, mito$PO_2$; mitochondrial oxygen tension. T0 and T1 are the time points of the mito$PO_2$ measurement. Data are presented as mean ± SD, * significant difference compared to baseline measurements ($p<0.05$); n=40 (8 rats/group).



## MITO$VO_2$ MEASUREMENTS

Mito$VO_2$ derives from the decay of the mito$PO_2$ slope during blocked microcirculatory blood flow and interrupted oxygen supply. At T0 the initial mito$PO_2$ was approximately 60 mmHg. Under baseline circumstances, blocking the microcirculation by local pressure with the measurement probe, caused a drop in mito$PO_2$ from 60 mmHg to approximately 10 mmHg in 10 s (Fig. 3); this resulted in a mito$VO_2$ of 4.4 mmHg. At T1 no significant changes were observed in the control groups. However, after inhibition of complex I by means of LPS, a significant decrease in mito$VO_2$ was observed from 4.5 ± 1.0 mmHg to 2.4 + 1.5 mmHg. This effect was also present (without signs of hypoperfusion) in the LPS + - group. Activation of complex II of the mitochondrial electron chain by succinate infusion maintained mito$VO_2$ at baseline values (Fig. 4a).

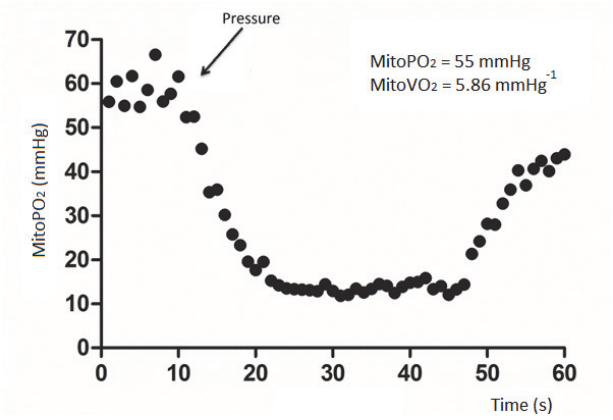


**Figure 3.** Typical example of *in vivo* mitochondrial respirometry measured at T0 on the abdominal skin of a rat. The mitoVO$_2$ was determined from the linear part of the oxygen disappearance curve by fitting equation 2. MitoPO$_2$ was the mean mitoPO$_2$ before the start of tissue compression.

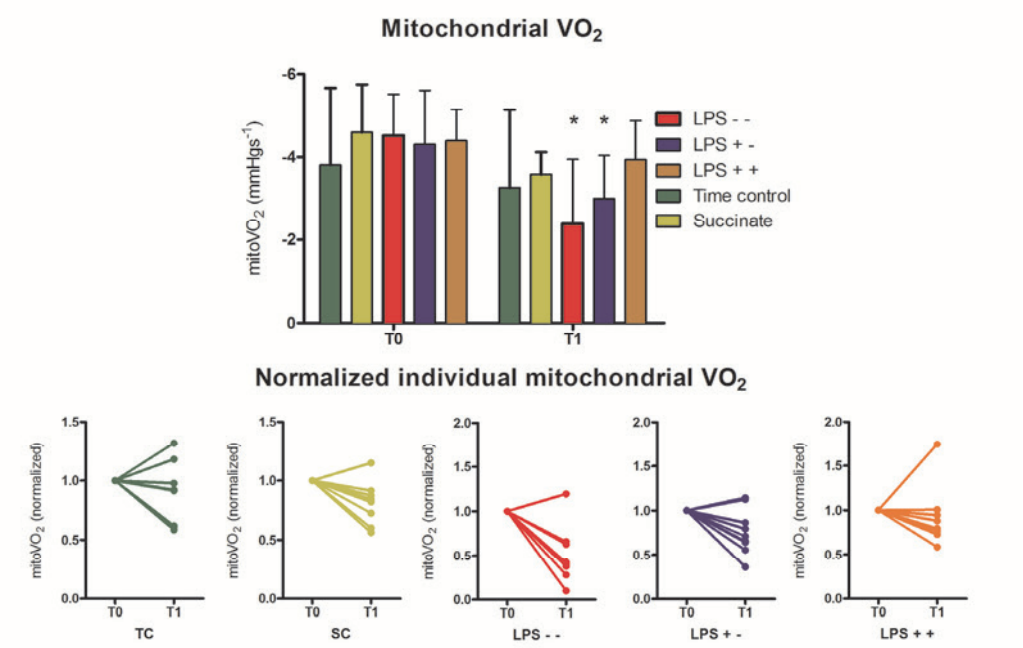


**Figure 4.** Panel A: mitoVO$_2$ at T0 and T1 in the different experimental groups. Panel B: Percentage change in mitoVO$_2$. TC; time control, SC; succinate control, LPS --; endotoxemia, LPS +-; endotoxemia with fluid resuscitation, LPS ++; endotoxemia with fluid resuscitation and succinate administration, LPS; lipopolysaccharide, mitoVO$_2$; mitochondrial oxygen consumption. T0 and T1 are the time points of mitoVO$_2$ measurement. Data are presented as mean ± SD, * significant difference compared to baseline measurements ($p<0.05$); n=40 (8 rats/group).

## DISCUSSION

The present study undertook further validation of *in vivo* mitoVO$_2$ measurements by means of PpIX-TSLT. The underlying concept was derived from reproducing the positive effect of succinate on mitochondrial oxygen consumption, as demonstrated *in vitro* by muscle biopsies from LPS-treated animals in skin *in vivo* [18, 21]. Until now, these effects could only be determined in isolated mitochondria. However, because we produced results similar to those found in isolated mitochondria, we propose that our novel measurement method enables efficient monitoring of alterations in mitochondrial function.

The administration of LPS causes inhibition of complex I of the mitochondrial electron transport chain [17], resulting in a decrease in mitochondrial oxygen consumption. In our *in vivo* respirometry experiments, the induction of LPS resulted in decreased mitoVO$_2$. Fluid resuscitation in the LPS +- group prevented tissue hypoperfusion, which often occurs after rapid and/or long-term LPS infusion. Unaltered and adequate tissue oxygenation in the control groups (TC and SC) resulted in unchanged mitoPO$_2$. Despite unchanged mitoPO$_2$ values, the mitoVO$_2$ of the LPS +- treated rats showed a significant difference between the control groups. However, the greatest difference was observed in the LPS ++ group, in which mitoVO$_2$ values recovered to baseline values. It is known from classical mitochondrial respirometry experiments that mitochondrial oxygen consumption restores after administration of succinate [18, 21]. This effect is probably caused by increased activity of complex II. In our *in vivo* experiments, the application of succinate in the LPS-treated rats also resulted in restoration of mitoVO$_2$ to baseline values. This demonstrates that *in vivo* mitoVO$_2$ measurements allow to show alterations in mitochondrial oxygen consumption. Importantly, PpIX-TSLT is able to detect alterations in mitochondrial oxygen consumption that are independent of the oxygen pressure in the mitochondrion. This may allow to make a distinction between problems related to oxygen supply or oxygen consumption on the cellular level in critical illness.

Earlier studies have shown the protective effects of succinate on mitochondrial function [22, 23]. Although this was not a primary goal in the present study, our rat model of endotoxemia also demonstrated the protective effect of succinate on mitochondrial oxygen consumption. However, since our data only demonstrate the capability of our experimental technique, further research is needed to test the clinical relevance of the protective effect of succinate in mitochondrial dysfunction. In the future, PpIX-TSLM could

become a useful clinical tool to monitor the deterioration and recovery of mitochondrial function in critically ill patients.

The applicability of PpIX-TSLT in humans [7, 12] provides an opportunity to develop a non-invasive monitoring tool which will provide *in vivo* information on mitochondrial function without tissue damage and functional loss. Therefore, our method may overcome some of the current disadvantages [3] and might pave the way for clinical bedside monitoring. The PpIX-TSLT could prove to be a valuable tool for ongoing research and treatment of mitochondrial dysfunction in sepsis, as suggested by Jeger et al. [3].

## CONCLUSION

This study shows the feasibility to monitor mitochondrial function in endotoxemic rats by means of cutaneous PpIX-TSLT measurements. A decrease in mito$VO_2$ in the presence of preserved or restored mito$PO_2$ suggests that mitochondrial dysfunction may contribute to metabolic failure in sepsis, even in the absence of hemodynamic shock. These results will hopefully lead to a clinical mitochondrial monitoring technique. It is expected that clinical implementation of this technique will contribute to our understanding of mitochondrial dysfunction in sepsis and the development of therapeutic approaches aimed at restoring aerobic metabolism and cellular function.

## ACKNOWLEDGMENTS

The authors thank Jacqueline Voorbeijtel and Patricia Specht for their expert biotechnical help. This research is financially supported by a Life Sciences Pre-Seed Grant (grant no. 40-41300-98-9037) from the Dutch Organization for Health Research and Development (ZonMW).

**CONFLICT OF INTEREST**

Dr. E.G. Mik is founder and shareholder of Photonics Healthcare B.V., a company aimed at making the delayed fluorescence lifetime technology available to a broad public. Photonics Healthcare B.V. holds the exclusive licenses to several patents regarding this technology, filed and owned by the Academic Medical Center in Amsterdam and the Erasmus Medical Center in Rotterdam, The Netherlands.

## References


1. Fink, M.P., *Bench-to-bedside review: Cytopathic hypoxia.*, in *Crit Care*. 2002. p. 491-499.
2. Nederlof, R., et al., *Pathophysiological consequences of TAT-HKII peptide administration are independent of impaired vascular function and ensuing ischemia.* Circ Res, 2013. **112**(2): p. e8-13.
3. Crocchiolo, P.R., et al., *CD4+:neopterin ratio correlates with p24 antigenaemia in HIV infected patients.* J Clin Lab Immunol, 1990. **31**(2): p. 55-7.
4. Brealey, D., et al., *Mitochondrial dysfunction in a long-term rodent model of sepsis and organ failure.* American Journal of Physiology - Regulatory Integrative and Comparative Physiology, 2004. **286**(3 55-3): p. R491-R497.
5. Harada, A., et al., *Biatrial isolation--a new surgical treatment for supraventricular tachycardia.* Jpn Circ J, 1990. **54**(1): p. 100-8.
6. Konrad, F.M., et al., *Acute Normovolemic Hemodilution in the Pig Is Associated with Renal Tissue Edema, Impaired Renal Microvascular Oxygenation, and Functional Loss.* Anesthesiology, 2013. **119**(2): p. 256-269.
7. Mik, E.G., *Measuring Mitochondrial Oxygen Tension: From Basic Principles to Application in Humans.* Anesth Analg, 2013.
8. Esposito, F., et al., *Isolation of cDNA fragments hybridizing to rat brain-specific mRNAs.* Dev Neurosci, 1990. **12**(6): p. 373-81.
9. Callahan, L.A. and G.S. Supinski, *Sepsis induces diaphragm electron transport chain dysfunction and protein depletion.* Am J Respir Crit Care Med, 2005. **172**(7): p. 861-8.
10. Piffaretti, F., et al., *Optical fiber-based setup for in vivo measurement of the delayed fluorescence lifetime of oxygen sensors.* J Biomed Opt, 2011. **16**(3): p. 037005.

11. Ishii, N., *Role of oxidative stress from mitochondria on aging and cancer.* Cornea, 2007. **26**(9 Suppl 1): p. S3-9.
12. Harms, F.A., et al., *Cutaneous respirometry by dynamic measurement of mitochondrial oxygen tension for monitoring mitochondrial function in vivo.* Mitochondrion, 2012.
13. Mik, E.G., et al., *In vivo mitochondrial oxygen tension measured by a delayed fluorescence lifetime technique.* Biophys J, 2008. **95**(8): p. 3977-90.
14. Mik, E.G., et al., *Mitochondrial PO2 measured by delayed fluorescence of endogenous protoporphyrin IX.* Nat Methods, 2006. **3**(11): p. 939-45.
15. Choi, J.K., et al., *Evaluation of mean skin temperature formulas by infrared thermography.* Int J Biometeorol, 1997. **41**(2): p. 68-75.
16. Harms, F.A., et al., *Oxygen-dependent delayed fluorescence measured in skin after topical application of 5-aminolevulinic acid.* J Biophotonics, 2011. **4**(10): p. 731-9.
17. Choumar, A., et al., *Lipopolysaccharide-induced mitochondrial DNA depletion.* Antioxid Redox Signal, 2011. **15**(11): p. 2837-54.
18. Singh, K.K., *Mitochondria damage checkpoint, aging, and cancer.* Ann N Y Acad Sci, 2006. **1067**: p. 182-90.
19. Golub, A.S., et al., *Analysis of phosphorescence in heterogeneous systems using distributions of quencher concentration.* Biophys J, 1997. **73**(1): p. 452-65.
20. Bodmer, S.I., et al., *Microvascular and mitochondrial PO(2) simultaneously measured by oxygen-dependent delayed luminescence.* J Biophotonics, 2012. **5**(2): p. 140-51.
21. Edeas, M., , Weissig, V., *Strategies, Innovations & Clincal Applications*, in *Targeting Mitochondria*, M. Edeas, , Weissig, V., Editor. 2014: Berlin.
22. Ferreira, F.L., et al., *Prolongation of survival time by infusion of succinic acid dimethyl ester in a caecal ligation and perforation model of sepsis.* Horm Metab Res, 2000. **32**(8): p. 335-6.
23. Malaisse, W.J., et al., *Protective effects of succinic acid dimethyl ester infusion in experimental endotoxemia.* Nutrition, 1997. **13**(4): p. 330-41.

# CHAPTER 7

# *Cutaneous mitochondrial respirometry: towards clinical monitoring of mitochondrial function*

Floor A. Harms[1], Sander I.A. Bodmer[1], Nicolaas J.H. Raat[1], Egbert G. Mik[1,2]

1 Department of Anesthesiology, Laboratory of Experimental Anesthesiology, Erasmus MC – University Medical Center Rotterdam, 's-Gravendijkwal 230, 3015 CE Rotterdam, The Netherlands

2 Department of Intensive Care, Erasmus MC – University Medical Center Rotterdam, 's-Gravendijkwal 230, 3015 CE Rotterdam, The Netherlands

**Short title**: Towards clinical monitoring of mitochondrial function

Published in: J Clin Monit Comput, 2014; Article in press

**ABSTRACT**

The recently developed technique for measuring cutaneous mitochondrial oxygen tension ($mitoPO_2$) by means of the Protoporphyrin IX - Triplet State Lifetime Technique (PpIX-TSLT) provides new opportunities for assessing mitochondrial function *in vivo*. The aims of this work were to study whether cutaneous mitochondrial measurements reflect mitochondrial status in other parts of the body and to demonstrate the feasibility of the technique for potential clinical use.

The first part of this paper demonstrates a correlation between alterations in mitochondrial parameters in skin and other tissues during endotoxemia. Experiments were performed in rats in which mitochondrial dysfunction was induced by a lipopolysaccharide-induced sepsis (n = 5) and a time control group (n = 5). $MitoPO_2$ and mitochondrial oxygen consumption ($mitoVO_2$) were measured using PpIX-TSLT in skin, liver and buccal mucosa of the mouth. Both skin and buccal mucosa show a significant $mitoPO_2$-independent decrease ($P<0.05$) in $mitoVO_2$ after LPS infusion (a decrease of 37% and 39% respectively). In liver both $mitoPO_2$ and $mitoVO_2$ decreased significantly (33% and 27% respectively).

The second part of this paper describes the clinical concept of monitoring cutaneous mitochondrial respiration in man. A first prototype of a clinical PpIX-TSLT monitor is described and its usability is demonstrated on human skin. We expect that clinical implementation of this device will greatly contribute to our understanding of mitochondrial oxygenation and oxygen metabolism in perioperative medicine and in critical illness. Our ultimate goal is to develop a clinical monitor for mitochondrial function and the current results are an important step forward.

**INTRODUCTION**

The maintenance of cellular activity and normal physiological organ function depends on cellular energy production by the mitochondria. Adequate production of adenosine triphosphate (ATP) depends on sufficient oxygen supply and the unhampered use of oxygen. During the last decades numerous publications have shown the involvement of mitochondrial dysfunction in a variety of human disorders, such as cardiovascular [1] and neurodegenerative diseases [2]. Mitochondrial dysfunction also occurs in acute illness like sepsis, a phenomenon originally termed ‘cytopathic hypoxia’[3-5]. Sepsis-related

mitochondrial dysfunction makes it important to investigate possible mitochondrial therapies [6]. Unfortunately, most mitochondrial interventions have led to little conclusive evidence of any therapeutic effect [6, 7]. The absence of a therapeutic effect could be explained by unknown factors related to the pathogenesis of sepsis and the poorly understood mechanisms behind mitochondrial dysfunction *in vivo*. Studies have shown discrepancies between respiration measured in isolated mitochondria and intact cells [8, 9]. Therefore, there is need for monitoring systems that enable assessment of mitochondrial function *in vivo* at the bedside.

Most of our knowledge about mitochondrial dysfunction in sepsis is derived from animal experiments in isolated mitochondria [10-12]. Ethical and technical difficulties constrain the availability of vital human biopsy tissue, especially when repeated sampling is required to monitor disease progression. Hence, a non-invasive monitoring tool that can be used *in vivo* and in human beings will contribute to a better understanding, diagnosis and treatment of sepsis. The recently developed technique to measure the mitochondrial $PO_2$ ($mitoPO_2$), by means of the Protoporphyrin IX - Triplet State Lifetime Technique (PpIX-TSLT) [13, 14] provides a new opportunity to measure mitochondrial function *in vivo*. With PpIX-TSLT $mitoPO_2$ can be measured by means of the oxygen-dependent change in lifetime of 5-aminolevulinic acid (ALA) induced endogenous protoporphyrin IX (PpIX). PpIX-TSLT is the first technique that allows measurements of $mitoPO_2$ in living cells and also can be applied *in vivo* [13-15]. Recently we measured $mitoPO_2$ in human skin by topical application of ALA [16,17].

PpIX-TSLT can monitor mitochondrial function *in vivo* and has been proposed as a potential clinical non-invasive tool in human beings [18, 19]. Our idea is to combine PpIX-TSLT-based $mitoPO_2$ measurements with the principles of oxygen disappearance rate (ODR) measurements [20-23]. The ODR principle is based on the dynamic measurement of the change in $PO_2$ after the cessation of oxygen supply. Combining steady-state $mitoPO_2$ and ODR measurements can provide useful information about mitochondrial oxygenation and oxygen consumption and can be applied *in vivo* and in humans. We have developed mitochondrial respirometry for monitoring $mitoPO_2$ and mitochondrial oxygen consumption ($mitoVO_2$) in skin [24]. The principle has been tested in experimental animals and we constructed a first clinical applicable prototype for $mitoPO_2$ monitor in humans being. Recently the Medical Ethics Committee of the Erasmus University Medical Center approved the PpIX-TSLT measurements in healthy volunteers. In this paper we provide the results of a rat study aimed at studying the relevance of measuring mitochondrial

parameters in skin. In addition, we describe the clinical mitoPO$_2$ monitor and its first use in healthy volunteers.

The first part of this paper investigates the relation between mitochondrial respiration and PO$_2$ in skin, liver and buccal mucosa in a rat model of lipopolysaccharide (LPS)-induced sepsis. We also further validated the technique for measuring mitoPO$_2$ in an additional group of rats. To this end we investigated the response of cutaneous tissue saturation, microvascular blood flow and mitoPO$_2$ on pharmacological hemodynamic interventions. Another part of this paper describes the clinical concept of the cutaneous PpIX-TSLT-based mitochondrial respirometry after topical application of ALA patches. Furthermore, a technical description of the developed clinical mitoPO$_2$ monitor prototype is given, followed by some first data from measurements in healthy volunteers.

## METHODS

### PRINCIPLE OF MITOPO$_2$ MEASUREMENTS

The background of the PpIX-TSLT is described in detail elsewhere [13, 14, 19]. In short, PpIX is the final precursor of heme in the heme biosynthetic pathway. PpIX is synthesized in the mitochondria, and administration of ALA substantially enhances the PpIX concentration. Since the conversion of PpIX to heme is a rate-limiting step, administration of ALA causes accumulation of PpIX inside the mitochondria. PpIX possesses a triplet state that reacts strongly with oxygen, making its lifetime oxygen-dependent. Population of the first excited triplet state occurs upon photo-excitation with a pulse of light. Relaxation to the ground state can occur either spontaneously, causing emission of red delayed fluorescence, or by collision with oxygen and subsequent energy transfer without emission of light (figure 1A). This quenching process makes the delayed fluorescence emission oxygen-dependent in a way that the presence of oxygen will shorten the lifetime (figure 1B). The delayed fluorescence lifetime is related to mitoPO$_2$ according to the Stern-Volmer equation:

$$mitoPO_2 = \left(1/\tau - 1/\tau_0\right)/k_q \qquad (1)$$

in which $\tau$ is the measured delayed fluorescence lifetime, $k_q$ is the quenching constant and $\tau_0$ is the lifetime at zero oxygen. In case of a non-homogenous oxygen distribution inside

the measurement volume, a reliable estimation of the average $PO_2$ can be made by the Rectangular Distribution Method (RDM) [25, 26]:

$$Y(t) = Y_0 \exp\left[-\left(1/\tau_0 + kq\langle mitoPO_2\rangle\right)t\right]\sinh(k_q\delta t)/k_q\delta t \qquad (2)$$

where Y(t) is the delayed fluorescence signal, t is the time from the beginning of the delayed fluorescence decay, $Y_0$ is the initial signal intensity at t = 0, <mitoPO$_2$> is the average mitochondrial oxygen tension and $\delta$ is the half-width of the $PO_2$ distribution.

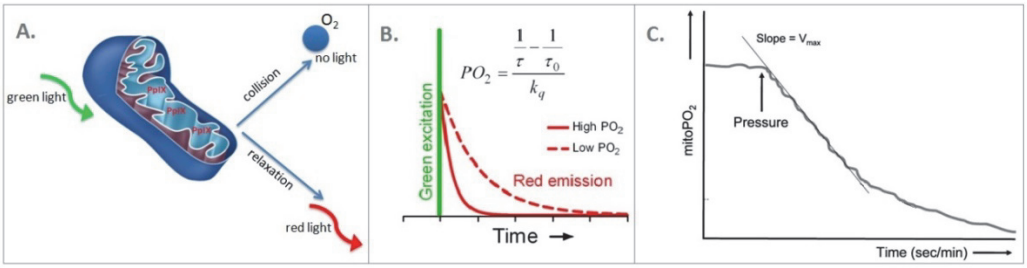


**Figure 1.** Background of the Protoporphyrin IX - Triplet State Lifetime Technique. Panel A shows the principle of the technique. Panel B shows the principle of measuring mitochondrial $PO_2$ by means of oxygen-dependent delayed fluorescence of PpIX, using pulsed excitation with green (510 nm) light. The delayed fluorescence lifetime is oxygen-dependent according to the Stern-Volmer equation, in which $k_q$ is the quenching constant and $\tau_0$ is the lifetime at zero oxygen. Panel C shows a theoretical time-course of mitoPO$_2$ during an ODR measurement



## PRINCIPLE OF MITOVO$_2$ MEASUREMENTS

Oxygen-dependent delayed fluorescence was induced by the administration of ALA, either by intraperitoneal injection or by applying an ALA containing adhesive patch to skin (explained in more detail below). Local occlusion of the microcirculation in the tissue was obtained by applying localized pressure with the measuring probe on the measurement volume. This simple procedure created stop-flow conditions and induced measurable oxygen disappearance due to cessation of microvascular oxygen supply and ongoing cellular oxygen consumption. MitoPO$_2$ in the measurement volume was measured, before and during application of pressure, by repeated measurements at a rate of 2 Hz using a single laser pulse per individual mitoPO$_2$ measurement. The rate of mitoPO$_2$ change during stop-flow conditions was determined from the linear part of the curve directly after the beginning of tissue compression, the decay from the slope was calculated as $\Delta$mitoPO$_2$/$\Delta$t as shown in Figure 1C [24].

EXPERIMENTAL PROCEDURES IN RATS

All animal care and handling was performed in accordance with the guidelines for Institutional and Animal Care and Use Committees and the protocol was approved by the Animal Research Committee of the Erasmus MC University Medical Center Rotterdam.

A total of 16 male Wistar rats (Charles River, Wilmington, MA, USA, body weight 275 - 325 g) were used in this experiment. The rats were assigned into one of the following three groups: a lipopolysaccharide (LPS) (n=5) ,a control group (n=5) and into a third separated group (n=6) wherein tissue saturation, flow and mito$PO_2$ of the skin was measured (FLOW-group).

To enhance mitochondrial PpIX concentration, all rats of the LPS and control groups received an intraperitoneal injection of 200 mg $kg^{-1}$ 5-aminolevulinic acid (ALA, Sigma-Aldrich, St. Louis, MO, USA) three hours before the start of experimental procedures. At the beginning of the experiment, animals were anesthetized by an intraperitoneal injection of a mixture of ketamine 90 mg $kg^{-1}$ (Alfasan, Woerden, The Netherlands), medetomidine 0.5 mg $kg^{-1}$ (Sedator Eurovet Animal Health BV, Bladel, The Netherlands), and atropine 0.05 mg $kg^{-1}$ (Centrofarm Services BV, Etten-Leur, The Netherlands). Mechanical ventilation was performed via tracheotomy. Ventilation was adjusted on end-tidal $PCO_2$, keeping the arterial $PCO_2$ between 35 and 40 mmHg. The inspired oxygen concentration was set at 40%. A polyethylene catheter (outer diameter 0.9 mm) was inserted into the right jugular vein for the intravenous administration of fluids. Arterial blood pressure and heart rate were monitored with a similar catheter in the right carotid artery. Ketamine (50 mg $kg^{-1}$ $h^{-1}$) and crystalloid solution (Ringer lactate, 5 mL $kg^{-1}$ $h^{-1}$) were infused intravenously for maintaining anaesthesia and fluid balance. Body temperature was measured rectally and kept at 38 $^{\circ}C \pm 0.5$ $^{\circ}C$ by means of a heating pad.

The hair of the abdominal skin was shaved and persistent hair was further removed with the aid of a commercially available hair removal cream (Veet, Reckitt Benckiser Co., Slough, UK). Directly after induction of anaesthesia in the FLOW-group a 2,5% ALA cream was applied topically on the abdominal skin of the rats. In the LPS and control groups a midline laparotomy was performed to gain access to the liver, and teeth of the rat were removed to gain access to the buccal mucosa. To prevent premature exposure of PpIX to light, the rat was covered with aluminium foil. The baseline measurements of the LPS and control group where started after a 30 minutes stabilisation period. Immediately after baseline measurements, sepsis was induced in the LPS group by intravenous LPS injection (10 mg $kg^{-1}$) (extracted from E. coli, serotype 0127:B8; Sigma-Aldrich Corp. St. Louis, MO,

USA). The LPS was dissolved at a concentration of 5 mg ml $^{-1}$ in a crystalloid solution. During the induction period of three hours, the LPS treated rats were resuscitated by infusion of a colloid solution (Voluven 0.6 mL kg$^{-1}$ h$^{-1}$). The final measurements under septic circumstances were performed three hours after the baseline measurements. The experiments of the FLOW-group were started three hours after the application of ALA. All mito$PO_2$ measurements on the rats were performed by an experimental laser setup that was not suitable for clinical use. The details of the experimental laser setup are described elsewhere [16]. At the end of the experiment the rats were terminated by euthanasia of the animal using an overdose of pentobarbital (ST Farma, Raamsdonksveer, The Netherlands).

MITOCHONDRIAL RESPIROMETRY IN DIFFERENT ORGANS OF RATS

The mito$VO_2$ is measured by the oxygen disappearance rate (ODR) after local cessation of the oxygen supply. The reflection probe was mounted on a height adjustable holder above the tissues, providing different settings of the probe-to-tissue distances. Local pressure with the measurement probe on the skin was applied by adjusting the holder direction 2 cm downwards to the cutaneous tissue. This procedure resulted in a local occlusion of the microvessels and created microvascular stop-flow conditions and allowed local measurement of oxygen disappearance rates [30]. Mito$PO_2$ was measured before and during a 45 seconds pressure period, at an interval of 2 Hz and using 1 laser pulse per measurement. We used one single probe for the measurements in the different locations; therefore the probe was removed and replaced during the measurements. The significance of the differences of the measurements between baseline and after LPS was tested with a Wilcoxon's signed rank test and difference between LPS group and control group was tested by the Mann-Whitney U test.

TISSUE SATURATION, FLOW AND MITO$PO_2$ MEASUREMENTS IN SKIN

Cutaneous tissue saturation (i.e. microvascular oxygen saturation, µ$HbO_2$) and microvascular flow were measured by a combined remission spectroscopy and doppler flowmetry system(Oxygen-To-See (O2C), LEA Medizintechnik, Giessen). The measurement probe (LF 1, LEA Medizintechnik, Giessen, Germany) of the O2C was fixated to the surface of the abdominal skin of the rats. Mito$PO_2$ measurement where performed simultaneously with the O2C measurements under four different circumstances. Under baseline conditions, 5 minutes after start of infusion of the vasoconstrictor phenylephrine (6 µg kg$^{-1}$ h$^{-1}$) (Sigma Chemical Co, St Louis,. Missouri, USA), 10 minutes after the infusion was stopped and 5 min after start of infusion of the vasodilatator urapidil (0.2 mg kg$^{-1}$ h$^{-1}$) (Nordic Pharma B.V., Paris, France). To enable a more direct comparison between the

mitoPO$_2$ readings and the O2C data, estimations of venous PO$_2$ were calculated from the tissue saturation using Hill's equation according to reference [27].

NOVEL CLINICAL MEASUREMENT SETUP

As an important step in the development of a new clinical mitochondrial monitoring technique, a novel prototype PpIX-TSLT setup has been build, ready for a practical and safe use in the clinic. The excitation source of the new clinical laser-setup was a custom build InnoLas 515 nm SpitLight-COMPACT DPSS Yb:YAG-laserhead (InnoLas, Krailling, Germany). The laser pulses had a specified duration of 11 ns at a wavelength of 515 nm. The laser was coupled by a 20 cm planoconvex lens into a custom-made excitation probe (IR 400, polymicro technologies Phoenix, AZ, USA). The excitation probe and the reflection probe, which consisted of two 400 µm probes both with a length of 1 meter (IR 400, polymicro technologies Phoenix, AZ, USA), mounted at the common end with a small distance between the probes. The common end of the probes were coupled trough a SMA connector into a bigger fiber with a diameter of 1000 µm and 4 cm length (P1000-2-VIS-NIR, Ocean Optics, Dunedin, FL, USA), covered in a stainless steel rod with a length of 5 cm and a diameter of 10 mm. The stainless steel rod forms a part of the measurement head and is integrated with a temperature controllable heating element, controlled by a control pad (Cal 3300, Cal Controls Ltd., Hitchin, UK). The measurement head was designed with a simple spring mechanism that can exert pressure on the skin. Finally, the measurement head was shelled with a nylon housing to prevent interference by background light during the measurements. A picture of the measurement head is presented in Figure 2.

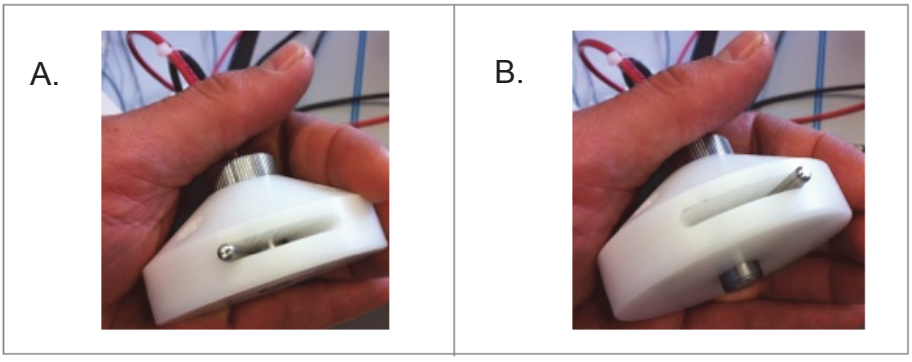


**Figure 2.** Picture of the measurement head with an integrated spring mechanism, which ensures no local pressure on the skin (panel A) or a reproducible amount of local pressure (panel B).

The light output of the excitation branch was measured by a FieldMate laser power meter with PowerMax PS19 measuring head (Coherent Inc., Santa Clara, CA, USA). A double switch footswitch (Footswitch XPEB311, Farnell InOne, Utrecht, The Netherlands) was

connected to the laser software and directly to the shutter of the laser in order to prevent unintentional use of the laser.

The PpIX signal was detected by a photomultiplier (PMT) module with gate function tube (H10304-20-NN, Hamamatsu Photonics, Hamamatsu, Japan). The detection probes were fit into an Oriel Fiber Bundle Focusing Assembly (Model 77799, Newport, Irvine, CA, USA) which was coupled to the PMT by an in-house built filter-holder, a plano convex lens (BK-7, Opto- Sigma, Santa Ana, CA, USA) with focal length of 90 mm and an electronic shutter (04 UTS 203, Melles Griot, Albuquerque, NM, USA). The shutter was controlled by an OEM Shutter Controller Board (59 OSC 205, Melles Griot, Albuquerque, NM, USA) and served as protection for the PMT, which was configured for the "normally on" mode. The PpIX emission light was filtered by a combination of a 590 nm longpass filter (OG590, Newport, Irvine, CA, USA) and a broadband (600–750 nm) bandpass filter (Omega Optical, Brattleboro, VT, USA). The output current of the photomultiplier was voltage-converted by an amplifier (Amplifier C6438-01, Hamamatsu Photonics, Hamamatsu, Japan) with an input impedance of 50 ohm, 500 times voltage amplification and a bandwidth around 50 Mhz.

Data-acquisition was performed by a PC-based data acquisition system containing a 2 MS/s simultaneous sampling data-acquisition board (NI USB-6356X, National Instruments, Austin, TX, USA). Control of the setup and analysis of the data was performed with software written in LabView (Version 10.0, National Instruments, Austin, TX, USA).
A schematic overview of all elements in the clinical measurement setup is given in Figure 3. All components of the clinical setup were build into a mobile housing (Minirack 19", Koning & Hartman B.V., Delft, The Netherlands). Electrical safety of the clinical setup was assured by three separation transformers (Separation transformers 1000 VA, Amplimo, The Netherlands) and was tested by a Bio-Tek 601Pro XL Safety Analyzer (Ultramedic LTD, Liverpool, UK)

MITOCHONDRIAL RESPIROMETRY IN A HUMAN VOLUNTEER

After institutional review board approval (CCMO registration: NL37911.078.11) we tested the new clinical setup in a healthy volunteer on the sternal skin. A self-adhesive patch containing 2 mg 5-aminolevulinic acid (ALA) was applied on the sternal skin and was protected from light for 5 hours. The mito$PO_2$ was measured under normal conditions and the ODR was determined by repeated mito$PO_2$ measurements on the ALA treated skin tissue, while locally blocking oxygen supply. The latter was achieved by applying local pressure with the measurement

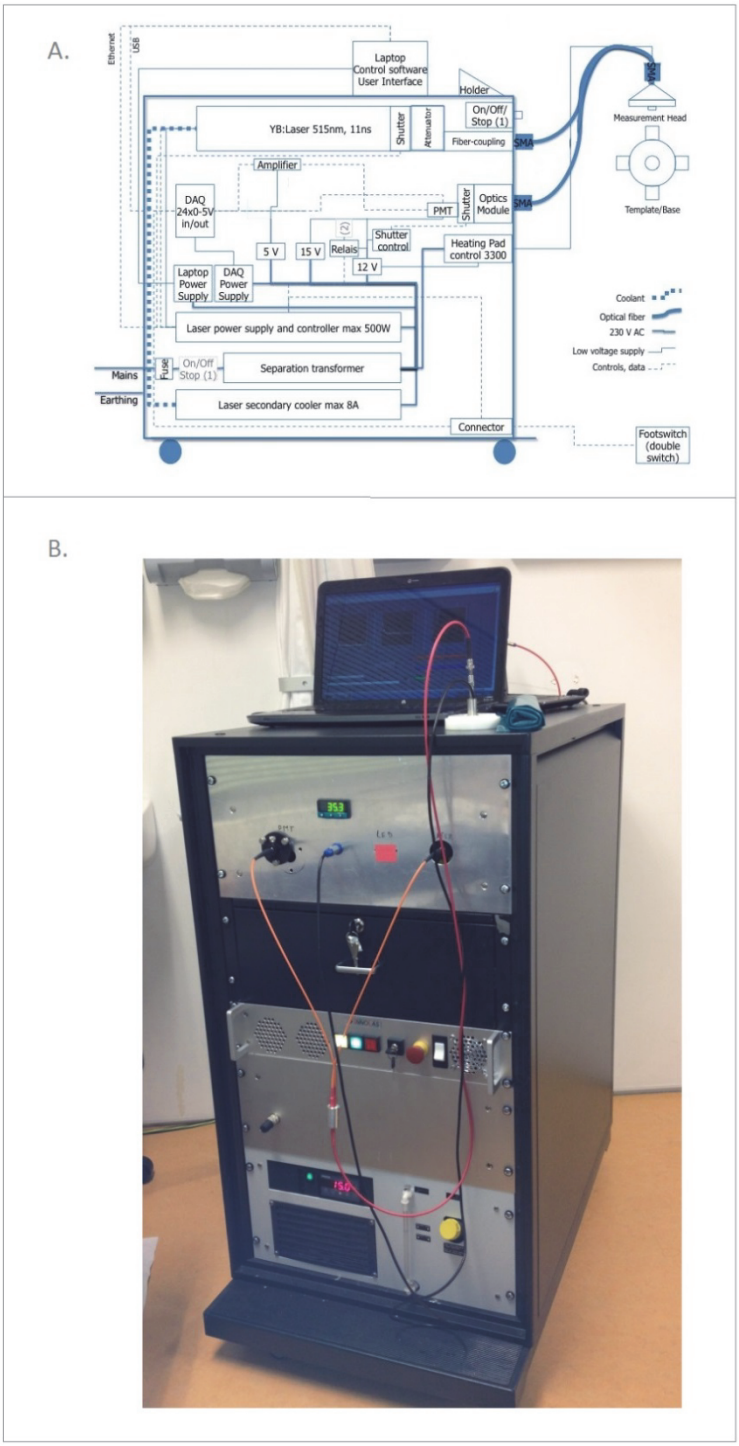


**Figure 3.** A schematic overview of the novel clinical PpIX-TSLT measurement setup (panel A) and a photograph of the working prototype in the policlinic (panel B).

probe generated by the spring mechanism integrated in the measurement head. Mito$PO_2$ was recorded before and during a period of 60 seconds compression of the microcirculation, at a 1 second interval and using 4 laser pulses per measurement.

## RESULTS

### MITOCHONDRIAL RESPIROMETRY IN DIFFERENT ORGANS OF RATS

The experiments were performed in two series of 5 rats in order to investigate the relationship between the mitochondrial function in the skin and other organs, like liver and buccal mucosa. The rats were assigned into two groups, a LPS and a control group. Table 1 shows the macro hemodynamic variables and laboratory values at baseline just before the start of the experiment ($t_1$) and 3 hours after ($t_2$). Before baseline measurements all rats were hemodynamic stable, and showed no signs of systemic hypoperfusion as witnessed by normal plasma lactate levels. Three hours after the induction of sepsis in the LPS group, significant ($P<0.05$) hemodynamic changes were observed compared to the control group. Macrocirculatory collaps and tissue hypoperfusion were avoided by means of fluid resuscitation, resulting in only a mild deterioration of mean arterial blood pressure and serum lactate.

**Table 1. Hemodynamic variables of the experimental animals**

| Variable | Baseline mean ± SE | After 3 h mean ± SE |
|---|---|---|
| CONTROL group | | |
| Heart rate, bpm | 257 ± 14 | 201 ± 5 |
| Mean arterial blood pressure, mmHg | 83 ± 2 | 72 ± 5 |
| Lactate | 0.7 ± 0.1 | 0.9 ± 0.1 |
| pH | 7.36 ± 0.03 | 7.26 ± 0.01 |
| Arterial blood $PO_2$, mmHg | 198 ± 6 | 207 ± 14 |
| Arterial blood PCO2, mmHg | 37 ± 3 | 39 ± 4 |
| LPS group | | |
| Heart rate, bpm | 247 ± 13 | 283 ± 8* |
| Mean arterial blood pressure, mmHg | 73 ± 1* | 59 ± 2 |
| Lactate | 0.8 ± 0.1 | 2.6 ± 0.4* |
| pH | 7.32 ± 0.03 | 7.11 ± 0.02* |
| Arterial blood $PO_2$, mmHg | 188 ± 13 | 216 ± 9 |
| Arterial blood $PCO_2$, mmHg | 37 ± 3 | 43 ± 1 |

Values are means ± SE, n = 5 in both groups.

* Significant difference ($P<0.05$) between control and LPS group

**Table 1.** Systemic variables and laboratory values of the experimental animals.

In both groups mitoPO$_2$ measurements were performed in three different organs (skin, liver and buccal mucosa) at time points $t_1$ and $t_2$. Analysis of mitoVO$_2$ by means of the ODR was done offline after the end of each experiment and the results are shown in figure 4. MitoVO$_2$ decreased significantly ($P < 0.05$) in the LPS group for all organs (skin, liver and buccal mucosa) at $t_2$ compared with baseline $t_1$. In contrast, mitoVO$_2$ of the control group remained unchanged overtime. To provide better insight into our data, figure 5 provides the individual responses of mitoPO$_2$ and mitoVO$_2$ in the rats upon infusion of LPS. Indeed, most individual rats responded to the induction of sepsis with the expected decrease in mitoVO$_2$. No relationship between the mitoPO$_2$ and the induction of sepsis is shown in the skin and the buccal mucosa. Only in liver a non-significantly decreased mitoPO$_2$ was observed. In contrast to the LPS group the values of the control group remain stable, with only mitoPO$_2$ in skin increasing significantly over time.

TISSUE SATURATION, FLOW AND MITOPO$_2$ MEASUREMENTS IN SKIN

The results of the experiments in the FLOW-group are shown in figure 6. Mean arterial pressure increased significantly during infusion of vasopressor (PE = phenylephrine), restored to baseline values after stopping phenylephrine infusion (NI = No Infusion) and dropped significantly below baseline during vasodilator infusion (UP = urapidil). Both vasopressor and vasodilator infusion increased blood flow in the abdominal skin. Due to relatively large variation in the flow readings the effects reached no significance. Both microvascular haemoglobin saturation (μHbO$_2$) and mitoPO$_2$ increased during vasopressor infusion. While μHbO$_2$ gradually increased further over the course of the experiment, mitoPO$_2$ stabilized at a level above baseline. While the trends of mitoPO$_2$ and venous PO$_2$ differed somewhat, the values of both variables were very similar.

MITOCHONDRIAL RESPIROMETRY IN A HUMAN VOLUNTEER

Figure 7 shows a typical example of a mitoPO$_2$ and mitoVO$_2$ measurement in a healthy volunteer. Panel 7A and 7B show delayed fluorescence signals measured before and during the application of local pressure on the skin with the measuring probe. In this case mitoPO$_2$ and mitochondrial oxygen disappearance rate were measured in primed sternal skin of a healthy male volunteer. After local tissue compression a decrease in mitoPO$_2$ was clearly observed due to cessation of oxygen supply and ongoing oxygen consumption in the mitochondria. In this example of a human ODR measurement baseline mitoPO$_2$ was typically around 63 mmHg and mitoVO$_2$ was 7.7 mmHg $s^{-1}$.

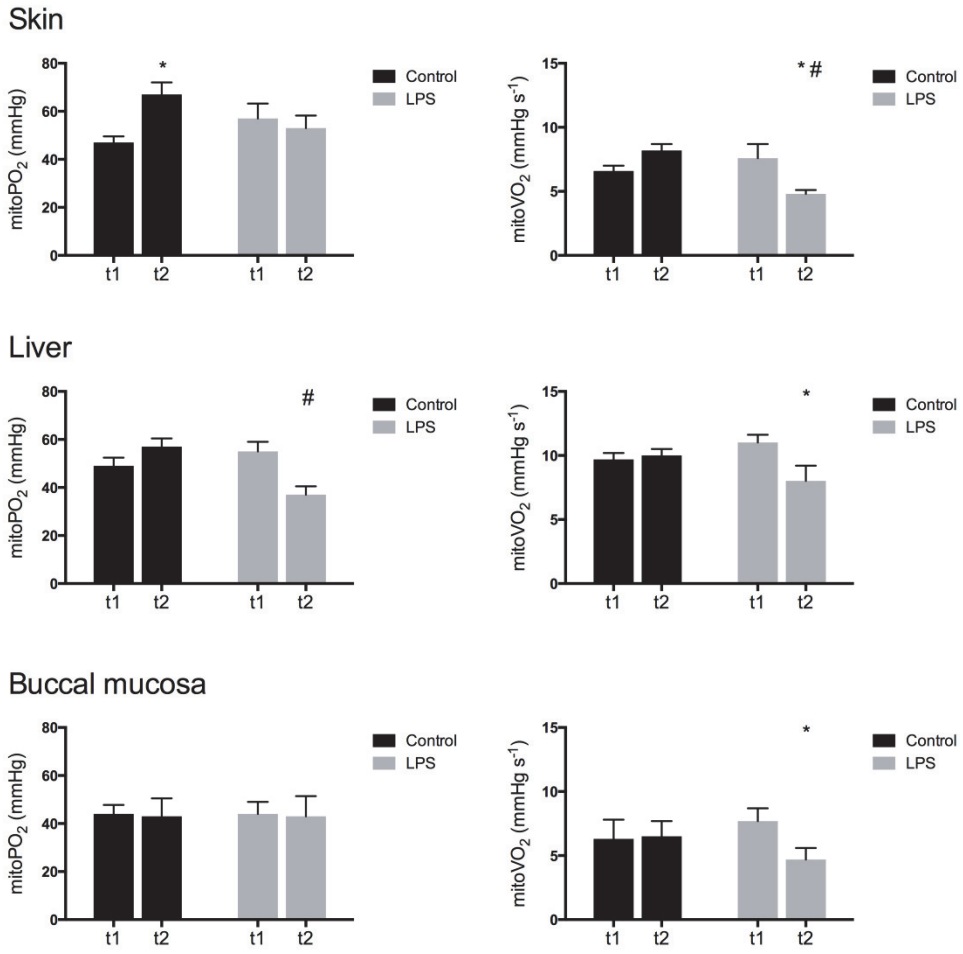


**Figure 4.** Average $mitoPO_2$ and $mitoVO_2$ obtained by *in vivo* respirometry in three different organs (skin, liver and buccal mucosa) at two different time points; baseline measurement ($t_1$) and three hours after baseline measurements ($t_2$). $mitoVO_2$: Mitochondrial oxygen consumption, $mitoPO_2$: Mean $mitoPO_2$ before stop-flow. *: $p < 0.05$ vs t1 and #: $p < 0.05$ vs control

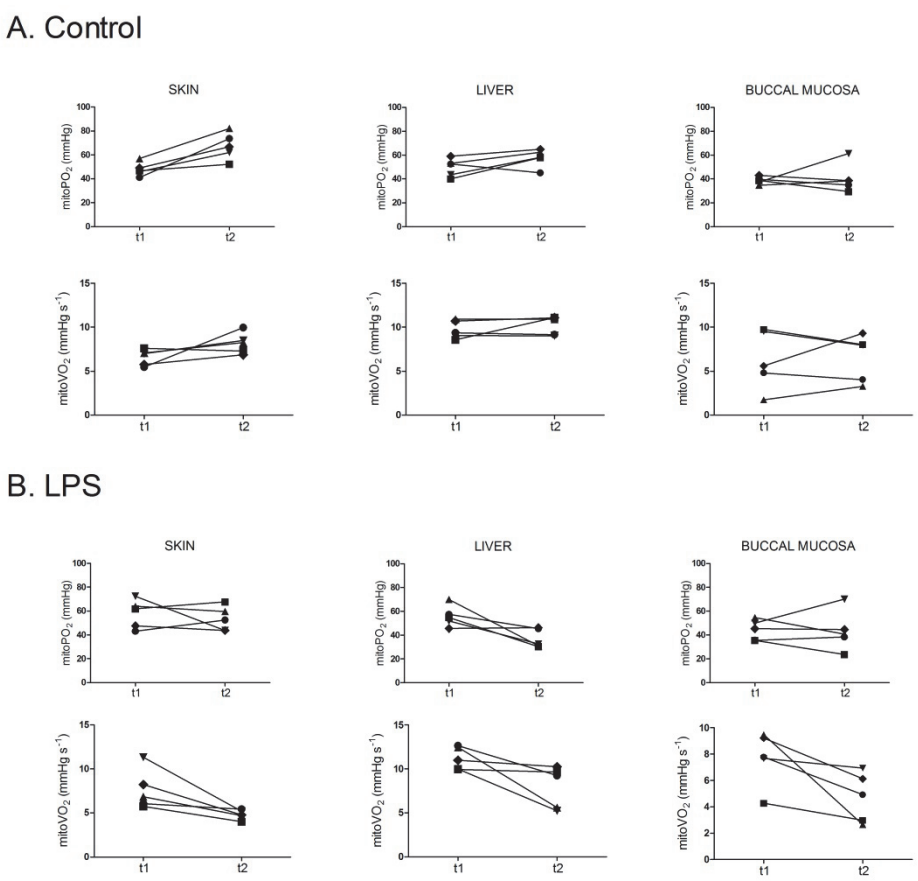


**Figure 5.** Panel A shows the individual time courses of the control rats regarding mitoVO$_2$ (upper three graphs) and mitoPO$_2$ (lower three graphs) at baseline ($t_1$) and three hours later ($t_2$). The individual mitoVO$_2$ (upper three graphs) and mitoPO$_2$ (lower three graphs) of the experimental rats at baseline measurement ($t_1$) and three hours after after the induction of sepsis($t_2$) are shown in panel B.
mitoVO$_2$: mitochondrial oxygen consumption, mitoPO$_2$: Mean PO$_2$ before stop-flow

MITOCHONDRIAL RESPIROMETRY IN A HUMAN VOLUNTEER

Figure 7 shows a typical example of a mitoPO$_2$ and mitoVO$_2$ measurement in a healthy volunteer. Panel 7A and 7B show delayed fluorescence signals measured before and during the application of local pressure on the skin with the measuring probe. In this case mitoPO$_2$ and mitochondrial oxygen disappearance rate were measured in primed sternal skin of a healthy male volunteer. After local tissue compression a decrease in mitoPO$_2$ was clearly observed due to cessation of oxygen supply and ongoing oxygen consumption in the mitochondria. In this example of a human ODR measurement baseline mitoPO$_2$ was typically around 63 mmHg and mitoVO$_2$ was 7.7 mmHg s$^{-1}$.

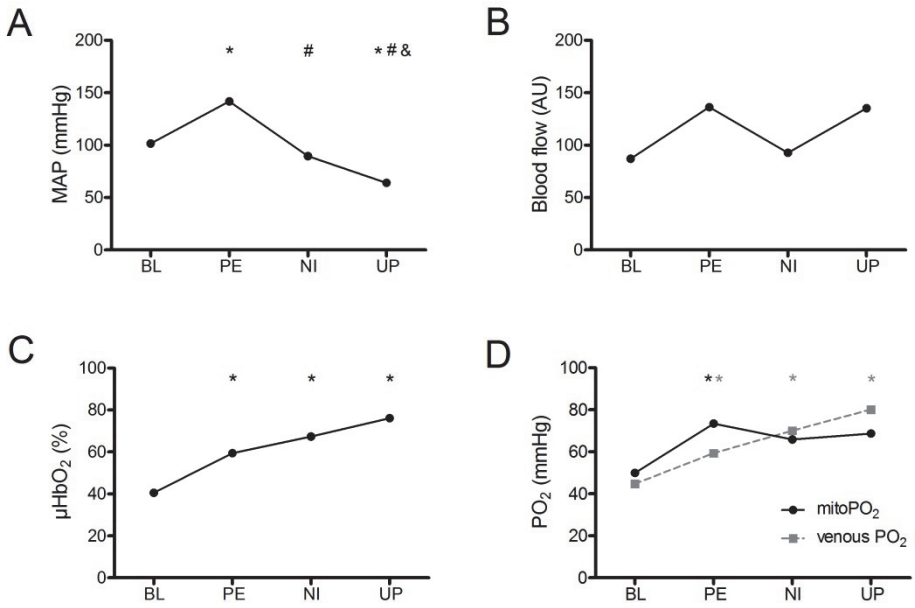


**Figure 6.** Microvascular blood flow, hemoglobin saturation and mito$PO_2$ in rat abdominal skin. Panel A shows the response of the mean arterial blood pressure (MAP) during infusion of the vasopressor phenylephrine (PE) and the vasodilator urapidil (UP). BL = baseline and NI = no infusion of vasoactive drugs. Panel B shows the response of the microvascular blood flow as measured by laser Doppler. AU = arbitrary units. Panel C shows the microvascular hemoglobin saturation as measured by the O2C and D shows the mitochondrial $PO_2$ measured by PpIX-TSLT after topical application of ALA cream. The grey squares are venous $PO_2$ values derived from the µ$HbO_2$ data. *: $p < 0.05$ vs BL, #: $p < 0.05$ vs PE and &: $p < 0.05$ vs NI.



No permanent damage to the skin was observed in cutaneous mitochondrial respirometry measurements. Only direct after repeated mito$PO_2$ and mito$VO_2$ measurements, a small red spot with the size of the measuring probe was observed on the sternal skin. This was likely caused by a hyperaemic response of the skin tissue after repeated temporary occlusion of the microcirculation. One day after the measurements no remaining marks at the skin were observed. The light dose was kept well below the recommended exposure limits [28] by setting the light output of the excitation branch at approximately 20 µJ/pulse as measured by a FieldMate laser power meter. The excitation probe was in direct contact with the skin, this occurs in an illuminated spot with minimally the same diameter as the excitation probe, 1000 µm. Therefore the resulting maximum fluencies were 2.6 mJ/$cm^2$ per pulse and 0.23 J/$cm^2$ per mitochondrial respiration measurement which is two orders of magnitude below typical fluencies used for photodynamic therapy. The novel PpIX-TSLT clinical measurement setup has been tested for electrical safety, whereby a residual-current far below statutory safety requirements [29] was measured.

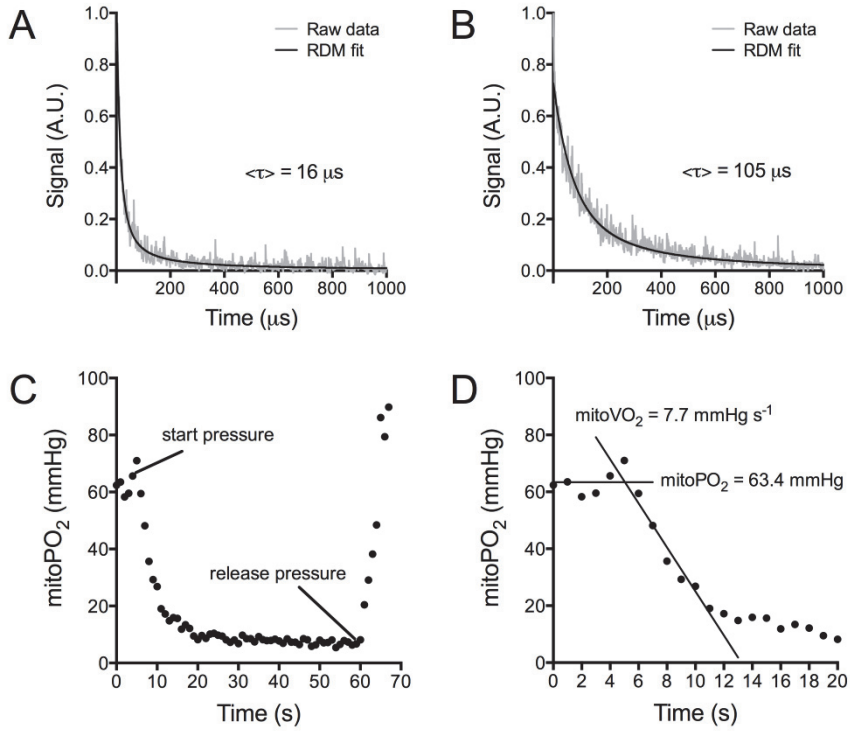


**Figure 7.** Typical example of mitochondrial respirometry in the presternal skin of a human volunteer. Panel A and B show raw delayed fluorescence data with corresponding RDM fit before and during application of pressure with the measuring probe respectively. Panel C shows an example of an ODR measurement and panel D shows the first 20 seconds of the same measurement with analysis of $mitoPO_2$ and $mitoVO_2$. $mitoVO_2$ was determined from the linear part of the oxygen disappearance curve. $mitoPO_2$ was the mean $mitoPO_2$ before the start of tissue compression.

## DISCUSSION

In this work we describe a novel monitoring technique to determine *in vivo* mitochondrial oxygen tension and consumption, ultimately allowing cutaneous mitochondrial respirometry in a clinical setting. Previously, the PpIX-TSLT technique was calibrated in cell lines, liver and heart [13-15]. We recently demonstrated that oxygen-dependent delayed fluorescence signals can be measured in skin after topical application of ALA-crème [16]. Furthermore, validation of these delayed fluorescence lifetimes to determine cutaneous $mitoPO_2$ was successfully executed [17]. Subsequently, we have developed a method for mitochondrial respirometry *in vivo,* which enables us to monitor $mitoPO_2$ and $mitoVO_2$ in

skin [30]. However, even after demonstrating its feasibility, a few more steps are necessary towards clinical use of PpIX-TSLT. Important remaining questions are, for example, the clinical relevance of cutaneous measurements, practical usability in man and the safety of the technique. In the presented work we addressed some of these questions.

We looked at the potential clinical relevance of the measurements in skin by comparing the values and responses of cutaneous mito$PO_2$ and mito$VO_2$ with other organs, like liver, kidney and gastrointestinal tract. The results show that the absolute value of mito$VO_2$ in the skin may not be the same as in other organs. Indeed, previous experiments have also demonstrated that metabolic alterations found in locomotive muscle are not the same as in a respiratory muscle [31]. Therefore care should be taken when extrapolating results from one organ to another. On the other hand, mitochondrial oxygen consumption in all studied organs decreased after the infusion of LPS (Figure 5). Importantly, no significant differences in mito$PO_2$ values were observed between the different experimental groups and organs, suggesting that the oxygen consumption is not dependent on the initial oxygen tension. These data suggest that the effects of systemic mitochondriopathies, like LPS-induced mitochondrial dysfunction, can be monitored in the skin. We found a relation between alterations in mitochondrial parameters in the skin and other tissues and organs that are considered more vital for life, like the liver. Therefore, we hypothesize that the skin can be used as a substitute for other less accessible target organs to monitor alterations in mitochondrial respiration in critical illness like sepsis and septic shock.

We used an acute sepsis model in this study while other studies show variable findings in short-term septic models, with increased [32], decreased [10, 32, 33], or unaltered mitochondrial function [34, 35]. More consisting data of decreased mitochondrial function were observed in long-term models lasting for > 16 hours [36]. These inconsistent findings can be explained by the different phases of sepsis. Rosser et al. [37] reported a rise in resting oxygen consumption rate at 1 hour and 6 hours after LPS infusion and the values returned to control after 24 hours. Maximal oxygen consumption rates were increased at 6 hours as well. However, exposure to endotoxin for 24 hours significantly reduced maximal oxygen consumption rates compared to the controls. This result suggests a phase-dependent variation in mitochondrial respiration in sepsis, whereby the late phase is characterized by decrease in mitochondrial function [10]. In the future, the PpXI-TSLT on the skin can play an important role in increasing our understanding of mitochondrial function and oxygen metabolism in the different phases in sepsis. A follow-up study in a long-term sepsis model in which the mitochondrial function of the skin is compared with organ function of vital organs would be of great value.

Mitochondria are the most important oxygen sinks in tissues and mitochondrial oxygen consumption creates oxygen gradients that drive the diffusion of oxygen from the microcirculation into the tissue cells. Therefore, mito$PO_2$ can be expected to be on lowest end of the oxygen distribution in tissues. Nevertheless, baseline mito$PO_2$ as measured by the PpIX-TSLT technique appears relatively high, e.g. in this study approximately 50 mmHg in skin of rats breathing 40% oxygen. PpIX-TSLT has been calibrated in skin [38] and our stop-flow experiments clearly demonstrate that the technique is capable of measuring low $PO_2$ values. However, to further exclude that the high baseline mito$PO_2$ readings are not caused by a bias in the PpIX-TSLT technique we performed a series of experiments in which we simultaneously measured mito$PO_2$, hemoglobin saturation ($\mu HbO_2$) and microvascular blood flow (the latter by using O2C). According to the manufacturer the O2C typically measures hemoglobin saturation in small venules and veins. Therefore, both PpIX-TSLT and O2C provide information from the lower end of oxygenation spectrum. In our experiments mito$PO_2$ and capillary-venous $PO_2$ were in the same $PO_2$ range and this clearly argues against a technical issue with PpIX-TSLT. Furthermore, mito$PO_2$ reflects a balance between oxygen supply and demand [39] and therefore is expected to be dependent on local blood flow, as verified by our data.
In order to develop a monitoring technique for human use, demonstrating the safety of our technique will be essential prior to clinical use. Therefore, we developed a novel laser setup that complies with the strict safety requirements regarding electrical safety. Furthermore, safety requirements also boasts limitations on the power output of the laser light, enabling repeated mito$PO_2$ measurements without exceeding the maximum light doses for the skin [28]. An advantage of fiber-based PpIX-TSLT measurements on the skin is that mitochondrial oxygenation parameters can be obtained without any tissue destruction. Another clear advantage of the PpXI-TSLT measurements on the skin is the reduced potential side-effects of topical application of ALA, in contrast to systemic administration. Nowadays, the topical application of ALA is widely used in dermatology, in the treatment of non-melanoma skin lesions with photodynamic therapy. Photodynamic therapy is known as a safe treatment with little concerns about photosensitization [30, 40]. Therefore, the mito$PO_2$ measurements in which a relatively low dose of topically applied ALA is used can be safely applied in human beings.

The applicability of our novel clinical PpIX-TSLT setup was demonstrated on human skin in a healthy volunteer, 5 hours after the application of a self-adhesive ALA-patch. The measured mito$PO_2$ and mito$VO_2$ values were comparable to previous findings in the skin of rats [30].

## CONCLUSION

Our findings show that the PpIX-TSLT allows non-invasive monitoring of mitochondrial oxygenation and respiration. We expect that clinical implementation of the method will greatly contribute to our understanding of tissue oxygenation and oxygen metabolism in patients. For example, monitoring mito$PO_2$ and mito$VO_2$ might greatly improve our understanding of mitochondrial pathology in the different phases in sepsis. Because the measurements can be performed without any tissue destruction our method overcomes the ethical and technical difficulties of current techniques (tissue biopsies) to assess mitochondrial function in patients. PpIX-TSLT provides us with future opportunities to monitor mitochondrial function by means of *in vivo* respirometry in long-term septic animal studies, clinical trials and possibly daily clinical practice.

## ACKNOWLEDGEMENTS

This work was financially supported by a Life Sciences Pre-Seed Grant (grant no 40-41300-98-9037) from the Netherlands Organization for Health Research and Development (ZonMW).

## CONFLICT OF INTEREST

Dr. E.G. Mik is founder and shareholder of Photonics Healthcare B.V., a company aimed at making the delayed fluorescence lifetime technology clinically available. Photonics Healthcare B.V. holds the exclusive licenses to several patents regarding this technology, filed and owned by the Academic Medical Center in Amsterdam and the Erasmus Medical Center in Rotterdam, The Netherlands.

## REFERENCES

1. Ballinger, S.W., *Mitochondrial dysfunction in cardiovascular disease.* Free Radic Biol Med, 2005. 38(10): p. 1278-95.
2. Schapira, A.H. and M. Gegg, *Mitochondrial contribution to Parkinson's disease pathogenesis.* Parkinsons Dis, 2011. 2011: p. 159160.

3. Fink, M., *Cytopathic hypoxia in sepsis.* Acta Anaesthesiol Scand Suppl, 1997. 110: p. 87-95.
4. Fink, M.P., *Cytopathic hypoxia. A concept to explain organ dysfunction in sepsis.* Minerva Anestesiol, 2000. 66(5): p. 337-42.
5. Fink, M.P., *Cytopathic hypoxia in sepsis: a true problem?* Minerva Anestesiol, 2001. 67(4): p. 290-1.
6. Wagner, F., et al., *Sepsis therapy: what's the best for the mitochondria?* Crit Care, 2008. 12(4): p. 171.
7. Galley, H.F., *Bench-to-bedside review: Targeting antioxidants to mitochondria in sepsis.* Crit Care, 2010. 14(4): p. 230.
8. Fontaine, E.M., et al., *Cytoplasmic cellular structures control permeability of outer mitochondrial membrane for ADP and oxidative phosphorylation in rat liver cells.* Biochem Biophys Res Commun, 1995. 213(1): p. 138-46.
9. Saks, V., et al., *Correlation between degree of rupture of outer mitochondrial membrane and changes of kinetics of regulation of respiration by ADP in permeabilized heart and liver cells.* Biochem Biophys Res Commun, 1995. 208(3): p. 919-26.
10. Brealey, D., et al., *Mitochondrial dysfunction in a long-term rodent model of sepsis and organ failure.* American Journal of Physiology - Regulatory Integrative and Comparative Physiology, 2004. 286(3 55-3): p. R491-R497.
11. Crouser, E.D., et al., *Endotoxin-induced mitochondrial damage correlates with impaired respiratory activity.* Crit Care Med, 2002. 30(2): p. 276-84.
12. Gellerich, F.N., et al., *Impaired energy metabolism in hearts of septic baboons: Diminished activities of complex I and complex II of the mitochondrial respiratory chain.* Shock, 1999. 11(5): p. 336-341.
13. Mik, E.G., et al., *In vivo mitochondrial oxygen tension measured by a delayed fluorescence lifetime technique.* Biophys J, 2008. 95(8): p. 3977-90.
14. Mik, E.G., et al., *Mitochondrial PO2 measured by delayed fluorescence of endogenous protoporphyrin IX.* Nat Methods, 2006. 3(11): p. 939-45.
15. Mik, E.G., et al., *Mitochondrial oxygen tension within the heart.* J Mol Cell Cardiol, 2009. 46(6): p. 943-51.
16. Harms, F.A., et al., *Oxygen-dependent delayed fluorescence measured in skin after topical application of 5-aminolevulinic acid.* J Biophotonics, 2011. 4(10): p. 731-9.
17. Choi, J.K., et al., *Evaluation of mean skin temperature formulas by infrared thermography.* Int J Biometeorol, 1997. 41(2): p. 68-75.
18. Mik, E.G., *Methods and devices for assessment of mitochondrial function.* 2009: US 2011/0182825 A1.

19. Mik, E.G., *Special article: measuring mitochondrial oxygen tension: from basic principles to application in humans.* Anesth Analg, 2013. 117(4): p. 834-46.
20. Buerk, D.G., et al., *Interpretation of oxygen disappearance curves measured in blood perfused tissues.* Adv Exp Med Biol, 1986. 200: p. 151-61.
21. Gaab, M.R., B. Poch, and V. Heller, *Oxygen tension, oxygen metabolism, and microcirculation in vasogenic brain edema.* Adv Neurol, 1990. 52: p. 247-56.
22. Golub, A.S., M.A. Tevald, and R.N. Pittman, *Phosphorescence quenching microrespirometry of skeletal muscle in situ.* Am J Physiol Heart Circ Physiol, 2011. 300(1): p. H135-43.
23. Reneau, D.D. and J.H. Halsey, Jr., *Interpretation of oxygen disappearance rates in brain cortex following total ischaemia.* Adv Exp Med Biol, 1977. 94: p. 189-98.
24. Harms, F.A., et al., *Cutaneous respirometry by dynamic measurement of mitochondrial oxygen tension for monitoring mitochondrial function in vivo.* Mitochondrion, 2013. 13(5): p. 507-14.
25. Golub, A.S., et al., *Analysis of phosphorescence in heterogeneous systems using distributions of quencher concentration.* Biophys J, 1997. 73(1): p. 452-65.
26. Bodmer, S.I., et al., *Microvascular and mitochondrial PO(2) simultaneously measured by oxygen-dependent delayed luminescence.* J Biophotonics, 2012. 5(2): p. 140-51.
27. Mik, E.G., T. Johannes, and C. Ince, *Monitoring of renal venous PO2 and kidney oxygen consumption in rats by a near-infrared phosphorescence lifetime technique.* Am J Physiol Renal Physiol, 2008. 294(3): p. F676-81.
28. *Directive 2006/25/EC of the European parliament and the council of 5 April 2006 on the (artificial optical radiation).* E.p.a.t.c.o.A. 2006, Editor. 2006.
29. *Medische elektrische apparatuur.* . 2006.
30. Harms, F.A., et al., *Cutaneous respirometry by dynamic measurement of mitochondrial oxygen tension for monitoring mitochondrial function in vivo.* Mitochondrion, 2012.
31. Fredriksson, K. and O. Rooyackers, *Mitochondrial function in sepsis: respiratory versus leg muscle.* Crit Care Med, 2007. 35(9 Suppl): p. S449-53.
32. Poderoso, J.J., et al., *Liver oxygen uptake dependence and mitochondrial function in septic rats.* Circ Shock, 1994. 44(4): p. 175-82.
33. Llesuy, S., et al., *Oxidative stress in muscle and liver of rats with septic syndrome.* Free Radic Biol Med, 1994. 16(4): p. 445-51.
34. Geller, E.R., S. Jankauskas, and J. Kirkpatrick, *Mitochondrial death in sepsis: a failed concept.* J Surg Res, 1986. 40(5): p. 514-7.

35. Garrison, R.N., D.J. Ratcliffe, and D.E. Fry, *The effects of peritonitis on murine renal mitochondria.* Adv Shock Res, 1982. 7: p. 71-6.
36. Singer, M., *Mitochondrial function in sepsis: acute phase versus multiple organ failure.* Crit Care Med, 2007. 35(9 Suppl): p. S441-8.
37. Rosser, D.M., et al., *Endotoxin reduces maximal oxygen consumption in hepatocytes independent of any hypoxic insult.* Intensive Care Med, 1998. 24(7): p. 725-9.
38. Harms, F.A., et al., *Validation of the protoporphyrin IX-triplet state lifetime technique for mitochondrial oxygen measurements in the skin.* Opt Lett, 2012. 37(13): p. 2625-7.
39. Mik, E.G., *Measuring Mitochondrial Oxygen Tension: From Basic Principles to Application in Humans.* Anesth Analg, 2013.
40. Ibbotson, S.H., *Adverse effects of topical photodynamic therapy.* Photodermatol Photoimmunol Photomed, 2011. 27(3): p. 116-30.

# CHAPTER

# 8

# *Cutaneous respirometry as novel technique to monitor mitochondrial function: a feasibility study in healthy volunteers*

Floor A. Harms, MD[1], Robert J. Stolker, MD, PhD[1], Egbert G. Mik, MD, PhD[1,2]

1 Department of Anesthesiology, Laboratory of Experimental Anesthesiology, Erasmus University Medical Center Rotterdam, 's-Gravendijkwal 230, 3015 CE Rotterdam, The Netherlands

2 Department of Intensive Care, Erasmus University Medical Center Rotterdam, 's-Gravendijkwal 230, 3015 CE Rotterdam, The Netherlands

**Short Title:** Mitochondrial function measurements in healthy volunteers

Submitted for publication

## ABSTRACT

**Background:** The protoporphyrin IX-triplet state lifetime technique (PpIX-TSLT) is proposed as a potential clinical non-invasive tool to monitor mitochondrial function. This technique has been evaluated in several animal studies. Mitochondrial respirometry allows measurement *in vivo* of mitochondrial oxygen tension (mitoPO$_2$) and mitochondrial oxygen consumption (mitoVO$_2$) in skin. This study describes the first use of a clinical prototype in skin of humans.

**Methods:** The clinical prototype was tested in 30 healthy volunteers. A self-adhesive patch containing 2 mg 5-aminolevulinic acid (ALA) was applied on the skin of the anterior chest wall (sternal) for induction of mitochondrial protoporphyrin IX and was protected from light for 5 h. MitoPO$_2$ was measured by means of oxygen-dependent delayed fluorescence of protoporphyrin IX. MitoVO$_2$ was determined by dynamic mitoPO$_2$ measurements on the primed skin, while locally blocking oxygen supply by applying local pressure with the measurement probe. MitoPO$_2$ was recorded before and during a 60-s period of compression of the microcirculation, at an interval of 1 Hz. Oxygen consumption was calculated from the decay of the mitoPO$_2$ slope.

**Results:** Oxygen-dependent delayed fluorescence measurements were successfully performed in the skin of 27 volunteers. The average value (± SD) of mitoPO$_2$ was 44 ± 17 mmHg and mean mitoVO$_2$ values were 5.8 ± 2.3 and 6.1 ± 1.6 mmHg s$^{-1}$ at a skin temperature of 34$^{o}$C and 40$^{o}$C, respectively. No major discomfort during measurement and no long-term dermatological abnormalities were reported in a survey performed 1 month after measurements.

**Conclusion**: These results show that the clinical prototype allows measurement of mitochondrial oxygenation and oxygen consumption in humans. The development of this clinically applicable device offers opportunities for further evaluation of the technique in humans and the start of first clinical studies.


## INTRODUCTION

An adequate supply of oxygen to tissue and its subsequent use in oxidative phosphorylation in the mitochondria is essential for preserving cellular integrity and, ultimately, life. Therefore, a non-invasive and *in vivo* monitoring system able to monitor mitochondrial parameters, like oxygenation and oxygen consumption, could be a valuable tool for clinicians [1]. The currently available techniques to determine mitochondrial

function are not suitable for clinical monitoring. The most commonly used techniques for assessment of mitochondrial function are *ex vivo* measurements on isolated mitochondria [2] or *in situ* detection in permeabilized cells/tissue [3]. Although these classical approaches provide highly specific information on the function of the organelle, their *ex vivo* use is a well-recognized limitation. Determination of mitochondrial function under physiological or pathophysiological circumstances is essential to understand and evaluate changes in oxidative phosphorylation [4], To overcome these *ex vivo* limitations, Fick's principle has been applied in humans for many years to measure tissue $VO_2$ by combining data of regional blood flow and arterial-venous oxygen content difference. However, measurements based on Fick's principle can generate data with a high variability and, therefore, its use for clinical decision-making has been questioned [5, 6].

The protoporphyrin IX-triplet state lifetime technique (PpIX-TSLT) is proposed as a potential novel approach to determine mitochondrial oxygen consumption [7]. The first detailed description of the PpIX-TSLT was published in 2006 [8]. PpIX-TSLT enables mitochondrial oxygen ($mitoPO_2$) measurements by means of the oxygen-dependent optical properties of protoporphyrin IX (PpIX). PpIX-TSLT was the first technique to allow measurements of $mitoPO_2$ in living cells and can be applied *in vivo* [9-11]. Our group has been working on the development of PpIX-TSLT from its use in cell cultures to a monitoring system of mitochondrial function in humans [12]. This technique has been tested and calibrated for use on isolated organs [10, 11] and *in vivo* [11]. Subsequently, oxygen-dependent quenching of delayed fluorescence of PpIX has been observed in skin [9] and validation of the quenching constants needed to calculate $mitoPO_2$ from the signals has been successful [13]. In addition to direct non-invasive measurement of $mitoPO_2$, it is also technically possible to gain information on mitochondrial function. This information is derived by means of mitochondrial oxygen consumption ($mitoVO_2$), which can be determined by dynamic $mitoPO_2$ measurements while blocking local oxygen supply [14]. Oxygen consumption can be calculated from the decay of the $mitoPO_2$ [14]. As proposed earlier [9, 12, 14], it should be technically possible to apply PpIX-TSLT in humans.

In the present study, we demonstrate for the first time the ability to measure $mitoPO_2$ and $mitoVO_2$ in human skin, using a clinical prototype of PpIX-TSLT. The safety and feasibility of our method is investigated and data are presented on the inter- and intra-individual distribution of mitochondrial oxygen measurements.

Our ultimate goal is to develop the PpIX-TSLT as a non-invasive monitor that allows direct assessment of mitochondrial dysfunction in sepsis. Although mitochondrial dysfunctions

are thought to be related to the pathogenesis of sepsis and multiorgan failure [15, 16], inconsistent data have been reported. These conflicting results may be due to the wide variety of methods used to determine mitochondrial dysfunction in sepsis [1]. Therefore, a standard method to monitor mitochondrial dysfunction could further elucidate the role of the mitochondria during septic conditions. When the PpIX-TSLT has proven to do this successfully, opportunities will arise for novel strategies in the treatment of severe sepsis.

## METHODS

The study was performed in compliance with the Code of Ethics of the World Medical Association (Declaration of Helsinki) and approved by the Institutional Review Board at the Erasmus MC **(**MEC-2011-397)**.** A total of 30 volunteers were drawn from a pool of young, healthy students and hospital staff aged 18-30 years. Written informed consent was obtained from volunteers prior to study participation.

### PRINCIPLE OF MITOPO$_2$ MEASUREMENTS

The background of the PpIX-TSLT is described in detail elsewhere [8, 11]. In short, PpIX is the final precursor of heme in the heme biosynthetic pathway. PpIX is synthesized in the mitochondria, and administration of 5-aminolevulinic acid (ALA) substantially enhances the PpIX concentration. PpIX possesses a triplet state that reacts strongly with oxygen, making its lifetime oxygen-dependent. Population of the first excited triplet state occurs upon photo-excitation with a pulse of light, and causes the emission of red delayed fluorescence. The delayed fluorescence lifetime is related to mitoPO$_2$ according to the Stern-Volmer equation:

$$mitoPO_2 = \left(1/\tau - 1/\tau_0\right)/k_q \qquad (1)$$

in which $\tau$ is the measured delayed fluorescence lifetime, $k_q$ is the quenching constant and $\tau_0$ is the lifetime at zero oxygen. In case of a non-homogenous oxygen distribution inside the measurement volume, a reliable estimation of the average PO$_2$ can be made by the rectangular distribution method (RDM) [17, 18].

The signal/noise ratio (SNR) of resulting traces was calculated and defined as the ratio of maximum signal amplitude to the peak-to-peak noise. Lifetime analysis operates stably at

moderate SNR (SNR >20) [11]. Therefore, only delayed fluorescence signals with a SNR <20 were analyzed and included in the present dataset.

## PRINCIPLE OF MITOVO$_2$ MEASUREMENTS

MitoVO$_2$ is measured by means of the oxygen disappearance rate after local occlusion of the oxygen supply. Local occlusion of the microcirculation in skin was obtained by application of pressure with the measurement probe. This simple procedure created reliable stop-flow conditions and induced measurable oxygen disappearance rates, due to cessation of microvascular oxygen supply and ongoing cellular oxygen consumption. MitoPO$_2$ was measured before and during application of pressure at an interval of 1 Hz, using 4 laser pulses per measurement. We have described the basic principles behind the technology and have provided a working implementation of the technique for mitoVO$_2$ measurements [14] as well as a method to calculate mitoVO$_2$. Figure 1 presents an example of the analysis of mitoVO$_2$.

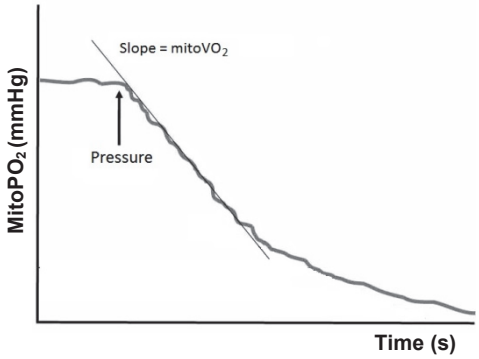


**Figure 1.** Principle of respirometry by local cessation of the oxygen supply. The mitochondrial oxygen consumption (mitoVO$_2$) is calculated from the linear part of the oxygen disappearance curve following local compression of the microcirculation by the measurement probe.

## EXPERIMENTAL SETUP

Prior to oxygen measurements the heart rate, blood pressure and peripheral oxygen saturation were determined in all volunteers, and a standard preoperative evaluation form was obtained from all these participants.

Oxygen measurements were performed by means of a clinical prototype PpIX-TSLT device (Chapter 6). A self-adhesive patch containing 8 mg ALA (Alacare®; Spirig AG, Egerkingen, Switzerland) was applied on the skin of the anterior chest wall (sternal), for induction of

PpIX. To enhance ALA penetration adequate skin preparation was essential. If present hair was shaved, and the skin was rubbed with a fine abrasive pad of a standard ECG sticker to remove parts of the stratum corneum. After ALA application, the skin was protected from light for 5 h. During these 5 h a suitable concentration of PpIX was synthesized to enable measurements of mito$PO_2$ and mito$VO_2$. A schematic overview of the skin preparations before the measurements is presented in Figure 2. To minimize the influence from ambient light, the experiments were performed in dimmed light. First, three successive mito$PO_2$ measurements were performed, during a period of 90 s, under baseline conditions. Subsequently, mito$VO_2$ was determined with a heated measurement probe at 34$^{o}$C and 40$^{o}$C. Warming of the measurement probe was done to prevent local vasoconstriction due to a cold probe, and to eliminate the effect of differences in skin temperature on the measurements. The temperature of 34$^{o}$C was chosen because this was the maximal skin temperature determined in 10 healthy volunteers in a normal environment, measured by infrared thermography. To determine the effect of hyperthermia on mito$VO_2$ a probe temperature of 40$^{o}$C was chosen. This temperature was well above the mean skin temperature [19] and low enough not to induce skin burns. One month after the experiments an evaluation form was completed by all the volunteers. The form consisted of questions about any pain during the measurements and the appearance of dermatological symptoms, such as erythema, pruritus and hyperpigmentation of the skin.

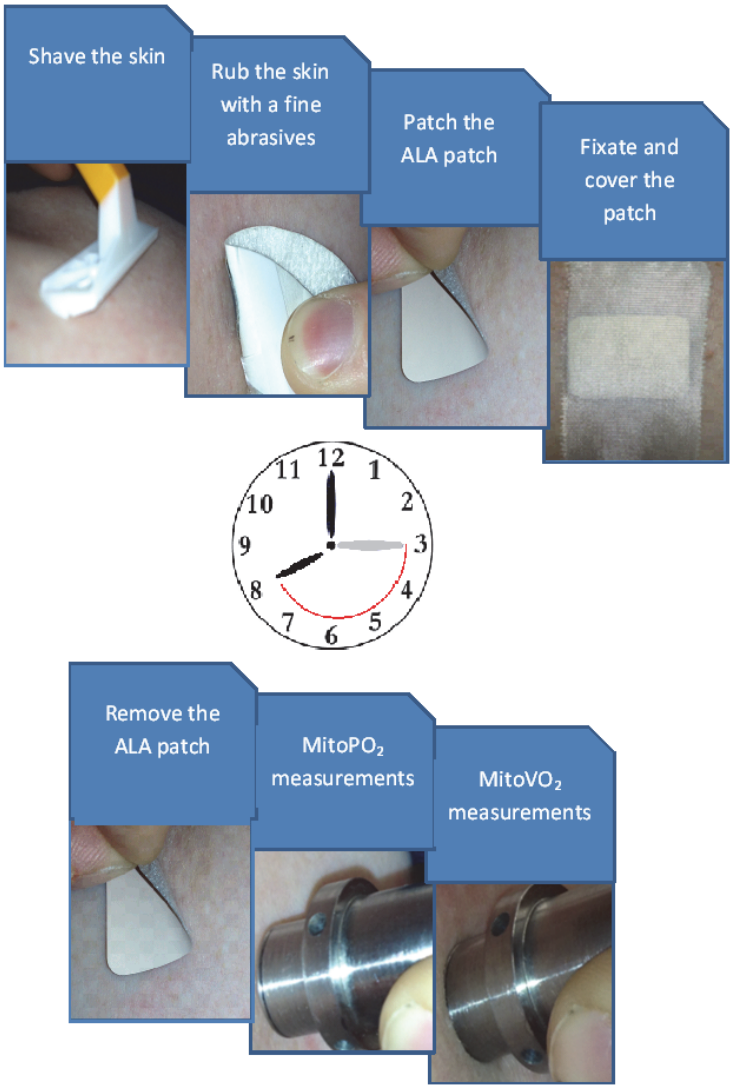


**Figure 2**. Schematic overview of the preparations before the measurements.

STATISTICAL ANALYSIS

Unless stated otherwise, reported values are mean ± SD. Normality of the data was tested using the Shapiro-Wilk test. Correlation between the two variables was tested by Pearson's correlation analysis.

## RESULTS

Basic characteristics of the 30 healthy volunteers are shown in Table 1. All participants had normal results for the physical parameters, such as heart rate, blood pressure and arterial oxygen saturation. Due to insufficient signal-to-noise ratio the measurements of three volunteers were excluded from further analysis.

**Table 1.** Characteristics healthy volunteers

| Characteristics | Volunteers (n=30) |
|---|---|
| Age (years) | 26 ± 5 |
| Sex, n (%) | |
| Men | 19 (63) |
| Women | 11 (37) |
| Smokers, n (%) | 1 (3) |
| Alcohol consumption, n (%) | |
| 0 drinks/day | 3 (10) |
| 1-2 drinks/day | 25 (83) |
| > 2 drinks/day | 2 (7) |
| Heart rate (bpm ± SD) | 69 ± 13 |
| Systolic blood pressure (mmHg ± SD) | 128 ± 12 |
| Diastolic blood pressure (mmHg ± SD) | 76 ± 10 |
| Arterial saturation (% ± SD) | 99 ± 1 |

### MITO$PO_2$ MEASUREMENTS

A typical example of a baseline mito$PO_2$ measurement is presented in Figure 3a. Due to the heterogeneous oxygenation in the skin a marked intra-individual variation was observed during the baseline measurement due to movement (breathing) in combination with a small measuring area (the diameter of the detection fiber was only 1 mm). Therefore, the mean mito$PO_2$ (red line) over a period of 90 s was used in the analysis of mito$PO_2$.

From the total of 27 experiments, mean mito$PO_2$ was 44 ± 17 mmHg (Figure 3b). This finding is consistent with previous values derived from animal studies [12, 14]. Despite the movement-induced variation in baseline mito$PO_2$, the mean data regress towards a normal distribution (p=0.73; skewness=0.07 ± 0.45, kurtosis = -0.46 ± 0.87) (Figure 3c).

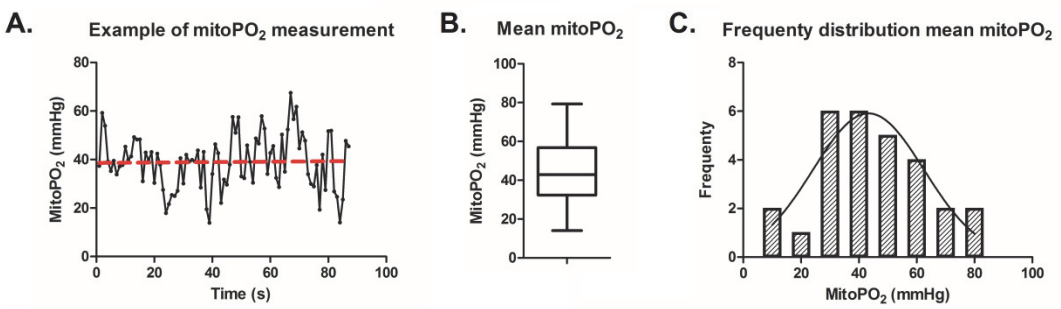


**Figure 3. A.** Example of a baseline mitoPO$_2$ measurement. The median mitochondrial oxygen tension (mitoPO$_2$) (red line) is calculated over a period of 90 second. **B.** The mitoPO$_2$,is presented in a box-and-whisker graph, **C.** Frequency distribution of all ratio differences of the mitoPO$_2$.

## MITOVO$_2$ MEASUREMENTS

A typical example of an oxygen disappearance curve on human skin is presented in Figure 4a. The mean mitoVO$_2$ values, measured in the skin of 27 healthy volunteers, were 5.8 ± 2.3 and 6.1 ± 1.6 mmHg s$^{-1}$ for a probe temperature of 34$^{o}$C and 40$^{o}$C, respectively (Figure 4b). The distribution of the data is presented in Figure 4c. The Shapiro-Wilk test demonstrates that mitoVO$_2$ measured at a temperature of 34$^{o}$C follows a normal distribution (p-value=0.069, skewness=0.9, kurtosis=1.9). However, the same analysis of mitoVO$_2$ at a temperature of 40$^{o}$C does not follow a normal distribution (p-value=0.047, skewness= 0.72 ± 0.45, kurtosis= -0.29 ± 0.87).

## CORRELATION BETWEEN MITOPO$_2$ AND MITOVO$_2$

We found a weak positive correlation between mitoVO$_2$ and baseline mitoPO$_2$ for 27 data pairs (Figure 5). This indicates that mitoVO$_2$ of the skin is not completely independent of baseline mitoPO$_2$ levels. However, the correlation is mainly determined for very high and/or very low mitoPO$_2$ values.

## SAFETY OF THE MEASUREMENTS

All healthy volunteers experienced the skin preparation and measurements as non-problematic. Due to either the skin preparation or the ALA patch, 45% of the volunteers suffered from mild pruritus and/or erythema on the actual measurement day; these minor complaints were no longer present the day after the measurements. Only two volunteers had transient hyperpigmentation of the skin after the measurements, possibly due to premature exposure of the primed area to sunlight (against our advice). The hyperpigmentation was temporary and disappeared within one month. None of the volunteers sustained long-term skin damage, as established one month after the experiments.

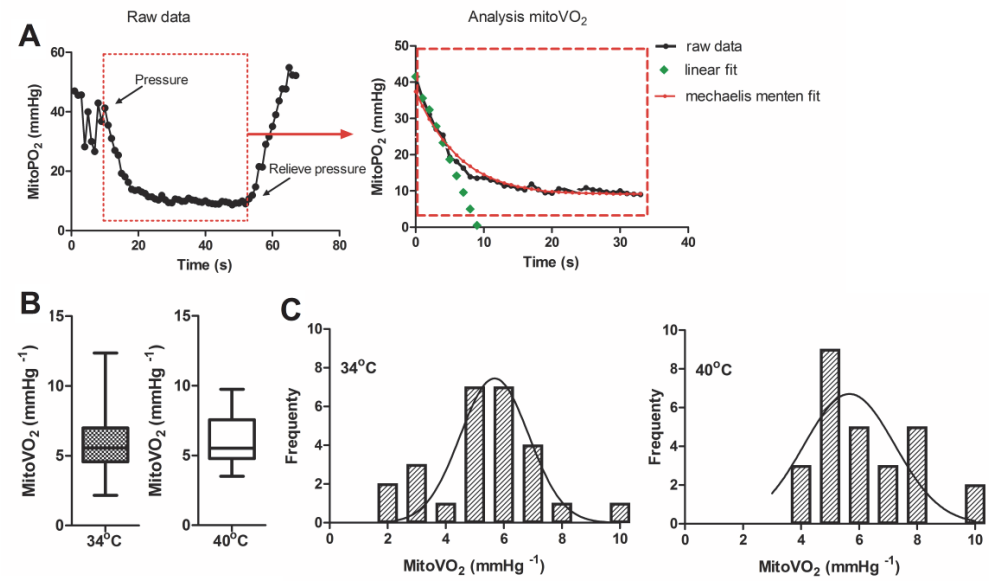


**Figure 4. A**. Typical example of the analysis of the mitochondrial oxygen consumption (mitoVO$_2$). The first panel shows an example of the oxygen disappearance rate after local occlusion of the microcirculation. In the second panel we demonstrate the analysis of the mitochondrial oxygen tension (mitoPO$_2$), the green line represents the linear fit ($\Delta PO_2(t)/\Delta t$) of the oxygen disappearance rate. **B**. The mitoVO$_2$ are presented in a box-and-whiskers graph. The boxes extend from the 25$^{th}$ percentile to the 75$^{th}$ percentile, with a line at the median, the whiskers extend above and below the box to show the highest and lowest values. Presented data are measured with two different probe temperatures (34$^{o}$C and 40$^{o}$C, respectively). **C.** Frequency distribution of all ratio differences of the mitoVO$_2$ at 34$^{o}$C and 40$^{o}$C.

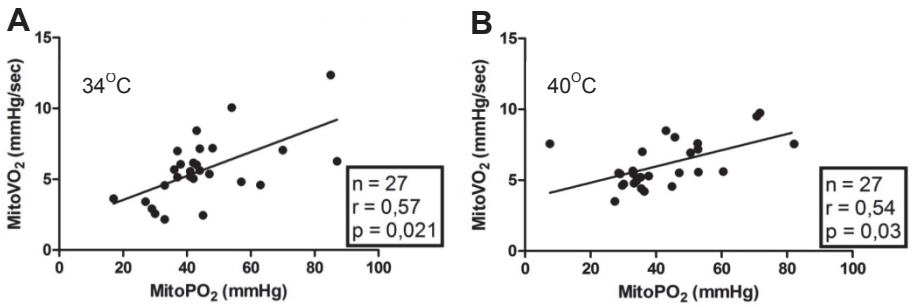


**Fig 5.** Correlation plot of the initial mitochondrial oxygen tension (mitoPO$_2$) and the mitochondrial oxygen consumption (mitoVO$_2$) at 34 $^{o}$C (A) and 40 $^{o}$C (B).

## DISCUSSION

This study presents the first results of a clinical prototype of a novel non-invasive monitoring device based on PpIX-TSLT. This device enables measurement of mitochondrial oxygenation and oxygen consumption in human skin. The PpIX-TSLT appears to be a feasible and safe non-invasive measurement tool that allows to perform a functional optical biopsy in intact skin.

Following topical application of ALA on the skin above the sternum, after 5 h we could detect delayed fluorescence signals, of which the lifetime kinetics could be analyzed in 27 of the 30 healthy volunteers. Three volunteers were excluded from the analysis because the SNR was insufficient; this was caused by technical problems with the light source at the time of measurement (laser output unstable and with reduced intensity). Mean mito$PO_2$ values were around 45 mmHg. This is slightly lower than previously measured in rats [14] and is probably explained by inter-species differences, as well as differences in the fractional inspired oxygen concentration ($FiO_2$). The $FiO_2$ in rats was 0.40 versus an atmospheric $FiO_2$ in healthy volunteers.

We observed a large variation in mito$PO_2$ in humans. This is probably due to the small measurement volume in a highly heterogenic tissue surface, whereby small movements of the measuring probe relative to the skin can lead to large changes in mito$PO_2$. However, large variations are also found in other commonly used methods to measure tissue oxygenation in human skin [20, 21].

Our group is currently working on a measuring probe with revised optics to increase the detection area on the skin. Combined with the ability to be placed flat on the skin and be affixed above the measuring spot, this is expected to substantially reduce the intra-individual variation in mito$PO_2$ readings.

In this first set of human mito$VO_2$ measurements, under stop flow conditions, we chose to calculate the oxygen consumption by a simple fit of the $\Delta PO_2/\Delta t$ curve. This resulted in a mito$VO_2$ of around 6 mmHg $s^{-1}$. The measured values for mito$VO_2$ in human sternal skin are comparable to the results reported for the abdominal skin of rats [15], i.e. 5.8 ± 2.3 mmHg $s^{-1}$ and 5.0 ± 0.3 mmHg $s^{-1}$ respectively.

The mito$VO_2$ measurements were performed with a heated measurement probe at 34°C and at 40°C. Although increased oxygen consumption was expected at a higher skin temperature, no difference was observed in these experiments.

The weak correlation between mitoVO$_2$ and initial mitoPO$_2$ (Figure 5) is possibly partly due to the used method for analysis of the oxygen disappearance rate. A disadvantage of the linear fit procedure is that it is dependent on the inflection point. At low initial oxygen levels the inflection point has a greater influence on the fitting procedure. This difficulty might be solved by using a different analyzing method for the oxygen disappearance rate [14]. Although this more complex method of analysis has been evaluated for use in rats, it has yet to be validated for use in humans; therefore, for the present study, we chose to use a simple linear fit procedure.

The PpIX-TSLT is a novel noninvasive measurement tool that might be of considerable benefit in emergency, intensive care and peri-operative medicine. For example, mitoPO$_2$ measurements could be useful to optimize oxygenation or hemodynamic status [22], or to guide treatment in critically ill patients [12].

This study is the first to demonstrate that measurement of mitochondrial parameters by PpIX-TSLT is feasible in humans. Although the technique still needs further development and optimization, the prototype allows evaluation in humans and the clinical setting. Therefore, we conclude that the method itself is feasible to measure mitoPO$_2$ and mitoVO$_2$ in humans. We expect that clinical implementation of the PpIX-TSLT will make a valuable contribution to our knowledge on mitochondrial function and oxygen metabolism under healthy and pathophysiological circumstances. For example, this technique could be a useful tool to evaluate topical skin treatment, for guidance of systemic mitochondrial therapy, and to monitor mitochondrial function in critically ill patients.

**ACKNOWLEDGEMENTS**

This research was financially supported by a Life Sciences Pre-Seed Grant (grant no. 40-41300-98-9037) from the Netherlands Organization for Health Research and Development (ZonMW).

## CONFLICT OF INTEREST

Dr. E.G. Mik is founder and shareholder of Photonics Healthcare B.V., a company aimed at making the delayed fluorescence lifetime technology available to a broad public. Photonics Healthcare B.V. holds the exclusive licenses to several patents regarding this technology, filed and owned by the Academic Medical Center in Amsterdam and the Erasmus Medical Center Rotterdam, the Netherlands.

## REFERENCES


1. Jeger, V., et al., *Mitochondrial function in sepsis.* Eur J Clin Invest, 2013. **43**(5): p. 532-42.
2. Piffaretti, F., et al., *Optical fiber-based setup for in vivo measurement of the delayed fluorescence lifetime of oxygen sensors.* J Biomed Opt, 2011. **16**(3): p. 037005.
3. Ishii, N., *Role of oxidative stress from mitochondria on aging and cancer.* Cornea, 2007. **26**(9 Suppl 1): p. S3-9.
4. Perry, C.G., et al., *Methods for assessing mitochondrial function in diabetes.* Diabetes, 2013. **62**(4): p. 1041-53.
5. Marson, F., et al., *Correlation between oxygen consumption calculated using Fick's method and measured with indirect calorimetry in critically ill patients.* Arq Bras Cardiol, 2004. **82**(1): p. 77-81, 72-6.
6. Smithies, M.N., et al., *Comparison of oxygen consumption measurements: indirect calorimetry versus the reversed Fick method.* Crit Care Med, 1991. **19**(11): p. 1401-6.
7. Mik, E.G., *Methods and devices for assessment of mitochondrial function.* 2009: US 2011/0182825 A1.
8. Mik, E.G., et al., *Mitochondrial PO2 measured by delayed fluorescence of endogenous protoporphyrin IX.* Nat Methods, 2006. **3**(11): p. 939-45.
9. Harms, F.A., et al., *Oxygen-dependent delayed fluorescence measured in skin after topical application of 5-aminolevulinic acid.* J Biophotonics, 2011. **4**(10): p. 731-9.
10. Mik, E.G., et al., *Mitochondrial oxygen tension within the heart.* J Mol Cell Cardiol, 2009. **46**(6): p. 943-51.
11. Mik, E.G., et al., *In vivo mitochondrial oxygen tension measured by a delayed fluorescence lifetime technique.* Biophys J, 2008. **95**(8): p. 3977-90.

12. Mik, E.G., *Measuring Mitochondrial Oxygen Tension: From Basic Principles to Application in Humans.* Anesth Analg, 2013.
13. Harms, F.A., et al., *Validation of the protoporphyrin IX-triplet state lifetime technique for mitochondrial oxygen measurements in the skin.* Opt Lett, 2012. **37**(13): p. 2625-7.
14. Harms, F.A., et al., *Cutaneous respirometry by dynamic measurement of mitochondrial oxygen tension for monitoring mitochondrial function in vivo.* Mitochondrion, 2013. **13**(5): p. 507-14.
15. Fink, M.P., *Cytopathic hypoxia. A concept to explain organ dysfunction in sepsis.* Minerva Anestesiol, 2000. **66**(5): p. 337-42.
16. Garrabou, G., et al., *The effects of sepsis on mitochondria.* J Infect Dis, 2012. **205**(3): p. 392-400.
17. Golub, A.S., et al., *Analysis of phosphorescence in heterogeneous systems using distributions of quencher concentration.* Biophys J, 1997. **73**(1): p. 452-65.
18. Bodmer, S.I., et al., *Microvascular and mitochondrial PO(2) simultaneously measured by oxygen-dependent delayed luminescence.* J Biophotonics, 2012. **5**(2): p. 140-51.
19. Choi, J.K., et al., *Evaluation of mean skin temperature formulas by infrared thermography.* Int J Biometeorol, 1997. **41**(2): p. 68-75.
20. Schwarz, G., et al., *Cerebral oximetry in dead subjects.* J Neurosurg Anesthesiol, 1996. **8**(3): p. 189-93.
21. Ekbal, N.J., et al., *Monitoring tissue perfusion, oxygenation, and metabolism in critically ill patients.* Chest, 2013. **143**(6): p. 1799-808.
22. Martin, D.S., et al., *Concepts in hypoxia reborn.* Crit Care, 2010. **14**(4): p. 315.

# CHAPTER 9

# *In vivo* assessment of mitochondrial oxygen consumption

Floor A. Harms[1], Egbert G. Mik[1,2]

1 Department of Anesthesiology, Laboratory of Experimental Anesthesiology, Erasmus MC – University Medical Center Rotterdam, 's-Gravendijkwal 230, 3015 CE Rotterdam, The Netherlands.

2 Department of Intensive Care, Erasmus MC – University Medical Center Rotterdam, 's-Gravendijkwal 230, 3015 CE Rotterdam, The Netherlands.

**Short title:** Assessment of mitochondrial oxygen consumption

Published in: Methods in molecular Biology 2014, in press

**ABSTRACT**

The Protoporphyrin IX - Triplet State Lifetime Technique (PpIX-TSLT) has been proposed by us as a potential clinical non-invasive tool for monitoring mitochondrial function. We have been working on the development of mitochondrial respirometry for monitoring mitochondrial oxygen tension (mitoPO$_{2)}$ and mitochondrial oxygen consumption (mitoVO$_2$) in skin. In this work we describe the principles of the method in experimental animals.

**INTRODUCTION**

Recently, growing interest in mitochondrial pathophysiology has led to a continuing increasing number of scientific papers about the impact of mitochondrial dysfunction in a variety of human disorders, like process of cellular aging and cancer [1], cardiovascular diseases [2], sepsis and septic shock [3-5]. This increased knowledge about mitochondrial related disorders is associated with a growing interest and research in treatment strategies aimed at 'Targeting Mitochondria' [6]. However, as is well known the mitochondria play a central role in energy metabolism and cellular survival. Pharmacological intervention on the mitochondrial level might have negative impact on these processes and could have side effects with serious consequences for affected organisms. Such side effects will potentially result in a small therapeutic window for future mitochondrial-targeted drugs. Therefore, the ability to monitor mitochondrial function for diagnosis, treatment effects, and the occurrence of side effects in patients might be of great benefit.

The in 2006 introduced Protoporphyrin IX - Triplet State Lifetime Technique (PpIX-TSLT) [7] opens opportunities to monitor mitochondrial oxygenation and oxygen consumption *in vivo* [8, 9]. This relative new technique enables us to measure mitochondrial oxygen tension (mitoPO$_2$) by means of the oxygen-dependent optical properties of 5-aminolevulinic acid (ALA) induced mitochondrial protoporphyrin IX (PpIX) [10]. But the technique does also provide us the possibility to monitor the respiration rate of the mitochondrial respiratory chain [11]. In this work we describe in detail the technical details and application of this novel method for *in vivo* respirometry in small animals, based on dynamic measurement of mitoPO$_2$ during local blockage of microvascular blood flow.

**MATERIALS**

LASER SETUP (Figure 1)

1. A computer-controlled tunable laser (Opolette 355-I, Opotek, Carlsbad, CA, USA), providing pulses with a specified duration of 4–10 ns and over the tunable range of 410 to 670 nmA.
2. Fiber Delivery System (Opotek, Carlsbad, CA, USA) consisting of 50 mm planoconvex lens, x-y fibermount and a fibre with a length of 2m and a core diameter of 1000µm (FOA-Inline, Avantes b.v., Eerbeek, The Netherlands).
3. Two 1000 µm optical fibers both with a length of 1 meter (P1000-2-VIS-NIR, Ocean Optics, Dunedin, FL, USA).
4. A stainless steel rod with a length of 5 cm and a diameter of 10 mm.
5. Gated microchannel plate photomultiplier tube (MCP-PMT R5916U series, Hamamatsu Photonics, Hamamatsu, Japan).
6. A gated socket assembly (E3059-501, Hamamatsu Photonics, Hamamatsu, Japan).
7. A thermoelectric cooler (C10373, Hamamatsu Photonics, Hamamatsu, Japan).
8. A regulated high-voltage DC power supply (C4848-02, Hamamatsu Photonics, Hamamatsu, Japan).
9. Oriel Fiber Bundle Focusing Assembly (Model 77799, Newport, Irvine, CA, USA).
10. Planoconvex lens with focal length of 90 mm (BK-7, Opto- Sigma, Santa Ana, CA, USA).
11. Electronic shutter (04 UTS 203, Melles Griot, Albuquerque, NM, USA).
12. OEM Shutter Controller Board (59 OSC 205, Melles Griot, Albuquerque, NM, USA).
13. Longpass filter, 590 nm (OG590, Newport, Irvine, CA, USA).
14. Broadband bandpassfilter, 600–750 nm (Omega Optical, Brattleboro, VT, USA).
15. Amplifier (Amplifier C6438-01, Hamamatsu Photonics, Hamamatsu, Japan) with an input impedance of 50 ohm, 500 times voltage amplification and a bandwidth around 50 Mhz.
16. PC-based data acquisition system containing a 10 MS/s simultaneous sampling data-acquisition board (NI-PCI-6115, National Instruments, Austin, TX). (Figure 1.3)
17. BNC interface (BNC-2090A, National Instruments, Austin, TX).

18. Control software, for example written in LabView (Version 10.0 or higher, National Instruments, Austin, TX, USA).

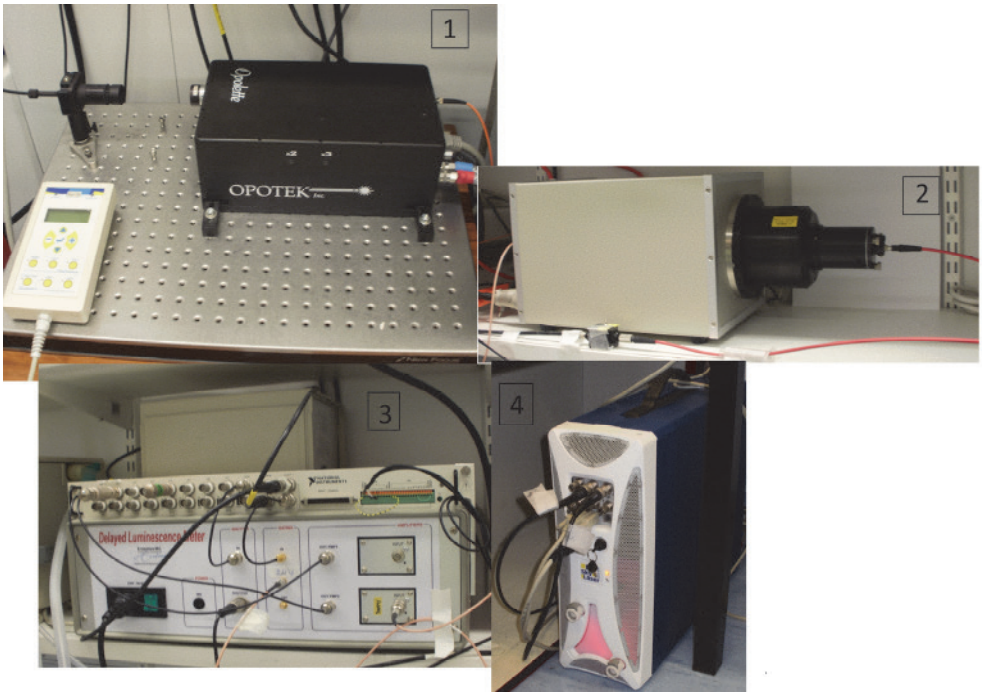


**Figure 1.** Measurement setup. 1. Opolette 355-I – computer controlled tunable laser with fiber coupling, both mounted on an optical bench. 2. Gated microchannel plate photomultiplier tube with gated socket assembly and thermoelectric cooler in a standard housing (gray part) with the measuring fiber coupled to the detector by in house build optics (black part). 3. The data-acquisition sytem and housing of the electronics (power supplies, amplifier and gating circuits). The shown case houses a two-channel setup for simultaneous measurements. 4. The powersupply/control unit of the Opolette 355-I.

ANIMALS

Adult Wistar rats with a bodyweight of 275-325 g (Charles River, Wilmington, MA, USA). All animal care and handling should be in accordance with the NIH Guide for the Care and Use of Laboratory Animals, or alternatively national law. In our case the experiments were approved by the Animal Research Committee of the ErasmusMC University Medical Center Rotterdam.

CHEMICALS, FLUID AND REAGENTS

1. Hydrophilic cremor lanette (Lanettecreme I FNA, Bipharma, Weesp, The Netherlands).
2. 5-aminolevulinic acid (ALA, Sigma- Aldrich, St. Louis, MO, USA).

3. Ketamine 90 mg kg $^{-1}$ (Alfasan, Woerden, The Netherlands).
4. Medetomidine 0.5 mg kg $^{-1}$ (Sedator Eurovet Animal Health BV, Bladel, The Netherlands).
5. Atropine 0.05 mg kg $^{-1}$ (Centrofarm Services BV, Etten-Leur, The Netherlands).
6. Hair removal cream (Veet, Reckitt Benckiser Co., Slough, UK).
7. Heparin solution 10 IE/ml (Leo Pharma BV Amsterdam NL).
8. Voluven (Fresenius Kabi 's Hertogenbosch NL).
9. Ringer solution (Baxter Utrecht NL).
10. Alcohol preps (Romed ® 65x30 mm)

SURGICAL TOOLS

1. Tube: enteral feeding tube L.40 cm-06Fr ref 310.06 Vygon, Ecouen, France, cut to a length of 1.5 cm with a marking at 1 cm.
2. Catheters: 15 cm fine bore polythene tubing PE50. 0.58mm ID, 0.96 OD (Portex Smiths medical Kent UK) connected to a 22 Ga x ½" needle (Luer stub Instech laboratories Inc.. Plymouth Meeting PA USA).
3. Syringes (1 ml).
4. Suture 4/0 (Silkam ® black BBraun Aesculap Tuttlingen Germany).
5. Heating pad with rails for connection fiber standard and BP transducer.
6. Spring scissors (Vannas-Tübingen FST curved 8.5 cm no. 15004-08).
7. Iris scissors (Strabismus FST 9 cm no.14075-09).
8. Forceps (Graefe Forceps FST 1x2 teeth tip width 0.8 mm no.11053-10).
9. Forceps fine (Dumont #7 Dumostar standard tip no.11297-00).
10. Hemostats (Halsted-Mosquito FST curved no.13009-12).
11. Clamp (Schwartz Micro Serrefines FST straight no.18052-01).
12. Hot Beads Sterilizer (FST 250 sterilizer no.18000-45).
13. Sterile towel 45x75 cm (Barrier® Mölnlyke Health Care Göteborg Sweden).
14. Operation microscope.

VENTILATION AND MONITORING

1. Dräger Babylog with anaesthetic breathing system paediatric.
2. Siemens Monitor SC 9000 XL.
3. Capnostat ® $CO_2$ sensor (Novametrix Medical system Inc Wallingford Connecticut USA no. 7167).
4. $CO_2$ cuvet neonatal.
5. Pritt poster buddies Henkel NL BV (for fixation of the $CO_2$ cuvet).

6. Oxygen 100% and air.
7. Data acquisition system PowerLab (ADInstruments Spechbach Germany).
8. Disposable BP transducer (MLT0699 ADInstruments) connected to a stopcock.
9. Simulator and tester Delta-Cal (Utah medical products Inc Westmeath Ireland).
10. T-type Implantable Thermocouple probe (IT-18 MLT1401 ADInstruments) in use with ML312 T-type Pod (ADInstruments).
11. T Copper-constantan thermocouple (MLT1403 ADInstruments) in use with ML290 Thermometer for T-type.
12. Infusion pump.
13. 20 ml syringes.
14. Stopcocks.
15. Extension line (L 100 cm Vygon Ecouen, France ref 71100.10).

**METHODS**

DELAYED LUMINESENCE SETUP:

Couple the excitation source of the pulsed tunable laser into the Fiber Delivery System and connect it trough a x-y connector with the excitation probe. Connect the excitation fiber with the reflection fiber by mounting the terminal tips of both fibers into an small aluminum rod with a separation of 1 mm between the fibers (Figure 2).

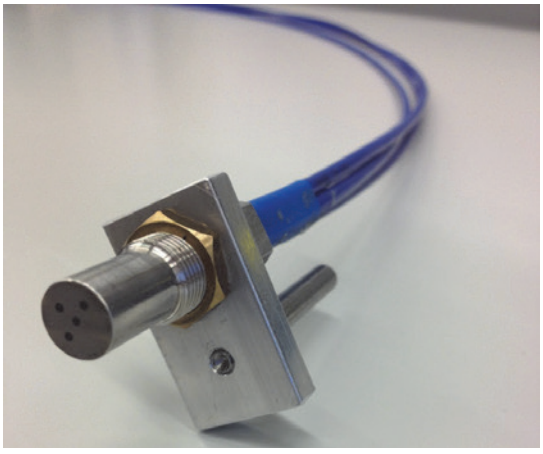

**Figure 2.** The measuring probe. Exitation and emission fibers are mounted in a small aluminum rod, allowing application of local pressure on the measurement volume. The shown probe has two additional fibers for spectroscopic measurements.

The MCP-PMT should preferably have enhanced (infra)red sensitivity. To this end our device has been custom adapted with an enhanced red-sensitive photocathode having a quantum efficiency of 24% at 650 nm. The MCP-PMT should be mounted on a gated socket assembly and cooled to -30$^{o}$C by the thermoelectric cooler. The MCP-PMT can be operated at a voltage between the range of 2000–2700V. Fit the emission branch of the reflection probe into an fiber bundling focusing assembly and couple it to the MCP-PMT by an optic assembly, which consists of a filter-holder, a plano convex lens (90 mm focusing distance) and an electronic shutter. The shutter protects the MCP-PMT, which is configured for the “normally on” mode. Filter out the PpIX emission light by a combination of a 590 nm longpass filter and a broadband (675 -25 nm) bandpassfilter fitted in the filter holder. Convert the output current of the photomultiplier to a voltage by an amplifier with an input impedance of 50 ohm, 500 times voltage amplification and a bandwidth around 50 Mhz. The data-acquisition is performed by a PC-based data acquisition system containing a 10 MS/s simultaneous sampling data-acquisition board. The amplifier is coupled to the DAQ-board by a BNC. The data-acquisition should preferably be performed at the highest possible rate of 10 mega samples per second, allowing for digital post-processing (e.g. low-pass filtering) if necessary. Control of the setup and analysis of the delayed luminescence signals can be performed with software written in LabView, using standard virtual instruments (VIs).

MitoPO$_2$ can be calculated from the delayed fluorescence lifetime by using the Stern-Volmer relationship:

$$mitoPO_2 = \left(1/\tau - 1/\tau_0\right)/k_q \qquad (1)$$

in which $k_q$ is the quenching constant (830 mmHg/s) and $\tau_0$ is the lifetime in the absence of oxygen (0.8 ms) [12]. So the task is now to recover the delayed fluorescence lifetime from the photometric signal by using an adequate fitting procedure.

Since mitochondrial oxygen tension, and thus delayed fluorescence lifetimes, are heterogenous in respiring tissues we do not advice to use a simple mono-exponential fitting procedure to the signal. This will lead to a bias towards longer lifetimes and thus results in underestimation of the average mitoPO$_2$. A convenient way to recover a good estimation of the average mitoPO$_2$ within the measuring volume is fitting a rectangular distribution to the delayed luminescence data [13].

$$Y(t) = Y_0 \exp\left[-\left(1/\tau_0 + kq\left\langle mitoPO_2\right\rangle\right)t\right]\sinh(k_q \delta t)/k_q \delta t \quad (2)$$

where Y(t) is the delayed fluorescence signal, t is the time from the start of the fit, $Y_0$ is the initial signal intensity at t = 0, <mitoPO$_2$> is the average mitochondrial oxygen tension and δ is the half-width of the $PO_2$ distribution.

The oxygen disappearance curve, i.e. the kinetics of mitoPO$_2$ after cessation of local blood flow, can be analyzed by an adapted Michaelis-Menten approach. In contrast to in vitro respiromety in oxygen-closed reaction vessels you have to take oxygen back diffusion into the measuring volume in account when performing analysis *in vivo*. We have previously shown that in skin the following formula can be used if autoconsumption of oxygen by the measuring technique is neglectible [11]:

$$dP_n/d_n = -\left(V_0 \cdot P_n\right)/\left(P_{50} + P_n\right) + Z\left(P_0 - P_n\right) \quad (3)$$

In this equation, $P_n$ is the measured $PO_2$ after excitation flash number *n*, $P_0$ is the mean $PO_2$ before stop-flow, Z is the inflow coefficient of oxygen, $P_{50}$ is the $PO_2$ at which cellular oxygen consumption is reduced to 1/2 $V_{0,}$ and $dP_n/dn$ is the rate of oxygen disappearance.

ANIMAL PREPARATION (Figure 3)

1. Anesthetize the rat with an intraperitoneal (IP) injection of a mixture of ketamine, medetomidine and atropine.
2. After that the rat reaches a surgical level of anesthesia, shave the skin of the abdomen and of the tracheal region.
3. Place the animals in a supine position and performed a tracheotomy. Insert a tube into the trachea until the tip is approximately 1 cm above the carina and fixate the tube with a suture around the trachea.
4. Connect the tube to the ventilation system, which consist a pediatric breathing system, breathing hoses, a $CO_2$ cuvet and a $CO_2$ monitor.
5. Fixate the $CO_2$ cuvet with Pritt poster buddies.
6. Start on the following standard ventilator settings: Inspiration time (Ti) 0.34 sec, expiration time (Te) 0.68 sec, ventilation frequency (fset) 59 bpm, inspiration-expiration ratio (I:E ratio) 1:2, inspired oxygen fraction ($FIO_2$) 40%, inspiratory pressur (Pins) 16 mbar, positive end-expiratory pressure (PEEP) 3.3 mbar. Adjust

the ventilator settings based on end-tidal $PCO_2$ and oxygenation needs and keep the arterial $PCO_2$ between 35 and 45 mmHg.

7. Insert a polyethylene catheter into the right jugular vein. Connect the catheter via an extension with an infusion pump for intravenous administration of fluids and maintenance anesthetics with ketamine.
8. Insert a similar catheter in the left femoral artery and connect it via the BP transducer with Powerlab, to monitor arterial blood pressure and heart rate.
9. Perform every hour an analysis of the arterial blood gas and if necessary adjust your ventilation settings.
10. Measure the body temperature with a rectally inserted thermometer and keep the temperature at 38 ± 0.5 °C by adjustments of the heating pad.

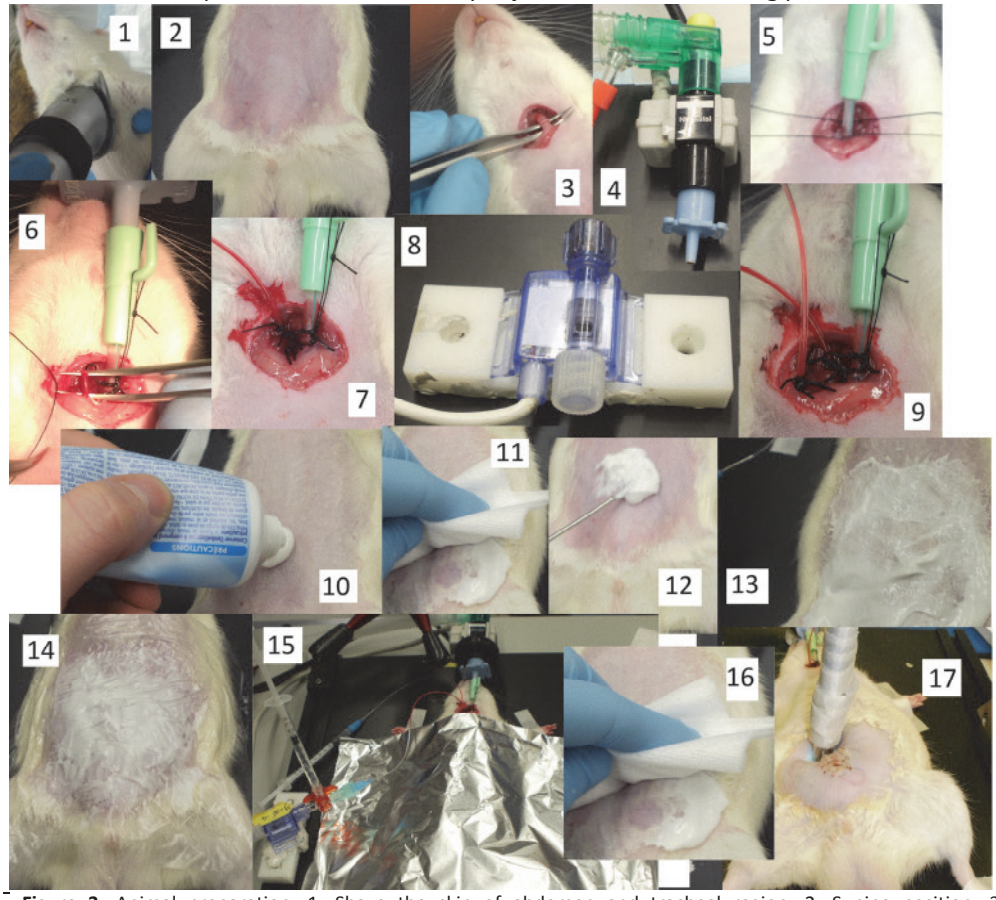


**Figure 3.** Animal preparation. 1. Shave the skin of abdomen and tracheal region, 2. Supine position, 3. Tracheotomy, 4. $CO_2$ cuvet, 5. Connect tube to ventilation system, 6. Carotid artery, 7. Catheter into carotid artery, 8. BP transducer, 9. Catheter into jugular vein, 10. Apply hair removal crème, 11. Remove hair removal crème. 12 -13. Apply 5-aminolevulinic acid crème, 14, Adhesive film, 15 cover area with aluminum foil, 16. Remove 5-aminolevulinic acid crème, 17. Start experiments.

EXPERIMENTAL PRCEDURES

1. Prepare the ALA cream by mixing hydrophilic lanette crème with 2,5% (mass percentage) 5-aminolevulinic acid.
2. Prepare the abdominal skin of the rats by shaving and removing remaining hairs with a hair removal cream. Remove the hair removal cream after 5 minutes and clean the abdominal skin with alcohol preps.
3. Apply the ALA cream topically on the prepared abdominal skin of the rats and leave it on for three hours.
4. To avoid evaporation, cover the exposed skin with an adhesive film and prevent premature light exposure of PpIX by covering the area with aluminum foil.
5. After three hours, there is a sufficient amount of PpIX converted in the mitochondria to start the mitochondrial oxygenation measurements.
6. Remove the ALA cream before the start of the measurements.
7. Perform the mitochondrial respiration measurements by repeated measurements of mito$PO_2$. Use the following settings for the PPIX-TSLT software: With these setting it is possible to measure the mito$PO_2$ at a frequency of e measurement every second during a period of 60 seconds.
8. Start for the first 10 seconds with the measurement of the initial mito$PO_2$, do this by keeping the probe just above the ALA-treated skin surface.
9. After the first 10 seconds apply local pressure with the measurement probe for a period of approximately 30 seconds. This local pressure blocks the oxygen supply by a temporally occluding the microvessels. After the flow arrest in the microvessels you will observe that the mito$PO_2$ gradually drops, this is due to the ongoing oxygen consumption inside the mitochondria.
10. Release the pressure on the abdominal skin after 30 seconds (you have to obtain a new steady mito$PO_2$ reading at a much lower level), hold the measurement probe in an stationary position above the measured area. Figure 4 shows a typical example of time course of mito$PO_2$ and figure 5 shows the result of fitting equation 3 to another example.

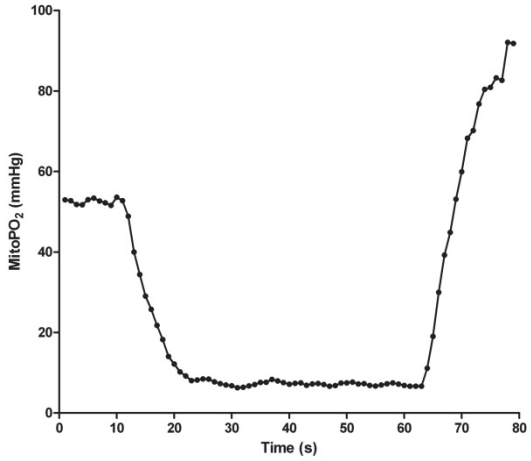


**Figure 4.** Dynamic mitoPO$_2$ measurement. Typical time course of mitoPO2 before, during (starting at 10 seconds) and after release (at 63 seconds) of local pressure with the measuring probe.

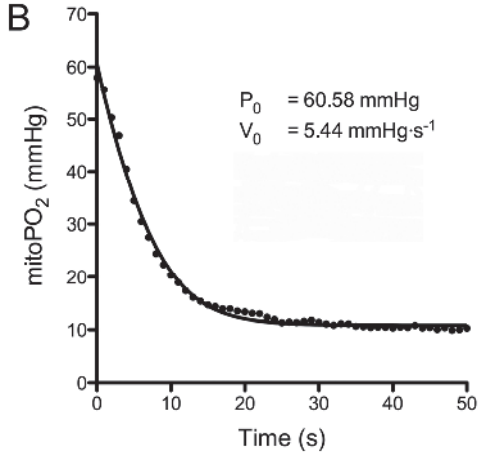


**Figure 5.** ***In vivo*** **respirometry.** Typical example of applying equation 3 to the mitochondrial oxygen disappearance signal. Recorded data (globules line) and the analysis of the data (straight line).



**NOTES**

1. Gating of the photomultiplier tube is essential to prevent saturation of the detector and electronics because of intense prompt fluorescence.
2. Reduce the excitation energy and the number of measurements to a usable minimum to prevent oxygen autoconsumption by the measuring method and excessive photoexcitation of the measuring volume.

3. We find that it is essential to keep the body temperature of the rats around the 38°C.
4. It's best to prepare the ALA cream fresh each time.
5. Store the stock ALA at 6°C and beware for this very hydrophilic compound to attract water.
6. We find that repeated oxygen consumption measurements are possible. However, we advise to change measurement sites on the ALA treated skin surface for repeated measurements.

**REFERENCES**


1. Ishii, N., *Role of oxidative stress from mitochondria on aging and cancer.* Cornea, 2007. **26**(9 Suppl 1): p. S3-9.
2. Ballinger, S.W., *Mitochondrial dysfunction in cardiovascular disease.* Free Radic Biol Med, 2005. **38**(10): p. 1278-95.
3. Fink, M.P., *Cytopathic hypoxia. Is oxygen use impaired in sepsis as a result of an acquired intrinsic derangement in cellular respiration?* Crit Care Clin, 2002. **18**(1): p. 165-75.
4. Galley, H.F., *Oxidative stress and mitochondrial dysfunction in sepsis.* Br J Anaesth, 2011. **107**(1): p. 57-64.
5. Garrabou, G., et al., *The effects of sepsis on mitochondria.* J Infect Dis, 2012. **205**(3): p. 392-400.
6. Edeas, M., , Weissig, V., *Strategies, Innovations & Clincal Applications*, in *Targeting Mitochondria*, M. Edeas, , Weissig, V., Editor. 2014: Berlin.
7. Mik, E.G., et al., *Mitochondrial PO2 measured by delayed fluorescence of endogenous protoporphyrin IX.* Nat Methods, 2006. **3**(11): p. 939-45.
8. Mik, E.G., et al., *Mitochondrial oxygen tension within the heart.* J Mol Cell Cardiol, 2009. **46**(6): p. 943-51.
9. Mik, E.G., et al., *In vivo mitochondrial oxygen tension measured by a delayed fluorescence lifetime technique.* Biophys J, 2008. **95**(8): p. 3977-90.
10. Mik, E.G., *Measuring Mitochondrial Oxygen Tension: From Basic Principles to Application in Humans.* Anesth Analg, 2013. **117**(4): p. 834-46.
11. Harms, F.A., et al., *Cutaneous respirometry by dynamic measurement of mitochondrial oxygen tension for monitoring mitochondrial function in vivo.* Mitochondrion 2013; **13** (5): 507-14.
12. Harms, F.A., et al., *Validation of the protoporphyrin IX-triplet state lifetime technique for mitochondrial oxygen measurements in the skin.* Opt Lett, 2012. **37**(13): p. 2625-7.
13. Golub, A.S., Tevald, M.A., Pittman, R.N., *Phosphorescence quenching microrespirometry of skeletal muscle in situ.* Am J Physiol Heart Circ Physiol, 2011; **300**, H135-143.

# GENERAL DISCUSSION AND FUTURE PERSPECTIVES

## GENERAL DISCUSSION

Mitochondria are the energy-producing subcellular organelles and, therefore, essential for maintaining life. Despite the importance of mitochondrial function and the major role of mitochondrial dysfunction in the pathophysiology of various diseases, no practical clinical method is available for monitoring specific mitochondrial function. In this thesis we describe the development of a new device based on the protoporphyrin-IX triplet state lifetime technique (PpIX-TSLT), which enables non-invasive bedside monitoring of mitochondrial oxygenation and mitochondrial function. We started with an invasive method for use in laboratory animals and developed this with the aim to produce a tool for non-invasive clinical monitoring. Although the technique was developed and calibrated for use in cell cultures, isolated organs (heart and liver) and for *in vivo* use in animals [1-3], it was not yet appropriate for clinical use.

A clinical monitoring tool has to meet the following requirements of an 'ideal' monitoring device [4]:

- Causes no harm
- Provides accurate and reproducible measurements
- Provides measurement of relevant variables
- Provides interpretable data
- Is easy to use
- Is readily available
- Is operator-independent
- Should provide information that is able to guide therapy
- Is cost-effective
- Has a rapid response time.

'Causes no harm', by enabling the use of non-invasive monitoring, was the first step towards achieving a monitoring device for clinical use. To ensure non-invasive measurement of mitochondrial function it is important to measure on an easily accessible organ that interfaces with the environment, such as skin or mucosa. Therefore, we first investigated the possibility to acquire oxygen-dependent measurements on the skin.

In **Chapter 1** we demonstrate that cutaneous application of 5-aminolevulinic acid (ALA) enables measurable PpIX levels and induces oxygen-dependent lifetimes in the skin. Furthermore, we tested the most appropriate method to analyze the delayed fluorescence lifetimes for use in a real-time environment. Because the distribution of oxygen in skin is far from homogeneous, monoexponential analysis biases towards longer lifetimes (low $PO_2$), and a better estimation of mean $PO_2$ is obtained by analysis with the rectangular distribution method (RDM):

$$Y_R = \exp\left(-\left(\frac{1}{\tau_0} + k_q \langle PO_2 \rangle\right) t\right) \cdot \frac{\sin h\left(k_q \, \delta t\right)}{k_q \, \delta t}$$

where <$PO_2$> is mean $PO_2$ within the sample volume, $\tau_0$ is the lifetime in the absence of oxygen, and $k_q$ is the quenching constant. The calibration constants of $\tau_0$ and $k_q$ were previously determined. Unfortunately, because a calibration procedure as described for heart and liver is not applicable in skin, another procedure was needed to validate the previously found calibration constants. For this, we developed a method for simultaneous measurement of mito$PO_2$ and microvascular oxygen tension ($\mu PO_2$) in rats **(Chapter 2)**. These simultaneous measurements enabled to validate the calibration constants by comparing the $\mu PO_2$ and mito$PO_2$ under different circumstances **(Chapter 3)**, i.e. in normal respiring skin tissue at different inspired oxygen fractions ($FiO_2$), in non-respiring skin tissue due to the application of cyanide, and in anoxic skin tissue during ventilation with 100% nitrogen.

As shown in the study in **Chapter 4**, a further development of the PpIX-TSLT provides additional monitoring of the parameters of mitochondrial function, mitochondrial oxygen consumption (mito$VO_2$), and oxygen affinity of the mitochondrial respiratory chain (mito$P_{50}$). Both the 'accuracy and reproducibility' of these functions were demonstrated in normal and non-respiring rat skin.
Mitochondrial dysfunction is suggested to be a key issue in the pathophysiology of and recovery from sepsis [5, 6]. However, the literature shows conflicting results, most likely due to the lack of a valid and reliable measurement method [7]. To determine whether our method indeed provides 'relevant variables' and has the potential to become a future indispensable monitoring tool capable to 'provide information that is able to guide therapy', the PpIX-TSLT must be able to observe changes in mitochondrial function in clinically relevant models.
Therefore, in **Chapter 5**, we explore the possibility to monitor mito$PO_2$ and mito$VO_2$ in a model of acute critical illness, i.e. endotoxemia-induced sepsis. The results of this study show that it is possible to monitor changes in mitochondrial function, even after hemodynamic recovery or after restoration of hemodynamic stability.
The study presented in **Chapter 6** reproduces the results of *ex vivo* experiments with endotoxin-induced mitochondrial dysfunction [8] in our *in vivo* measurement setup. After the infusion of endotoxin, the intravenous administration of succinate resulted in an increased mito$VO_2$, highly resembling the classical *ex vivo* measurements [8]. This allows

us to conclude that the PpIX-TSLT is able to measure alterations down to the level of the mitochondrial respiratory chain. The results of this study also suggest that the administration of succinate might be a suitable therapy in the treatment of mitochondrial dysfunction [9, 10].

A new clinical device that is 'easy to use' is described in **Chapter 7**. In addition, we explored whether measurements on the skin 'provide interpretable data' about more systemic organs, by comparing the values and responses of cutaneous mito$PO_2$ and mito$VO_2$ with other organs. These data show that the effects of systemic mitochondriopathies, such as LPS-induced mitochondrial dysfunction, can be monitored in the skin.

Finally, after extensive testing in our animal studies, we describe the 'accuracy and reproducibility' of the measurements of our new clinical measurement device in healthy volunteers **(Chapter 8)**.

## FUTURE PERSPECTIVES

In the work presented in this thesis, not all requirements have been met to meet the properties of an 'ideal' clinical mitochondrial monitoring device [4]. Some additional steps are needed before this is achieved. First of all, for clinical use, the PpIX-TSLT monitor must meet all the international criteria (CE marking) for a medical device. Therefore, a first series of commercially available clinical monitors based on the PpIX-TSLT is currently under development (COMET, Photonics Healthcare, the Netherlands). It is expected that these COMET monitors will be available in 2015 for clinical use. This will enable a cumulative increase in data collection, as well as valuable knowledge, by providing a means to validate the PpIX-TSLT in multicenter clinical trials.

Hopefully, these developments will allow us to pave the way towards our final goal: clinical monitoring of mitochondrial function in septic patients in order to assess and treat the metabolic state of intensive care patients. Furthermore, this assessment technique can be used to determine the result of therapeutic interventions on the mitochondrial level. For all these goals, additional research is required. First of all, we are planning a longitudinal observational study in sepsis patients. Also, in addition to conducting clinical trials, pre-clinical studies will remain very valuable. On the shorter term, comparative studies are needed to test the relationship between our monitoring method and the

classical *ex vivo* techniques, in order to further elucidate the metabolic implications of the treatment of patients undergoing intensive care.

**REFERENCES**


1. Mik, E.G., et al., *Mitochondrial oxygen tension within the heart.* J Mol Cell Cardiol, 2009. 46(6): p. 943-51.
2. Mik, E.G., et al., *In vivo mitochondrial oxygen tension measured by a delayed fluorescence lifetime technique.* Biophys J, 2008. 95(8): p. 3977-90.
3. Mik, E.G., et al., *Mitochondrial PO2 measured by delayed fluorescence of endogenous protoporphyrin IX.* Nat Methods, 2006. 3(11): p. 939-45.
4. Vincent, J.L., et al., *Clinical review: Update on hemodynamic monitoring--a consensus of 16.* Crit Care, 2011. 15(4): p. 229.
5. Fink, M.P., *Cytopathic hypoxia. Is oxygen use impaired in sepsis as a result of an acquired intrinsic derangement in cellular respiration?* Crit Care Clin, 2002. 18(1): p. 165-75.
6. Galley, H.F., *Oxidative stress and mitochondrial dysfunction in sepsis.* Br J Anaesth, 2011. 107(1): p. 57-64.
7. Jeger, V., et al., *Mitochondrial function in sepsis.* Eur J Clin Invest, 2013. 43(5): p. 532-42.
8. Singh, K.K., *Mitochondria damage checkpoint, aging, and cancer.* Ann N Y Acad Sci, 2006. 1067: p. 182-90.
9. Ferreira, F.L., et al., *Prolongation of survival time by infusion of succinic acid dimethyl ester in a caecal ligation and perforation model of sepsis.Horm Metab Res,* 2000. 32(8) p.335-6.
10. Malaisse, W.J., et al., *Protective effects of succinic aciddimethyl ester infusion in experimental endotoxemia*, Nutrition. 1997 Apr;13(4):330-41.

# SUMMARY

## SUMMARY

In this thesis we describe the development of the protoporphyrin IX-triplet state lifetime technique (PpIX-TSLT) which is used to measure mitochondrial function at the bedside. The process started as an invasive method for use in laboratory animals and was developed into a clinical non-invasive monitoring tool. PpIX-TSLT allows to measure mitochondrial oxygen tension ($mitoPO_2$). The technique was originally developed and calibrated on cell cultures, isolated organs (heart and liver) and for *in vivo* use, but was not sufficiently developed for clinical use in humans. In daily clinical practice, however, measurement of mitochondrial function could play a key role in the monitoring and treatment of various diseases. For example, in the case of sepsis and septic shock, mitochondrial dysfunction may play an important role in the onset of multi-organ failure.

**Chapter 1** describes a method to induce and measure oxygen-dependent delayed fluorescence signals in skin. The method is based on the delayed fluorescence of protoporphyrin IX (PpIX), the final precursor in the synthesis of heme. PpIX is synthesized inside the mitochondria. Because the synthesis from PpIX to heme is rate limiting, the amount of PpIX can be increased by local administration of 5 aminolevulinic acid (ALA). After cutaneous application of ALA, it diffuses through the skin where it is converted to PpIX. We show that cutaneous application of ALA enables measurable PpIX levels and induces oxygen-dependent signals. We also examined three methods to analyze the delayed fluorescence lifetime on skin, i.e. mono-exponential analysis (MEA), the rectangular distribution method (RDM), and the exponential series method (ESM); of these, the RDM proved to be the most feasible for real-time monitoring.

The technique described in **Chapter 2** enables simultaneous measurement of microvascular and mitochondrial oxygen tension. Measurements of microvascular oxygen tension ($\mu PO_2$) are based on oxygen-dependent quenching of phosphorescence of the near-infrared phosphor Oxyphor G2. The $mitoPO_2$ measurements are based on oxygen-dependent quenching of delayed fluorescence of protoporphyrin IX (PpIX). We demonstrated that the favorable spectral properties of PpIX and Oxyphor G2 allow to measure the $\mu PO_2$ and $mitoPO_2$ with excitation by one single laser pulse. Due to the wide separation of the emission spectra of PpIX and Oxyphor G2, the delayed fluorescence and phosphorescence signals were easily separated and analyzed without mutual interference.

In **Chapter 3** we validate the previously determined calibration constants for $mitoPO_2$ measurement in skin. The validation was done by simultaneous measurements of

cutaneous $\mu PO_2$ and $mitoPO_2$ under different conditions, i.e. in normal skin tissue at different inspired oxygen fractions ($FiO_2$), in non-respiring skin tissue after the application of cyanide, and in anoxic skin tissue after ventilation with 100% nitrogen. During a stepwise decrease in $FiO_2$, we found decreased values in either the $\mu PO_2$ or the $mitoPO_2$. Similar values of $\mu PO_2$ and $mitoPO_2$ were found in non-respiring tissue and in anoxic skin. Overall, the results indicate that the calibration constants that were determined in heart and liver are also accurate for $mitoPO_2$ measurements in the skin.

**Chapter 4** describes further development of PpIX-TSLT, with the aim to provide a new technique to monitor oxygenation, oxygen consumption and oxygen affinity of the mitochondrial respiratory chain *in vivo*. Mitochondrial oxygen consumption ($mitoVO_2$) measurements were done by dynamic (repetition frequency of 1 Hz) $mitoPO_2$ measurements during a period of local compression (10 s before, 60 s during and 20 s after compression), which was achieved by applying local pressure with the measurement probe. This simple procedure created stop-flow conditions and induced measurable oxygen disappearance due to the cessation of microvascular oxygen supply and ongoing cellular oxygen consumption inside the mitochondria. Furthermore, we provide a method for analysis of oxygen disappearance kinetics, from which we can calculate the $mitoVO_2$ and $mitoP_{50}$. The reproducibility of the measurement method was demonstrated in rats. Finally, we show that blockade of the mitochondrial respiratory chain, due to the application of cyanide, leads to the disappearance of oxygen consumption inside the mitochondria.

The study in **Chapter 5** investigates whether it is possible to monitor alterations in $mitoPO_2$ and $mitoVO_2$ in an acute sepsis model. The results of the lipopolysacharride-induced sepsis groups show a significant decrease in $mitoVO_2$. However, decreased $mitoPO_2$ was only observed in the absence of proper resuscitation after the induction of sepsis. These results indicate that we are able to monitor alterations in mitochondrial function. Impaired $mitoVO_2$, despite normal $mitoPO_2$, suggests that persisting mitochondrial dysfunction does play a role in the pathophysiology of sepsis.

In **Chapter 6** we measure alterations in $mitoVO_2$ after intravenous administration of succinate. Previous *ex vivo* studies with toxin-induced mitochondria reported increased oxygen consumption after succinate administration. Our study shows that we were able to reproduce *in vivo* experiments under *in vivo* circumstances by means of PpIX-TSLT. These results demonstrate that *in vivo* $mitoVO_2$ measurements are valid to measure alterations in mitochondrial oxygen consumption.

**Chapter 7** addresses two important steps that are essential for clinical applicability of PpIX-TSLT. The first part of this chapter shows the that there is a relationship in the alterations of mitoPO$_2$ and mitoVO$_2$ between skin and other organs and tissues. Furthermore, a relationship was observed between blood flow, tissue oxygen saturation and mitoPO$_2$. The second part of the chapter describes the clinical concept of cutaneous PpIX-TSLT measurements and presents a technical description of the clinical prototype developed by our group.

In **Chapter 8** we present the first results of our clinical PpIX-TSLT prototype that was used in healthy volunteers to measure mitoPO$_2$ and mitoVO$_2$ in human skin. In this observational study, the measurements result in an average mitoPO$_2$ of 44 ± 17 mm Hg and a mitoVO$_2$ of 5.8 ± 2.3 mm Hg; these data correspond with earlier results derived from our rat studies. Although the values show a large variation, partly because of the technical implementation of our prototype, both mitoPO$_2$ and mitoVO$_2$ tend to regress toward a normal distribution. Our results demonstrate that the PpIX-TSLT method allows to acquire real-time information on mitochondrial oxygenation and mitochondrial oxygen consumption in humans.

**Chapter 9** provides a detailed description of the PpIX–TSLT for application in a rat model. This user-friendly manual will enable researchers to measure mitoPO$_2$ and mitoVO$_2$ in rats and other small animals.

# NEDERLANDSE SAMENVATTING

## NEDERLANDSE SAMENVATTING

In dit proefschrift beschrijven we de ontwikkeling van de Protoporphyrin IX-triplet state lifetime technique" (PpIX-TSLT) van een invasieve meetmethode toegepast in proefdieren naar een niet-invasieve methode klaar voor klinisch gebruik. De PpIX-TSLT stelt ons in staat om niet-invasief de zuurstofspanning in de mitochondriën te meten. De techniek is ontwikkeld en geijkt op celculturen, geïsoleerde organen (hart en lever) en voor *in vivo* gebruik, maar kon nog niet worden toegepast in de kliniek. Dit ondanks dat het meten van de mitochondriale functie in de dagelijkse klinische praktijk wel degelijk een belangrijke rol zou kunnen vervullen in het monitoren van verschillende ziektebeelden, zoals bijvoorbeeld sepsis en septische shock, waarbij het disfunctioneren van de mitochondriën mogelijk een sleutelrol speelt in het ontwikkelen van multi-orgaanfalen.

**Hoofdstuk 1** laat zien dat het mogelijk is om zuurstofafhankelijke vertraagde fluorescentie signalen te meten. Om deze signalen te kunnen detecteren maken we gebruik van Protoporfyrine IX (PpIX). Dit is de laatste precursor in de synthese van heem en wordt gesynthetiseerd in de mitochondriën. Doordat de synthese van PpIX naar heem traag verloopt is het mogelijk om de concentratie van PpIX te verhogen door het toedienen van de precursor 5-aminolevelinezuur (ALA). Bij de cutane applicatie van ALA, zal de ALA door de huid diffunderen waar het ter plaatse geconverteerd wordt naar PpIX. Wij laten zien dat deze cutane applicatie meetbare PpIX niveaus induceert en zuurstofafhankelijke signalen vertoont. Tevens onderzoeken we drie manieren (mono-exponentiële analyse (MEA), rechthoekig distributie methode (RDM) en exponentiële series methode (ESM)) om de vertraagde fluorescentie uitdooftijd in de huid te analyseren, waaruit blijkt dat de RDM de meest betrouwbare is.

Met de techniek die beschreven wordt in **Hoofdstuk 2** is het mogelijk tegelijkertijd zowel in de microcirculatie als in de mitochondriën de zuurstofspanning te meten. Bij deze simultane meting wordt de mitochondriale zuurstofspanning (mito$PO_2$) gemeten door middel van ALA geïnduceerde protoporferine IX en wordt de microvasulaire zuurstofspanning ($\mu PO_2$) gemeten met behulp van Oxyphor G2. Deze porfyrines hebben beide een ander emissiespectrum, hoewel het excitatiespectrum rond dezelfde golflengte ligt. Hierdoor kunnen Oxyphor G2 en PpIX simultaan geëxciteerd worden met eenzelfde golflengte laserlicht, wat het mogelijk is om de fluorescentie en vertraagde fluorescentie door middel van filters van elkaar te scheiden en te analyseren.

In **hoofdstuk 3** valideren we de eerder verkregen kalibratieconstanten voor het meten van de mitoPO$_2$ op de huid. Dit hebben we gedaan middels het vergelijken van simultaan gemeten µPO$_2$ en mitoPO$_2$ onder verschillende omstandigheden: in de normale huid, in niet-ademend huidweefsel door middel van de cutane applicatie van cyanide, en in anoxisch huidweefsel na de ventilatie van 100% stikstof. We vinden een afname in zowel de µPO$_2$ als mitoPO$_2$ bij een stapsgewijze daling van de fractionele inspiratoire zuurstofconcentratie (FiO$_2$). Verder vinden we vergelijkbare µPO$_2$ en mitoPO$_2$ in het niet-ademend weefsel en in de anoxische huid. Deze resultaten laten zien dat het mogelijk is om de eerder bepaalde kalibratieconstanten voor het hart en de lever ook toe te passen in de huid.

**Hoofdstuk 4** beschrijft een methode die naast het meten van de mitoPO$_2$ het ook mogelijk maakt om inzicht te krijgen in de functie van de mitochondriën door middel van de mitochondriale zuurstofconsumptie (mitoVO$_2$) en zuurstofaffiniteit (mitoP$_{50}$). De metingen worden uitgevoerd met behulp van een reeks kort opeenvolgende mitoPO$_2$ metingen (één meting per seconde) gedurende een (10 seconde voor, 60 seconde tijdens en 20 seconde na) lokale compressieperiode door druk uit te voeren met de meetprobe op het weefsel. Gedurende deze compressieperiode wordt er stop-flow conditie geïndiceerd in de microcirculatie. Hierdoor wordt de zuurstoftoevoer naar de mitochondriën geblokkeerd en door het persisterende zuurstofverbruik in de mitochondriën vertoont de mitoPO$_2$ een afname in de tijd. We beschrijven dat het mogelijk is om uit deze kinetiek de mitoVO$_2$ en mitoP$_{50}$ te berekenen. Van belang voor deze berekening is dat hierbij rekening wordt gehouden met de zuurstof influx vanuit de omgeving. Verder laten we zien dat een blokkade van de mitochondriale ademhalingsketen, door middel van cyanide, leidt tot het verdwijnen van de zuurstofconsumptie in de mitochondriën.

In **Hoofdstuk 5** wordt onderzocht of het mogelijk is om, met behulp van de mitoPO$_2$ en mitoVO$_2$, in een acuut sepsis model een afname in de mitochondriale functie te monitoren. De resultaten lieten in de geïnduceerde sepsis groepen een significante daling zien van de mitoVO$_2$. De mitoPO$_2$ werd alleen duidelijk beïnvloed wanneer er na het induceren van de sepsis geen resuscitatie plaatsvond. Deze resultaten impliceren dat we veranderingen in de mitochondriale functie kunnen monitoren. Hierbij doet de afname in de mitoVO$_2$ bij een gelijk blijvende of herstelde mitoPO$_2$ het vermoeden versterken dat mitochondriale dysfunctie wel eens een belangrijke rol zou kunnen hebben in het optreden van een falend metabolisch bij sepsis.

In **Hoofdstuk 6** meten we het effect op de mitoVO$_2$ na het intraveneus toedienen van succinaat. In eerdere *ex vivo* studies met toxine geïnduceerde mitochondriën vond men toegenomen zuurstofconsumptie na toediening van succinaat. We tonen in dit hoofdstuk aan dat we deze *ex vivo* metingen met de PpIX-TSLT *in vivo* kunnen reproduceren. Deze resultaten suggereren dat we met onze techniek daadwerkelijk veranderingen kunnen meten op het niveau van de mitochondriale ademhalingsketen.

**Hoofdstuk 7** beschrijft twee belangrijke stappen die essentieel zijn voor de klinische toepasbaarheid van de PpIX-TSLT. Als eerste wordt er in dit hoofdstuk aangetoond dat veranderingen die gemeten worden op de huid van de ratten tegelijkertijd ook tot uiting komen in de meer vitale organen, en dat deze veranderingen ook gemeten kunnen worden in organen zelf. Ten tweede wordt in dit hoofdstuk de ontwikkeling van een nieuw klinische prototype beschreven.

In **Hoofdstuk 8** wordt voor het eerst met behulp van PpIX-TSLT de mitoPO$_2$ en mitoVO$_2$ gemeten op de humane huid. De metingen van deze observationele studie resulteren in een gemiddelde mitoPO$_2$ van 44 ± 17 mmHg en een mitoVO$_2$ van 5.8 ± 2.3 mmHg, wat overeenkomt met de eerder gevonden data in ratten. Hoewel de waardes een grote variatie vertonen, observeren we zowel in de mitoPO$_2$ als in de mitoVO$_2$ data de intentie om zich normaal te verdelen. Deze resultaten suggereren dat de PpIX-TSLT ons in staat stelt om “real time” informatie te geven over de functie van de humane mitochondriën.

In **Hoofdstuk 9** wordt stapsgewijs beschreven hoe de PpIX-TSLT kan worden toegepast in ratten. Met behulp van deze gebruiksaanwijzing stellen we in de toekomst iedereen in staat om de mitoPO$_2$ en mitoVO$_2$ te meten.

# APPENDICES

**DANKWOORD**

Yes, het is gelukt! Zonder de steun en bijdragen van velen was dit proefschrift nooit tot stand gekomen, van wie ik in het bijzonder wil noemen.

**Prof. dr R.J. Stolker,** beste Robert Jan, bedankt voor het vertrouwen en de mogelijk die je mij hebt gegeven voor het uitvoeren van dit promotieonderzoek. Je kritische blik en adviezen bij het lezen van dit proefschrift heb ik erg gewaardeerd.

**Dr. E.G. Mik,** beste Bert, ik had me geen betere copromotor kunnen wensen. Jou onuitputtelijke enthousiasme en kennis over het meten zuurstof hebben me vanaf moment één weten te motiveren. Daarnaast is jou onvoorwaardelijke steun en hulp onmisbaar geweest voor de totstandkoming van dit proefschrift. Het was een eer om jouw wetenschappelijk kindje verder te mogen ontwikkelen.

**De leden van de kleine promotie commissie:** Dr. D.A.M.P.J. Gommers, Prof.dr. C. Ince en Prof.dr. C. Spies. Hartelijk dank voor de bereidheid zitting te nemen in de kleine commissie en voor de snelle beoordeling van het proefschrift. Prof.dr. C. Spies, Ihre Bereitschaft, an meiner Promotionsausschusses teilzunehmen, ist eine wahre Ehre.

**Overige leden van de grote promotiecommissie:** Prof. dr. W.F.F.A. Buhre, Prof. dr. D.J.G.M. Duncker, Prof. dr. C.M.F. Dirven, Prof.dr. A.G.J.M. Leeuwen en Prof.dr. J.H. Ravesloot. Hartelijk dank voor uw bereidheid om zitting te nemen in de grote commissie.

**Dr. H. Raat,** beste Harold, als senior onderzoeker op het laboratorium experimentele anesthesiologie was je de ideale sparingspartner. Jouw scherpzinnige blik heeft me vaak aan het denken gezet. Dank hiervoor.

**P. Specht,** beste Patricia, hoewel stiekem nog veel te jong, voor mij ben toch wel een beetje de moeder van het lab. Bedankt voor alles wat je me geleerd hebt, je hulp bij mijn experimenten en voor je luisterend oor. Ik ben je nog veel chocolade verschuldigd, maar dat gaat goed komen!

**J. Voorbijtel,** beste Jacqueline, bedankt voor de honderden ratjes die jij voor mij perfect prepareerde, zonder deze hulp was er geen enkel experiment geslaagd.

**M. Munker,** beste Micheal, wat was die klinische laser een drama! Tot op heden kan ik niet begrijpen dat het genereren van kleine pulsjes groen licht zo veel voeten in de aarde kan hebben. Bedankt voor het tripje naar Duitsland wat het licht weer liet schijnen. En sorry dat wetenschap niet zo snel gaat. Nog even geduld de COMET (het nieuwe meetapparaat) gaat er echt komen.

**Mede onderzoekers,** beste Minke, Marit, Sander, Mark, Nadia en Mariska, bedankt voor de gezelligheid, de adviezen en bedankt voor de support na elk mislukt experiment.

**Maatschap Anesthesiologie IJselland ziekenhuis,** beste Frans, Jelmer, Rob, Christine Patricia, Frodo, Mirjam, Jacomar en Branka, bedankt voor jullie steun en flexibiliteit tijdens de laatste fase van dit proefschrift.

**Paranimfen,** lieve Ellen, na alle zenuwslopen momenten die we de afgelopen jaren samen hebben meegemaakt, waarin ik je overigens altijd met veel plezier heb ondersteund, is het nu aan jou de taak om mijn zenuwen in bedwang te houden. Lieve Jolanda, bedankt voor alle hulp, steun en 'bank hang momentjes'. Ladies ik vind het echt super om jullie op deze belangrijke dag aan mijn zijde te hebben.

**Roei(st)ers,** bedankt voor alle perfecte roeihalen. Hoewel deze sommige trainingen maar schaars voorkwamen, heeft jullie streven naar perfectie de afgelopen jaren voor veel mooie 'joy momentjes', afleiding en broodnodige ontspanning gezocht.

**Anton, Heleen, Hilke en Koen Harms,** lieve papa en mama, zus en broer, een gepromoveerd(e) dochter/zusje, wie had dat ooit gedacht, bedankt voor de steun die ik altijd van jullie heb mogen ontvangen.

**Manasse Hutte,** lieve Manasse, gedurende mijn promotie traject heb ik je leren kennen. Jij gaf de noodzakelijke rust en orde. Ik verheug me op alle leuke dingen die we nog samen gaan doen en waar nu eindelijk tijd voor is. Maar eerst een mooi feestje! Ik hou van jou.

## PUBLICATIONS

**Harms FA,** Bodmer SI, Raat NJ, Mik EG;
*Cutaneous mitochondrial respirometry: non-invasive monitoring of mitochondrial function*.
J Clin Monit Comput, 2014; Article in press

**Harms FA**, Mik EG;
*In vivo assessment of mitochondrial oxygen consumption.*
Methods in Molecular Biology, 2014; Article in press

**Harms FA**, Mik EG;
*Op weg naar een nieuwe monitoringtechniek: In vivo meten van mitochondrialefunctie.*
NTvA, 2013; **26**(1): p.7-10

**Harms FA**, Bodmer SI, Raat NJ, Stolker RJ Mik EG;
*Validation of the protoporphyrin IX-triplet state lifetimetechnique for mitochondrial oxygen measurements in the skin.*
Opt Lett, 2012; **37**(13): p. 2625-7.

Bodmer SI, Balestra GM, **Harms FA**, Johannes T, Raat NJ, Stolker RJ, Mik EG;
*Microvascular and mitochondrial PO(2) simultaneously measured by oxygen-dependent delayed luminescence.*
J Biophotonics, 2012; **5**: p.140-151

**Harms FA**, de Boon WM, Balestra GM, Johannes T, Stolker RJ, Mik EG;
*Oxygen-dependent delayed fluorescence measured in skin after topical application of 5-aminolevulinic acid.*
J Biophotonics, 2011; **4**:p. 731-739.

**PhD PORTFOLIO**

| | |
|---|---|
| **Name PhD student**: | F.A. Harms |
| **Erasmus MC Department:** | Anesthesiology |
| **PhD period:** | 2011-2014 |
| **Promotor:** | Prof.dr. R.J. Stolker |
| **Supervisor:** | Dr. E.G. Mik |

**PhD training**

**General courses**

- BROK ('Basiscursus Regelgeving Klinisch Onderzoek') Erasmus University
- Artikel 9 ("Laboratory Animal Science") Groningen University
- Statistics

**Seminars and workshops**

- NVA young investigator day
- Lasercursus voor dermatologen

**Presentations**

- NVA wetenschapsdag 2011, Ede (The Netherlands) (oral)
- 22nd Annual Meeting of the European Society for Computing and Technology in Anesthesia and Intensive Care (ESCTAIC) 2011, Erlangen(Germany) (oral)
- Targeting Mitochondria 2011, Berlin (Germany) (poster)
- NVA wetenschapsdag 2012, Ede (The Netherlands) (oral)
- 23nd Annual Meeting of the European Society for Computing and Technology in Anesthesia and Intensive Care (ESCTAIC) 2012, Timisoara (Romania) (oral)
- Targeting Mitochondria 2012 Berlin (Germany) (oral)
- NVA wetenschapsdag 2013, Zeist (The Netherlands) (oral)
- Targeting Mitochondria 2012, Berlin (Germany) (oral, Award)

**(Inter)national conferences**

- NVA wetenschapsdag 2011, Ede (The Netherlands)
- Targeting Mitochondria 2011, Berlin (Germany)
- 22nd Annual Meeting of the European Society for Computing and Technology in Anesthesia and Intensive Care (ESCTAIC) 2011, Erlangen (Germany)
- NVA wetenschapsdag 2012, Ede (The Netherlands)
- Targeting Mitochondria 2012, Berlin (Germany)
- NVA wetenschapsdag 2012, Ede (The Netherlands)
- 23nd Annual Meeting of the European Society for Computing and Technology in Anesthesia and Intensive Care (ESCTAIC) 2012, Timisoara (Romania)
- Targeting Mitochondria 2013, Berlin (Germany)
- NVA wetenschapsdag 2013, Zeist (The Netherlands)

**Teaching**

- Supervising medical students (research project) 2011-2013

**CURRICULUM VITAE**

Floor Harms werd op 23 december 1983 geboren te ’s-Gravenhage. Na het behalen van het VWO diploma aan het Haagse Montessori Lyceum, begon ze in 2003 met de studie geneeskunde aan de Erasmus Universiteit Rotterdam. Na het afronden van het artsexamen in 2010 startte ze haar promotieonderzoek naar het monitoren van de mitochondriale oxygenatie en zuurstofconsumptie in het Erasmus MC, Rotterdam (promotor: Prof.dr. R.J. Stolker), leidend tot dit proefschrift. Vanaf oktober 2012 is zij werkzaam als arts-assistent in opleiding tot Anesthesioloog in het Erasmus MC, Rotterdam (opleider: Prof.dr. R.J. Stolker).